TECHNISCHE UNIVERSITÄT WIEN

Diplomarbeit

Scale Up of reverse Water-Gas Shift Catalysts

Autor: Richard Buchinger

Matrikelnummer: 11706003

Institut für Materialchemie, Bereich Physikalische Chemie

Betreuer:

Univ.-Prof. Dr. Christoph Rameshan

Dr. Noelia Barrabés Rabanal

Wien, am 10.01.2023

Unterschrift (Student):

Abstract

In the combat against global warming methods to reduce carbon dioxide (CO_2) emissions are of high interest. The reverse water-gas shift reaction (rWGS) not only allows to reduce CO_2 emissions but also converts CO_2 into carbon monoxide (CO) which is a useful chemical used to produce many base chemicals.

Novel perovskites (i.e. $Nd_{0.6}Ca_{0.4}Fe_{0.9}Co_{0.1}O_{3-\delta}$ – NCF-Co) proofed to be very active rWGS catalysts on the lab scale [1]. Thus, an up-scaling of this catalyst should be tried.

The perovskite material was prepared via the Pechini route. Besides of the NCF-Co phase, the formation of a brownmillerite phase was observed in X-ray diffraction (XRD) measurements for batches of larger size.

For up-scaling, pellets with the porogens starch and graphite which were sintered at different temperatures were prepared and tested in the reactor for their catalytic activity. It was found that higher porogen content and lower sintering temperature increase the activity. Pellets with Al_2O_3 as binder also performed well in the catalytic tests.

For pellets produced with alumina hydrates and NCF-Co it was found that pellets which contain more boehmite exhibit a higher mechanical stability. The reactor testing was done close to the thermodynamic equilibrium (close to real conditions). A higher activity compared to pure alumina was confirmed but it was difficult due to the problem of condensing water to distinguish between the NCF-Co containing catalysts.

Furthermore, it was tried to prepare composites with zeolites. First a pure zeolite was prepared (ZSM-5 “Si/Al=35”). This zeolite and two other ZSM-5 zeolites (ZSM-5 “pure Si” and ZSM-5 “Si/Al=140”) were tested for their stability via in-situ XRD in hot water vapor atmosphere. Two of these three zeolites were relatively stable (ZSM-5 “Si/Al=35” and ZSM-5 “Si/Al=140”) whereas for the zeolite ZSM-5 “pure Si” the formation of β-cristobalite was found.

For the preparation of composites two approaches were chosen:

- Zeolite added to the Pechini synthesis
- NCF-Co added to zeolite synthesis

For the approach “zeolite added to the Pechini synthesis” the formation of β-cristobalite and an almost completely destroyed zeolite was found for ZSM-5 “pure Si”, whereas for ZSM-5 “Si/Al=140” only partial destruction of ZSM-5 and the forming of various other phases apart from ZSM-5 and NCF-Co were found.

For the approach “NCF-Co added to zeolite synthesis” it was found in the XRDs that reflexes from both phases are present. A reduction of the brownmillerite phase was observed, when NCF-Co was added early in the course of the zeolite synthesis.

In the catalytic tests the same problems as described above arose. Nevertheless, the qualitative assessment that an early addition of NCF-Co to the zeolite synthesis leads to a flattening of the activity curve can be made.

For all investigated NCF-Co catalysts, exsolution was confirmed via ex-situ XRD.

Kurzfassung

Im Kampf gegen die Klimaerwärmung sind Methoden zur Reduktion von Kohlenstoffdioxid (CO_2) Emissionen von höchstem Interesse. Die reverse Wasser-Gas Shift (rWGS) Reaktion ermöglicht nicht nur eine Reduktion von CO_2 Emissionen, sondern auch die Umwandlung in eine nützliche Verbindung namens Kohlenstoffmonoxid (CO) welche für die Produktion von Grundchemikalien benötigt wird.

Neuartige Perowskite (z.B. $Nd_{0.6}Ca_{0.4}Fe_{0.9}Co_{0.1}O_{3-\delta}$ – NCF-Co) stellten sich bei Tests im Labormaßstab als sehr aktiv heraus [1]. Deshalb soll ein Up-Scaling dieses Katalysators versucht werden.

Der Perowskit wurde über die Pechini Synthese hergestellt. Neben der NCF-Co Phase wurde bei Röntgenbeugungsmessungen (XRD) auch eine Brownmillerit Phase gefunden.

Für den Up-Scaling Prozess wurden zuerst Pellets mit den Porogenen Stärke und Graphit, gesintert bei verschiedenen Temperaturen, hergestellt und in einem Reaktor die katalytischen Aktivitäten getestet. Es wurde festgestellt, dass sowohl ein höherer Gehalt an Porogenen als auch eine niedrigere Sintertemperatur die Aktivität erhöhen. Pellets mit Al_2O_3 als Binder lieferten eine gute katalytische Performance.

Für Pellets hergestellt aus Alumina Hydraten und NCF-Co wurde gefunden, dass Pellets mit höheren Böhmit Gehalten eine höhere mechanische Stabilität aufweisen. Für die Reaktortests sollte nahe am thermodynamischen Limit (nahe an reellen Bedingungen) gearbeitet werden. Eine erhöhte Aktivität zu reinem Alumina konnte belegt werden, aufgrund des Problems von kondensierendem Wasser kann jedoch nicht zwischen den verschiedenen Katalysatoren welche NCF-Co enthalten unterschieden werden.

Weiters wurde versucht Komposite mit Zeolithen herzustellen. Dazu wurde zunächst ein reiner Zeolith synthetisiert (ZSM-5 „Si/Al=35“). Dieser und zwei weitere ZSM-5 Zeolithe (ZSM-5 „pure Si“ und ZSM-5 „Si/Al=140“) wurden via in-situ XRD in Heißwasserdampfatmosphäre auf Stabilität geprüft. Zwei der drei getesteten Zeolithe waren relativ stabil (ZSM-5 „Si/Al=35“ und ZSM-5 „Si/Al=140“) wohingegen bei Zeolith ZSM-5 „pure Si“ die Bildung von β-Cristobalit beobachtet wurde.

Für die Herstellung von Kompositen wurden zwei Ansätze gewählt:

- Zeolithe zur Pechini Synthese zugegeben
- NCF-Co zugegeben zur Zeolith Synthese

Beim Ansatz „Zeolithe zugegeben zur Pechini Synthese“ wurde für Zeolith ZSM-5 „pure Si“ die Bildung von β-Cristobalit und eine beinahe vollständige Zerstörung von ZSM-5 beobachtet. Für ZSM-5 „Si/Al=140“ wurde eine geringere Zerstörung und Bildung von weiteren Phasen, abgesehen von ZSM-5 und NCF-Co, festgestellt.

Beim Ansatz „NCF-Co zugegeben zur Zeolith Synthese“ wurde in den XRDs gefunden, dass Reflexe beider Phasen vorhanden sind. Eine Reduktion der Brownmillerite Phase konnte beobachtet werden, wenn NCF-Co früh im Verlauf der Zeolith Synthese zugegeben wurde.

Die katalytischen Tests waren wiederum von dem oben bereits genannten Problem überlagert. Allerdings konnte die qualitative Beobachtung gemacht werden, dass sich eine frühe Zugabe von NCF-Co zur Zeolith Synthese in einer Abflachung der Aktivitätskurve äußert.

Exsolution wurde mittels ex-situ XRD für alle in den Reaktortests eingesetzten Perowskitkatalysatoren bestätigt.

Danksagung

Ich möchte mich bei Christoph Rameshan, seinen Arbeitsgruppenangehörigen und Noelia Barrabés meiner Co-Betreuerin einerseits dafür bedanken, dass ich meine Diplomarbeit hier abfassen durfte und andererseits dafür, dass ich bei meiner Arbeit tatkräftig unterstützt wurde.

Weiters möchte ich mich bei Laura Kronlachner für die ICP-OES Messungen, bei Johannes Zbiral für die XRF-Messungen und bei Werner Artner vom XRD-Zentrum, welcher mir bei Fragen immer mit Rat und Tat zur Seite stand, bedanken.

Auch bei den Zugehörigen des Instituts für Technische Elektrochemie, an welchem ich die Synthesen der Perowskite durchgeführt habe, möchte ich mich für ihre Gastfreundschaft bedanken.

Zu guter Letzt, aber definitiv nicht gering geschätzter, möchte ich mich bei meiner Familie und Freunden bedanken, die mich in dieser Zeit unterstützt haben.

Eidesstattliche Erklärung

Ich erkläre hiermit, dass ich die vorliegende Diplomarbeit selbständig angefertigt habe und keine anderen Hilfsmittel verwendet worden sind als die von mir als Quellen angegebenen. Wörtliche und sinngemäße Zitate sind entsprechend gekennzeichnet worden.

Wien, am 10.01.2023

Richard Buchinger

Table of Contents

1 Introduction

One hot topic of our modern society is the combat against climate change due to emissions of greenhouse gases like carbon dioxide (CO_2). Efficient ways to reduce CO_2 emissions as well as the fixation of already emitted CO_2 and the conversion into something useful are urgently needed. One way of CO_2 conversion is the reverse water-gas shift reaction (rWGS). In this reaction CO_2 and hydrogen (H_2) are reacted to carbon monoxide (CO) and water (H_2O). CO_2 is a very stable molecule, hence much energy and a catalyst are required for high conversions. If H_2 is used in excess, then H_2:CO with ratios in the order of 2:1 can be achieved. This gas mixture, called syngas, can be reacted to useful chemicals like hydrocarbons in Fischer-Tropsch reactions [2] or methanol and other alcohols [3].

Novel perovskites (i.e. $Nd_{0.6}Ca_{0.4}Fe_{0.9}Co_{0.1}O_{3-\delta}$) proved to be very active in the reverse water-gas shift reaction (rWGS) at lab-scale [4]. These perovskites are stable until high reaction temperatures and also cheap. Because of these very promising tests on the lab-scale, a scale-up of this catalyst should be tried.

1.1 Reverse Water-Gas Shift Reaction

The reverse water-gas shift reaction can be described by the chemical equation given in Equation 1:

$$CO_2 + H_2 \rightleftharpoons CO + H_2O \tag{1}$$

The rWGS is an endothermic and endergonic reaction as it can be seen from the thermodynamic data in Table 1.

Table 1: thermodynamic data of rWGS at 298 K [5]

ΔH_r (kJ·mol^{-1})	ΔS_r (J·mol^{-1}·K^{-1})	ΔG_r (kJ·mol^{-1})
36.2	42.0	23.7

In Figure 1 the conversion versus temperature for rWGS can be seen. From the viewpoint of thermodynamics, a high temperature would be favorable for high conversion.

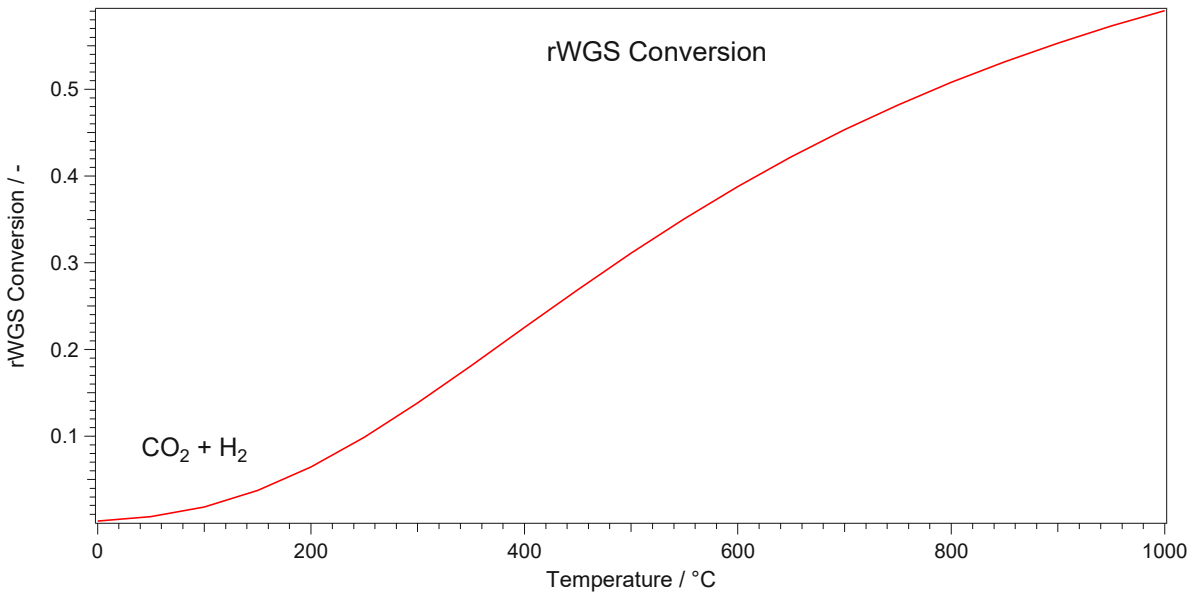

Figure 1: thermodynamically maximum possible rWGS conversion, thermodynamic values used for calculation of the rWGS conversion from [5]

A possible side reaction of rWGS is the formation of methane. This happens preferentially at lower temperatures, because this is an exothermic reaction, hence higher yields are possible from the viewpoint of thermodynamics [6].

1.2 Perovskites

The general formula of oxide-type perovskites is ABO_3. The crystal system is often orthorhombic or cubic, depending on the radii of the cations A and B and the stability of the perovskites can be determined by the Goldschmidt´s tolerance factor:

$$t = \frac{r_A + r_O}{\sqrt{2} \cdot (r_B + r_O)} \tag{2}$$

r_A .....radius of the A cation (pm)

r_B .....radius of the B cation (pm)

r_O .....radius of the anion (pm)

The A-site of the perovskites that was investigated for the upscaling was filled with Nd^{3+}-ions and was doped with Ca^{2+}-ions. These cations have rather large radii. The B-site sublattice was formed by Fe^{3+}-ions. The B-Site was doped with Co^{2+} ions. The B-site ions have smaller radii than the ones on the A-site. In Figure 2 the crystal structure of the perovskite $Nd_{0.6}Ca_{0.4}Fe_{0.9}Co_{0.1}O_{3-\delta}$ can be seen.

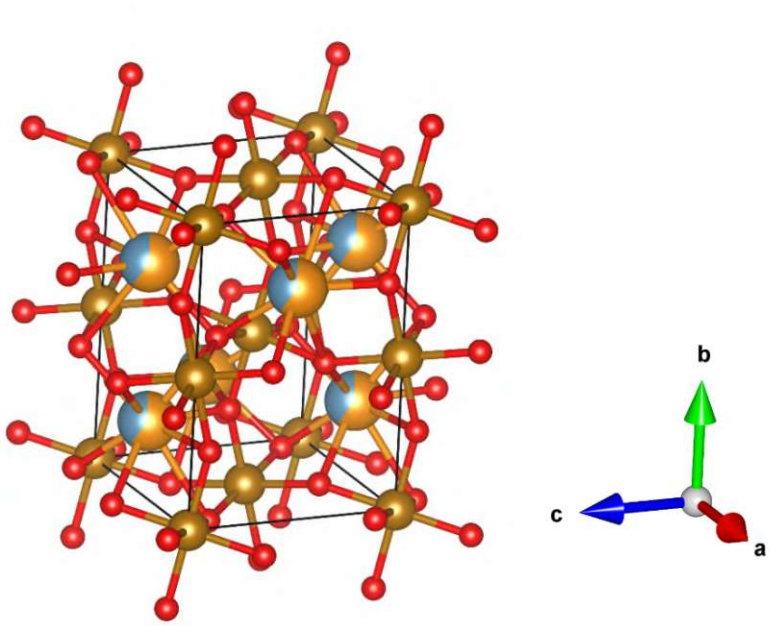

Figure 2: crystal structure of $Nd_{0.6}Ca_{0.4}Fe_{0.9}Co_{0.1}O_{3-\delta}$

Because of the A-site doping with cations with the charge +2, charge neutrality of the perovskite has to be achieved via different possible mechanisms: The first possibility is a partial oxidation of Fe-ions on the B-site (Fe^{3+} and Fe^{4+} are both present). Another possibility to achieve net neutral charge would be the formation of oxygen vacancies. Which of the two effects is dominant depends on the temperature and reaction conditions. Therefore, an unknown amount of oxygen vacancies is indicated in the formula as $ABO_{3-\delta}$.

Another phenomenon that can occur with these investigated perovskite is called exsolution. Under reductive conditions (reductive gases or electrochemical polarization), the B-site ions can get reduced,

causing them to migrate to the surface, where they form small metallic nanoparticles. These nanoparticles can catalyse chemical reactions like water gas shift [7] or reverse water gas-shift[4].

1.3 Process of Up-Scaling [8]

On the lab scale catalysts are often investigated in pure forms (e.g. as powders) or with a support material at best. When doing a scale-up, other factors such as mechanical, thermal and chemical stability play an important role. On a big scale it is also important to bring the catalyst into a suitable form that the pressure drop in the reactor does not exceed certain limits. Thus, it is necessary to prepare catalyst pieces in the range from millimeters or even bigger. Pelleting and extrusion are often used to get to this formed catalyst pieces. To meet all these requirements and to allow the forming process to function properly, catalysts are not used in pure forms anymore, instead various additives are used. Some additives only assist the forming process to get to formulations that can be pelletized or extruded but are eliminated from the final catalyst body later in a calcining or sintering process via decomposition of these additives. Other additives stay in the catalyst body to ensure proper operation in the catalytic reaction. In Figure 3 the typical tasks in the development of a technical catalyst can be seen.

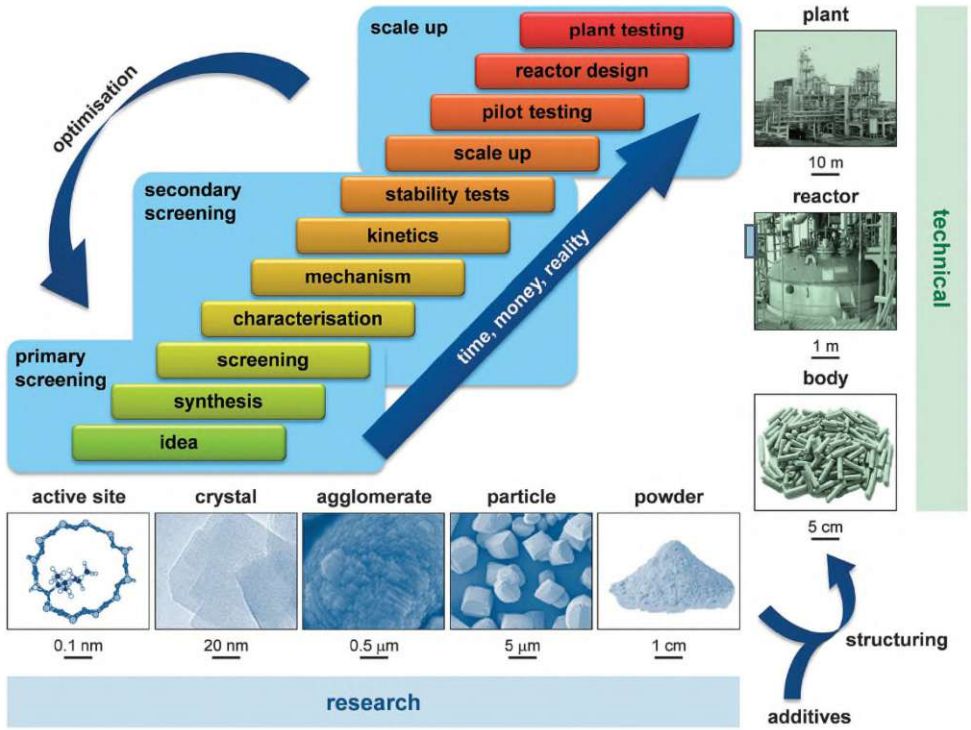

Figure 3: typical tasks in the development of a catalyst [8]

1.4 Zeolites [9]

Zeolites are made of Si-Al-oxide networks and very versatile materials. A very important parameter is the Si/Al ratio which can vary over a broad range for many zeolites. The introduction of Al into the network leads to a negative charge at the Al-site. Via cations like H^+ or Na^+ and some others a charge neutrality can be achieved. Besides Al, also other elements like Fe (but many others as well) can be introduced into the network [10, 11]. A key characteristic of zeolites is a well-defined pore structure. This pore structure leads to very high internal surface areas but also the external surface areas are typically relatively high. Zeolites are very stable and can be used up to high reaction temperatures. Typical applications of zeolites are:

- Adsorbents

- Catalysts (Petroleum Refining, Synfuels Production)
- Detergents

In Figure 4 the crystal structure of ZSM-5, a widely used zeolite, with the formula $Na_nAl_nSi_{96-n}O_{192}\cdot 16H_2O$ can be seen.

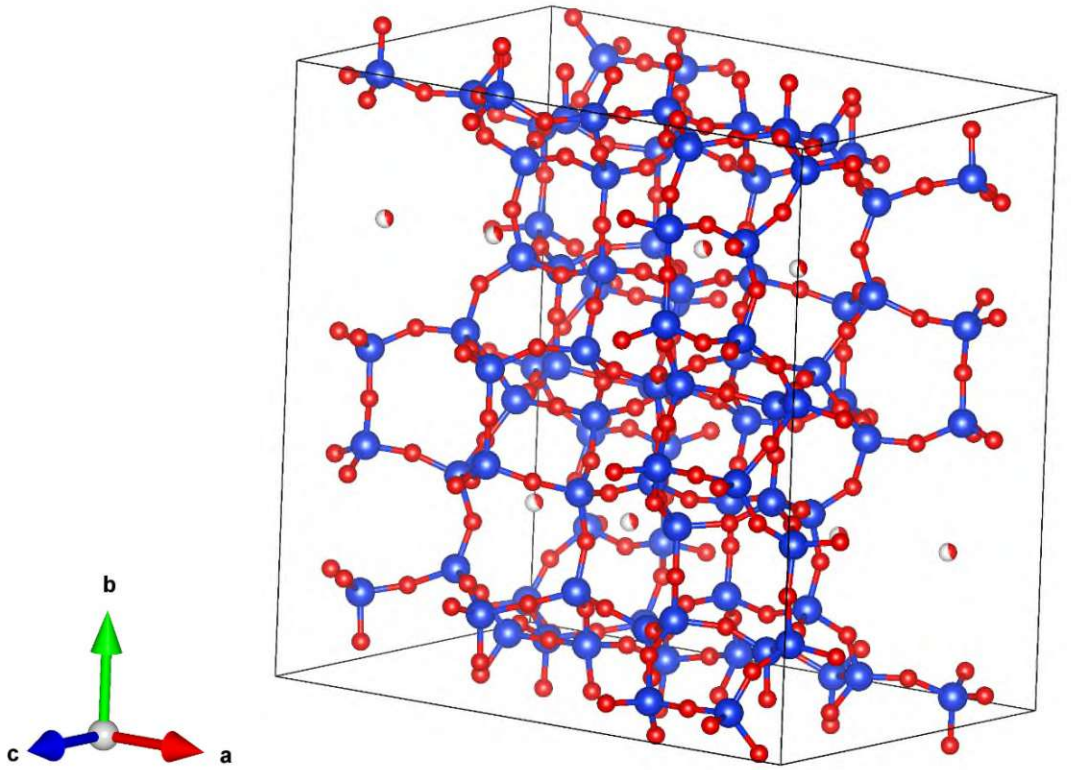

Figure 4: crystal structure of ZSM-5

The typical course of zeolite preparation is the following:

- Silica, alumina (or other metals) sources, a structure directing agent (SDA), basic reagents and water are mixed to form an aqueous gel
- Crystallization in an autoclave at increased temperature (100-200 °C)
- Separation of the zeolite from the aqueous phase via filtration or centrifugation
- Drying & calcination

Zeolites with higher Si content exhibit higher stability in hot water vapor since they have a higher hydrophobicity [12].

1.5 Alumina Hydrates [13]

Boehmite - γ-AlO(OH) - and bayerite - α-$Al(OH)_3$ - are so called alumina hydrates, (precursors of alumina - Al_2O_3). When sintering alumina hydrates, physiosorbed and crystal water can be eliminated from the structure and various polymorphs of alumina are formed. In Figure 5 it can be seen, which sintering temperature leads to which polymorph for the two before mentioned alumina hydrates. When the precursors are compacted before sintering, bodies with increased mechanical strength are the result. By mixing catalysts with the alumina precursor catalyst bodies with certain mechanical stability can be

obtained. These alumina hydrates are often used as supports or binders for catalysts used in refinery and chemical processes.

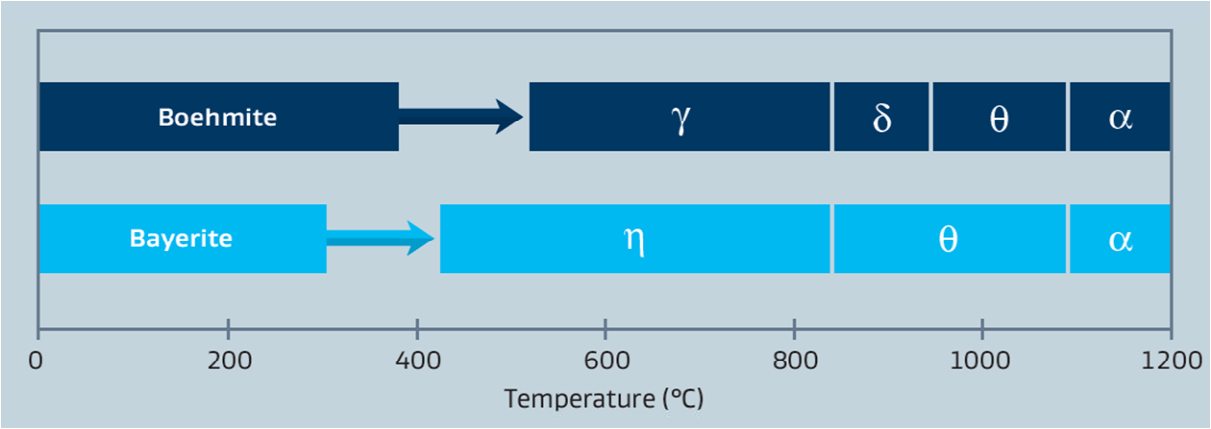

Figure 5: phase changes of alumina hydrates at the respective temperatures [13]

2 Methods

2.1 Catalytic Measurements

For the catalytic measurements, a tubular fixed bed reactor was used. To hold the perovskite powder in place, some glass wool was put in a quartz glass tube (outer diameter $6\ \mathrm{mm}$, inner diameter $4\ \mathrm{mm}$). After the catalyst was weighed in, the fixed bed reactor was inserted into the measuring equipment The gas feeds (all gases were provided by Messer Group GmbH, Bad Soden, Germany) were controlled by mass flow controllers (Bronkhorst, Ruurlo, Netherlands), which use the calorimetric principle. The gas flow was not recorded, but regularly checked. The gas mixture can either flow through the reactor, which is situated in a heating unit, or through a bypass. The temperature was controlled with a PID controller (EMSR EUROTHERM GmbH, Vienna, Austria): The temperature was measured using a type K thermocouple and was recorded every second. The tip of the thermocouple was positioned outside of the catalyst bed. After the reactor, the composition of the gas mixture was analyzed by a Micro-gas chromatograph (Micro-GC; Fusion 3000A, Inficon, Bad Ragaz, Switzerland). The Micro-GC had two columns. Column A uses a Rt-Molsieve 5Å with Ar as carrier gas and backflush injection. Column B uses a Rt-Q-Bond with He as carrier gas and variable volume injection. The detection for all gases (H_2, CO, CH_4, and O_2 in column A, CO_2 in column B) was done via a thermal conductivity detector. The Micro-GC took a measurement every 4 minutes. A scheme of the measurement setup can be seen in Figure 6

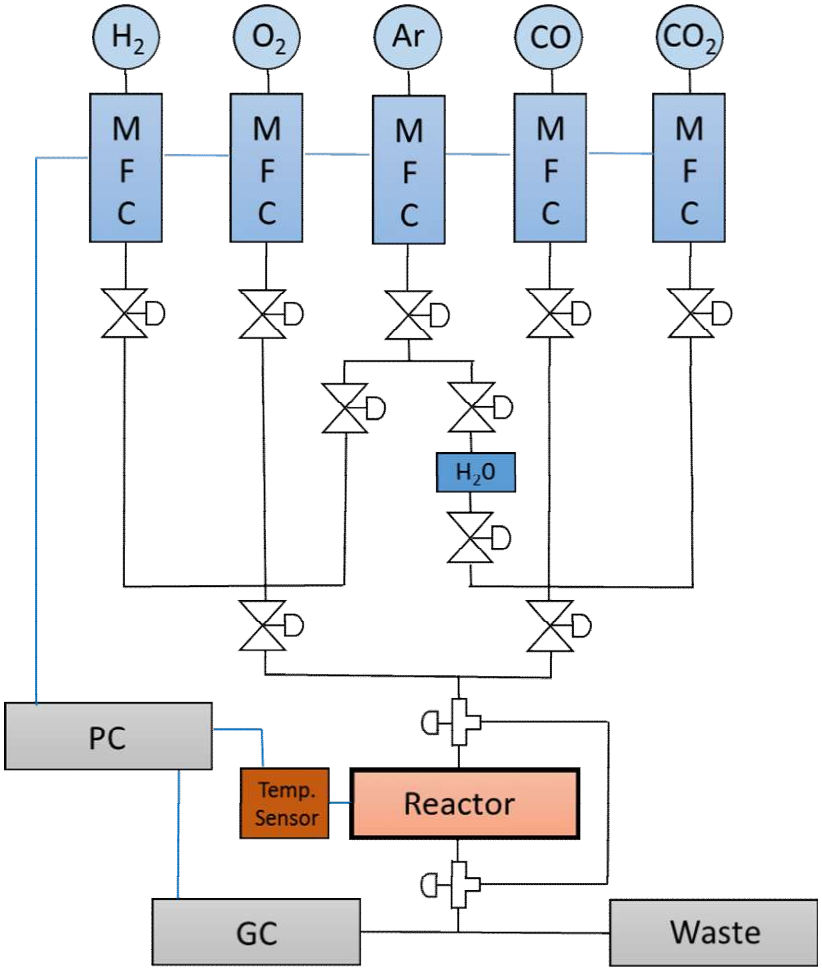

Figure 6: scheme of the measurement setup for catalytic measurements [14]

The yield was derived from Equation 3:

$$Yield = \frac{x_{CO}}{x_{CO_2,0}} \tag{3}$$

$x_{CO_2,0}$ .....molar ratio of CO_2 before the reactor (−)

x_{CO} .....molar ratio of CO after the reactor (−)

The specific activity a was derived from Equation 4:

$$a = \frac{x_{CO} \cdot p \cdot \dot{V}_{sum}}{R \cdot T \cdot m} \tag{4}$$

a .....specific activity ($\mathrm{mol \cdot g^{-1} \cdot s^{-1}}$)

p .....pressure ($p = 101{,}300$ Pa)

$\dot{V}_{\mathrm{sum}}$ .....overall volumetric flow ($\mathrm{m^3 \cdot s^{-1}}$)

R .....ideal gas constant ($R = 8.314\ \mathrm{J \cdot mol^{-1} \cdot K^{-1}}$)

T .....absolute temperature ($T = 273.15$ K)

m .....mass of catalyst (g)

The selectivity was derived from Equation 5:

$$Selectivity = \frac{x_{CO}}{x_{CO} + x_{CH_4}} \quad (5)$$

x_{CH_4} .....molar ratio of CH_4 after the reactor $(-)$

2.2 Scanning Electron Microscope

All Scanning Electron Microscope (SEM) images were recorded using secondary electrons on a Quanta 250 FEGSEM microscope (FEI Company, Hillsboro, OR, USA). For the voltage (HV…high voltage) and the working distance (WD) variable values were used. The values for WD and HV for each image can be found in the captions. All images were taken at room temperature.

The imaging process uses electron-sample interactions: When focusing a beam of electrons (primary electrons) on a solid sample, electrons of the outer shells of the sample are removed, leading to the so-called secondary electrons. These electrons have energies of just a few eV. A detector measures the number of secondary electrons. Due to the low energy of secondary electrons, only the ones of the outermost layer can reach the detector. The number of secondary electrons is proportional to the volume of which they originate from. Consequently, the intensity of secondary electrons for sloping surfaces is higher than for even surfaces. Therefore, SEM images give information about the topography of the specimen.

To record a picture of the whole sample, the electron beam scans over the surface, hence **scanning** electron microscopy.

2.3 Brunauer Emmett Teller

Gas molecules can adsorb on the surface of solids. Sorption isotherms describe the loading of the sorbent with sorbate in dependence of the equilibrium concentration of sorbate, for a given temperature. Different models exist to describe these isotherms. The model according to Brunauer-Emmett-Teller [15] is based on the assumption that sorbate can form monolayers (binding to the surface) as well as multilayers (binding to an already adsorbed gas molecule).

The isotherms were recorded using a Micrometrics ASAP 2020 system. The samples were degassed at $300\ °C$ under vacuum for $4\ \text{hours}$, followed by the measurement of full N_2 adsorption-desorption isotherms at $-196\ °C$ (liquid N_2). According to the BET-model the specific surface area can be calculated from the adsorption-desorption isotherms.

2.4 XRD & in-situ XRD

The XRD measurements were performed at room temperature with a PANalytical X´Pert Pro Diffractometer (Malvern Panalytical, Malvern, UK) in Bragg-Brentano geometry using a mirror for separating the Cu-$K_{\alpha 1,2}$ radiation and an X´Celerator linear detector (Malvern Panalytical, Malvern, UK).

The in-situ XRD measurements were performed in the temperature range from $25\text{-}700\ °C$ with a PANalytical X´Pert Pro Diffractometer (Malvern Panalytical, Malvern, UK) in Bragg-Brentano geometry with an in-situ cell XRK 700 using a mirror for separating the Cu-$K_{\alpha 1,2}$ radiation and an X´Celerator linear detector (Malvern Panalytical, Malvern, UK). The atmosphere was either He or Ar as inert gas, bubbled through water at room temperature to get about $3\ \%$ humidity of the inert gas.

Data analysis was done with the HighScore Plus software (Malvern Panalytical, Malvern, UK) and the PDF-4+2019 Database (ICDD-International Centre for Diffraction Data, Newtown Square, PA, USA)

XRD is used to determine the structure of crystals (e.g. atomic positions and lattice parameters). An X-ray beam hits the specimen under a certain diffraction angle and gets diffracted at electron shells of the ions or atoms of the crystal. A detector located on the other side of the sample (same angle between X-ray source and sample and between sample and detector) measures the intensity of the diffracted X-ray beam, depending on the diffraction angle. A schematic depiction of this geometry can be seen in Figure 7.

At certain angles, constructive interference occurs due to the periodic crystal structure of solids and a reflex can be observed in the diffractogram.

The connection between wavelength, lattice parameters, and the diffraction angle is given by Bragg´s Law (6):

$$n \cdot \lambda = 2 \cdot d \cdot \sin(\Theta) \tag{6}$$

n .....order of diffraction (−)

λ .....wavelength of the X-ray beam (Å)

d .....spacing between diffraction planes (Å)

Θ.....Bragg angle (°)

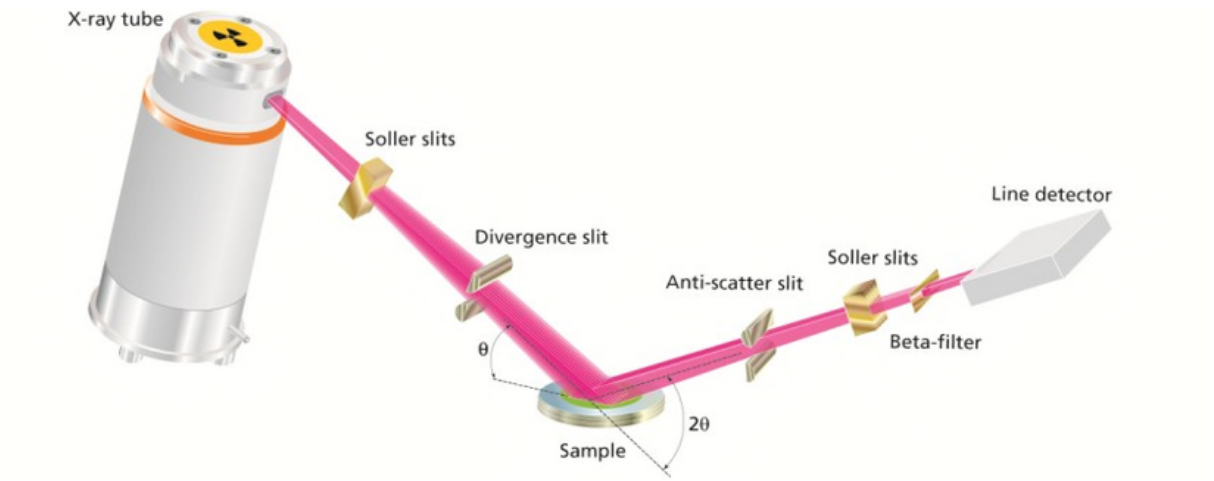

Figure 7: measurement setup of Bragg-Brentano geometry [16]

3 Pechini Syntheses

The preparation of the pure catalyst (NCF-Co) that should be used for up-scaling was done via the Pechini route. If not indicated differently, the typical workflow of a Pechini synthesis was always the same: The proper amounts of the precursors were dissolved in distilled water, with the solvation being facilitated by the addition of some nitric acid and heating. The respective solutions were combined in a quartz glass flask. In the next step, citric acid (excess of 20 % with regards to cations) was added to the solution. Citric acid complexes the cations and allows the co-precipitation of the ions. On a hot plate the water was evaporated, while formation of an orange sponge-like product could be observed. Further decomposition of organic material was performed over the Bunsen burner flame. After this step, the color of the intermediate changed to brown. Then the flasks were put in a muffle furnace for calcination (under normal atmospheric conditions). In Table 2 and Table 3 the reagents used for the syntheses can be seen.

Table 2: reagents used for the syntheses

Nd_2O_3		**$CaCO_3$**		**Fe**		**$Co(NO_3)_2{\cdot}6H_2O$**	
Designation	Description	Designation	Description	Designation	Description	Designation	Description
A	REO, 99 %	A	Sigma Aldrich, ≥99.995 % trace metal basis	A	Thermoscientific, 99.8 % metal trace basis	A	Roth, ≥98 %
B	Strategic elements, 99.9 %	B	From Noelia Barrabes lab, purity unknown	B	Mixture of Sigma Aldrich 99,98 % trace metal basis and Sigma Aldrich 99,99 % trace metal basis	B	Sigma Aldrich 99.999 %
		C	$CaCO_3$ precipitated, purissum (reagent very old)				

Table 3: reagents used for the syntheses

Citric acid		HNO_3		H_2O	
Designation	Description	Designation	Description	Designation	Description
A	PanReac Applichem, pure, pharma grade	A	Chemlab 65 % a.r.	Always used; not extra designated in tables later	In-house, doubly distilled
B	Sigma Aldrich 99,998 % (metals basis)	B	Sigma Aldrich, >= 65% orderd in-house/ from electrochemistry department		

Table 4 shows details about the syntheses like weighed in amounts, sintering program and yields for the first batches that were prepared.

Table 4: details about prepared batches of NCF-Co

Batch Date	Amount Nd_2O_3 (g)	Amount $CaCO_3$ (g)	Amount Fe (g)	Amount $Co(NO_3)_2{\cdot}6H_2O$ (g)	Amount citric acid (g)	Used reagent for: Nd_2O_3; $CaCO_3$, Fe; $Co(NO_3)_2{\cdot}6H_2O$; citric acid; HNO_3	Sintering program (heating rate in °C/min – holding temperature in °C – holding time in h – heating rate in °C/min – holding temperature in °C – holding time in h – cooling rate in °C/min)	Yield (g)
19.04.2022	2.4542	0.9685	1.2157	0.7037	11.3	B;A;B;B,B;B	/-/-/-5-800-5-5	4.54
22.04.2022	2.4418	0.9685	1.2158	0.7040	12.5	B;A;B;B,B;B	5-350-0,5-5-800-5-5	4.47
28.04.2022	2.7104	0.9685	1.2157	0.7040	12.5	B;A;B;B,B;B	5-350-0,5-5-800-5-5	4.71
23.05.2022	4.3363	1.5495	1.9451	1.1263	19.5	B;A;B;B,B;B	5-350-0,5-5-800-5-5	7.63
03.06.2022	6.504	2.3238	2.9173	1.6893	29.5	B;A;B;B,B;B	5-350-0,5-5-800-5-5	11.43

The XRDs of the first synthesized batches can be seen in Figure 8. Besides reflexes of NCF-Co also reflexes of a brownmillerite phase and sometimes of Fe_2O_3 appear. Fe_2O_3 appears due to a lack of Nd on the A-site and could be avoided by 9 % excess of Nd_2O_3. The most dominant reflex from the brownmillerite phase can be seen at an angle at 33.4° and is indicated in the XRD. All other reflexes correspond to NCF-Co. For bigger batches some reflexes corresponding to NCF-Co interestingly appear more intense.

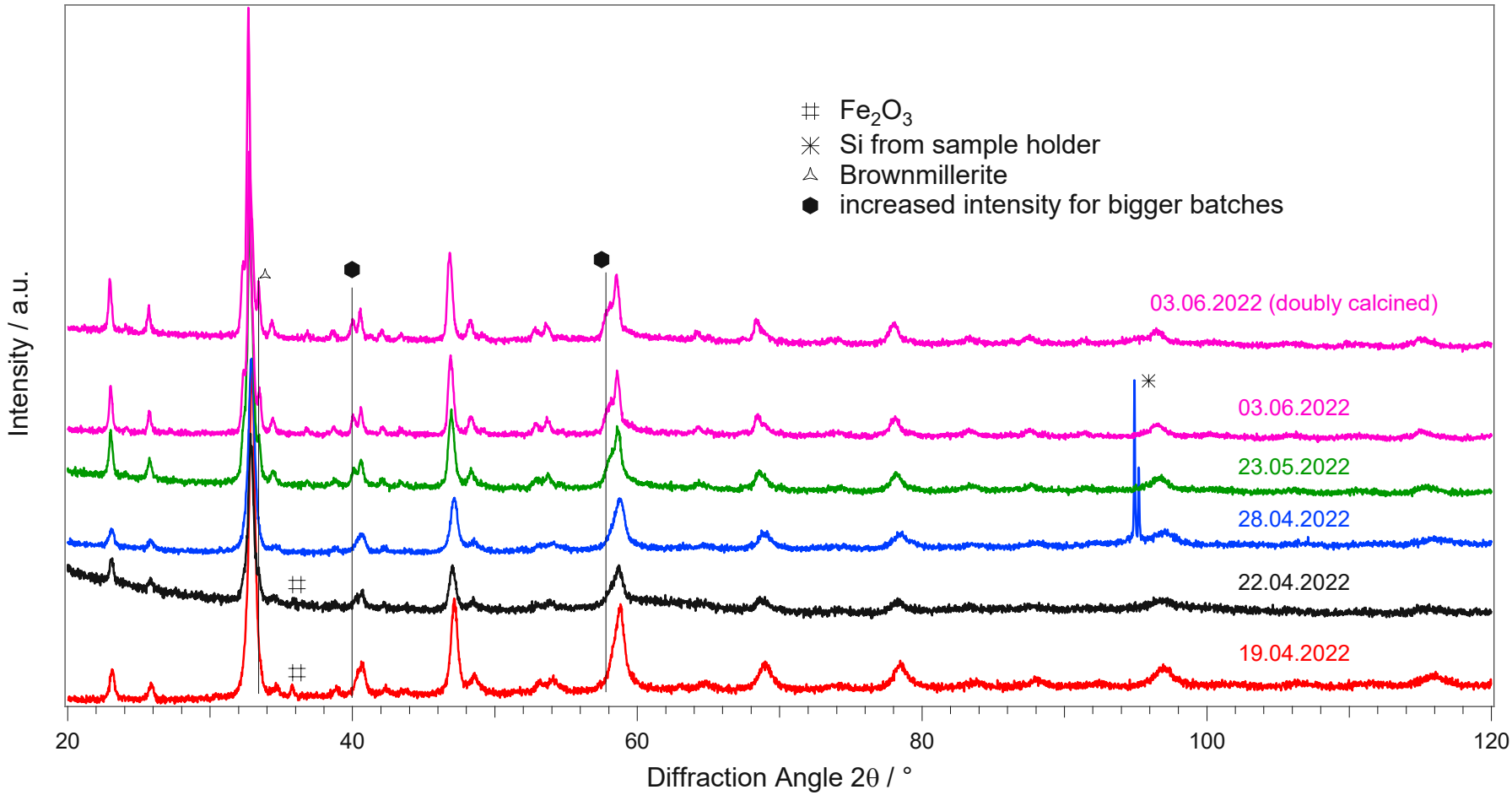

Figure 8: XRDs of first prepared NCF-Co batches, reflexes other than the ones from NCF-Co are indicated

Due to reproducibility reasons, and because the proper equipment (flame spray pyrolysis apparatus) for producing larger amounts of perovskite was not yet available, it was decided to make many Pechini synthesis and combine all batches to a big one. For the preparation of these batches cheaper reagents with lower purity should be used. To still get a good stoichiometry two batches were prepared, one where stochiometric amounts of the educts were used, and one with 10 % excess of Nd_2O_3, because this reagent is hygroscopic and previous synthesis often showed a deficit of Nd and thus formation of Fe_2O_3. Then ICP-OES measurements were conducted by Laura Kronlachner and the new amounts that should be weighed in were calculated. To account for water and other impurities in the educts, 4.85 % excess of Nd_2O_3, 1.46 % deficit of $CaCO_3$ and 12.3 % excess of $Co(NO_3)_2{\cdot}6H_2O$ were used. The details about these two syntheses can be seen in Table 5, the XRDs in Figure 9 and the results of the ICP-OES measurement in Table 6.

Table 5: synthesis details of the batches used for calculation of the amounts of educts

Batch name	Amount Nd_2O_3 (g)	Amount $CaCO_3$ (g)	Amount Fe (g)	Amount $Co(NO_3)_2{\cdot}6H_2O$ (g)	Amount citric acid (g)	Used reagent for: Nd_2O_3; $CaCO_3$, Fe; $Co(NO_3)_2{\cdot}6H_2O$; citric acid; HNO_3	Sintering program (heating rate in °C/min – holding temperature in °C – holding time in h – heating rate in °C/min – holding temperature in °C – holding time in h – cooling rate in °C/min)	Yield (g)
29.06.2022 stochiometric	3.9066	1.5495	1.9453	1.1272	19.6	A;A;A;A;A;A	5-350-0,5-5-800-5-5	7.59
29.06.2022 10 % Nd_2O_3 excess	4.2974	1.5494	1.945	1.1271	19.7	A;A;A;A;A;A	5-350-0,5-5-800-5-5	8.13

Table 6: results of ICP-OES measurements used for calculation of the amounts of educts, mol% only refer to the A-site (for Nd and Ca) or the B-site (for Fe and Co)

Batch name	Fe (mol%)	Co (mol%)	Nd (mol%)	Ca (mol%)	Ratio (Nd+Ca)/(Fe+Co)
stochiometric	0.910 ±0.001	0.090 ±0.001	0.585 ±0.002	0.415 ±0.002	0.989 ±0.004
10 % Nd_2O_3 excess	0.911 ±0.001	0.089 ±0.001	0.607 ±0.001	0.393 ±0.001	1.0400 ±0.003

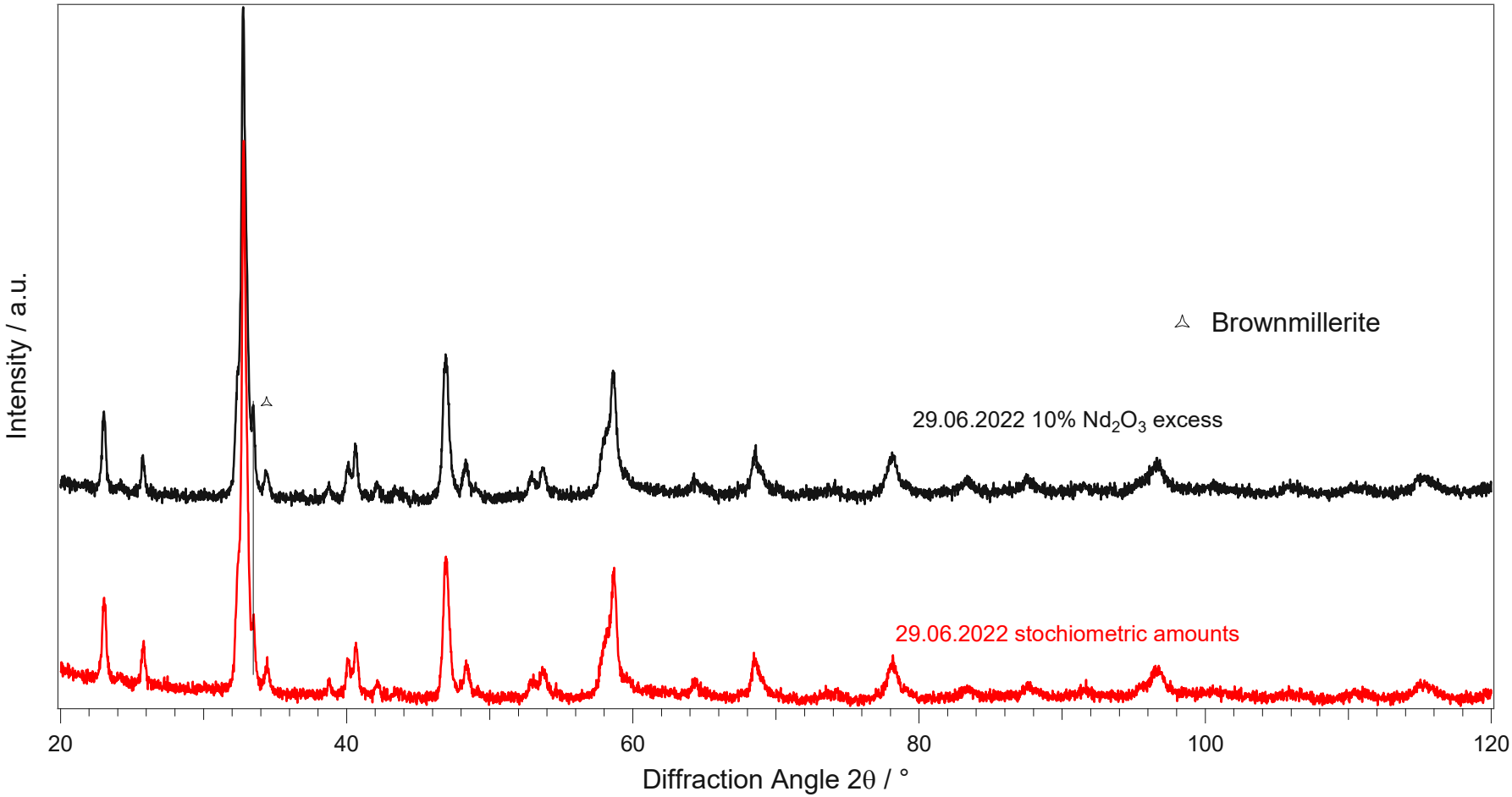

Figure 9: XRDs of first batches prepared with new reagents of less purity, reflexes other than from NCF-Co are indicated

In the next step 17 Pechini syntheses were carried out. The details about the syntheses can be seen in Table 7 and the XRDs in Figure 10.

Table 7: synthesis details of the batches used for combination to one big batch

Batch name	Amount Nd_2O_3 (g)	Amount $CaCO_3$ (g)	Amount Fe (g)	Amount $Co(NO_3)_2 \cdot 6H_2O$ (g)	Amount citric acid (g)	Used reagent for: Nd_2O_3; $CaCO_3$, Fe; $Co(NO_3)_2 \cdot 6H_2O$; citric acid; HNO_3	Sintering program (heating rate in °C/min – holding temperature in °C – holding time in h – heating rate in °C/min – holding temperature in °C – holding time in h – cooling rate in °C/min)	Yield (g)
220705	8.7035	3.2441	4.1332	2.6882	41.6	A;A;A;A;A	5-350-0,5-5-800-5-5	16.8
220706_A	8.7035	3.2442	4.1334	2.6881	41.5	A;A;A;A;A	5-350-0,5-5-800-5-5	16.7
220706_B	8.7032	3.2442	4.1334	2.6882	41.5	A;A;A;A;A	5-350-0,5-5-800-5-5	16.7
220707_A	8.7034	3.2443	4.1333	2.6881	41.5	A;A;A;A;A	5-350-0,5-5-800-5-5	16.7
220707_B	8.7033	3.2443	4.1332	2.6881	41.5	A;A;A;A;A	5-350-0,5-5-800-5-5	16.8
220708_A	9.7287	3.6262	4.6193	3.0046	46.4	A;A;A;A;A	5-350-0,5-5-800-5-5	18.7
220708_B	9.7284	3.6260	4.6195	3.0046	46.5	A;A;A;A;B	5-350-0,5-5-800-5-5	18.9
220711_A	9.7285	3.6260	4.6196	3.0045	46.7	A;A;A;A;B	5-350-0,5-5-800-5-5	18.8
220711_B	9.7284	3.6263	4.6195	3.0041	46.4	A;B;A;A;B	5-350-0,5-5-800-5-5	18.6
220712_A	9.7285	3.6264	4.6197	3.0048	46.6	A;B;A;A;B	5-350-0,5-5-800-5-5	18.8
220712_B	9.7280	3.6258	4.6193	3.0039	46.8	A;B;A;A;B	5-350-0,5-5-800-5-5	18.2
220713_A	9.7286	3.6266	4.6193	3.0048	46.7	A;B;A;A;B	5-350-0,5-5-800-5-5	18.5
220713_B	9.7288	3.6259	4.6195	3.0040	46.7	A;B;A;A;B	5-350-0,5-5-800-5-5	18.7
220714_A	9.7298	3.6267	4.6197	3.0041	46.9	A;A;A;A;B	5-350-0,5-5-800-5-5	18.8
220714_B	9.7285	3.6263	4.6195	3.0045	46.4	A;A;A;A;B	5-350-0,5-5-800-5-5	18.8
220715_A	9.7285	3.6264	4.6193	3.0041	46.7	A;C;A;A;B	5-350-0,5-5-800-5-5	18.7
220715_B	9.7286	3.6266	4.6198	3.0045	46.4	A;C;A;A;B	5-350-0,5-5-800-5-5	18.6

As already seen in previous syntheses a complete phase purity was not reached. A brownmillerite phase could be observed. Reflexes of Fe_2O_3 were absent.

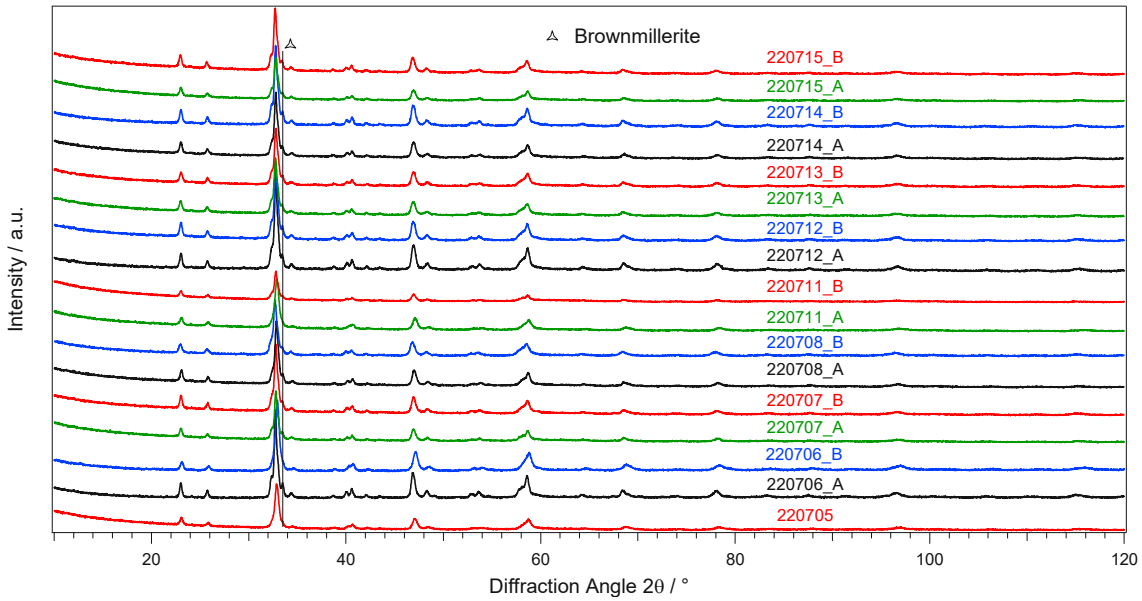

Figure 10: XRDs of batches that were combined to one big batch, reflexes other than from NCF-Co are indicated

In the next step all batches were combined to one big batch and a sieve fraction with grain sizes between 212-425 µm was prepared. The grains that were too big were further ground until mostly all of the batch was in the desired range of the grain size.

The results of an ICP-OES measurement after combination of all batches can be seen in Table 8. The results are not perfect but considering the purity of the used reagents the result is fine. The BET surface area of the combined batch is $4{,}63\ m^2 \cdot g^{-1}$.

Table 8: results of an ICP-OES measurement of the combined batch, mol% only refer to the A-site (for Nd and Ca) or the B-site (for Fe and Co)

Fe (mol%)	Co (mol%)	Nd (mol%)	Ca (mol%)	ratio (Nd+Ca)/(Fe+Co)
0.890 ±0.006	0.107 ±0.000	0.601 ±0.006	0.399 ±0.006	1.002 ±0.002

To roughly determine the wt% of NCF-Co and brownmillerite phase, Rietveld refinements were performed. From the uncombined batches only two Rietveld analyses were performed. For the batch 220706A (Figure 11) the presence of the brownmillerite phase was clearly visible from the XRD. For batch 220706B (Figure 12) it was not clearly apparent that a brownmillerite phase is present, however the Rietveld analysis revealed this phase is present too. Another Rietveld refinement was performed for the combined batch (Figure 13). Measured and refined intensities coincide well.

The following phases were used as a starting point for the Rietveld refinement:

- $NdFeO_3$ (PDF-Code: 04-014-5430) modified to $Nd_{0.6}Ca_{0.4}Fe_{0.9}Co_{0.1}O_3$
- $Ca_2Fe_2O_5$ (PDF-Code: 04-008-6821)

For the combined batch a Rietveld analysis was performed as well. The parameters that were fitted in the Rietveld refinement are:

Global Parameters:

- Specimen Displacement

NCF-Co:

- Scale Factor
- B overall
- Cell Parameter: a, b, c
- Nd: occupancy (0.5-0.7), Ca: occupancy (0.2-0.3)
- B isotropic of all atoms
- Profile Variables: Cagliotti u, Cagliotti v, Cagliotti w, Peak Shape 1, Peak Shape 2, Peak Shape 3

Brownmillerite $Ca_2Fe_2O_5$:

- Scale Factor
- B overall
- Cell Parameter: a, b, c
- Profile Variables: Cagliotti u, Cagliotti v, Cagliotti w, Peak Shape 1, Peak Shape 2, Peak Shape 3

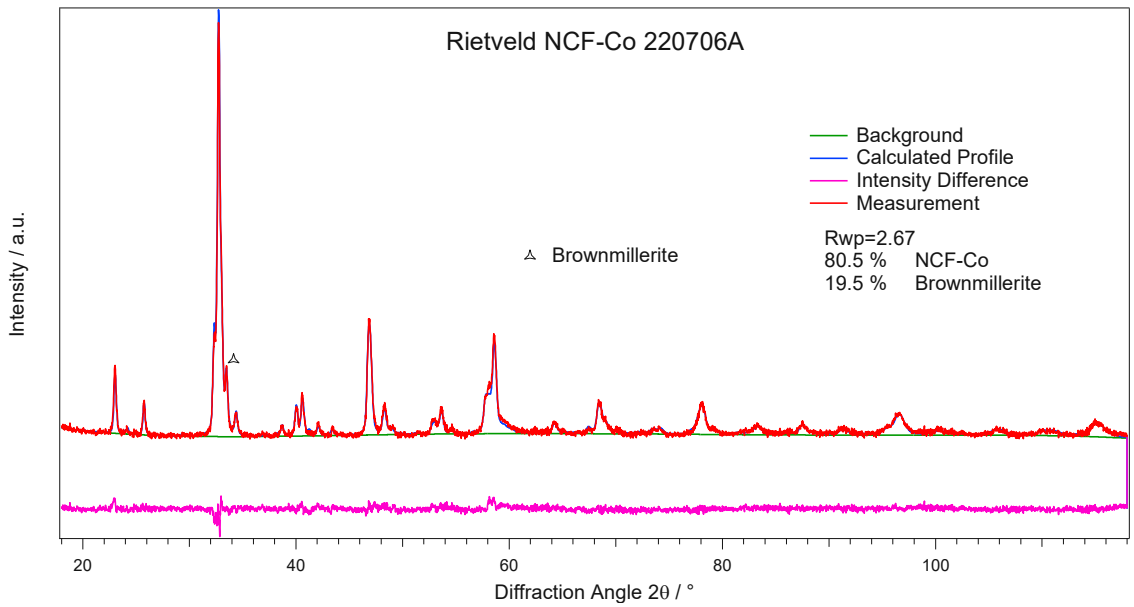

Figure 11: XRD & Rietveld fit of batch 220706A, reflexes other than from NCF-Co are indicated

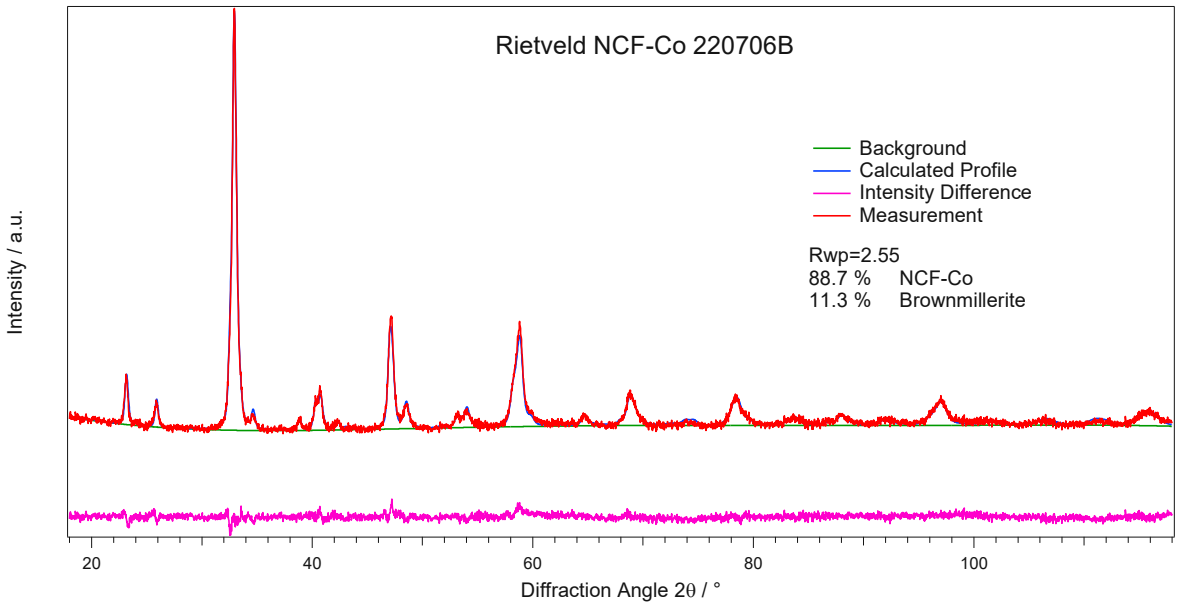

Figure 12: XRD & Rietveld fit of batch 220706B, reflexes other than from NCF-Co are indicated

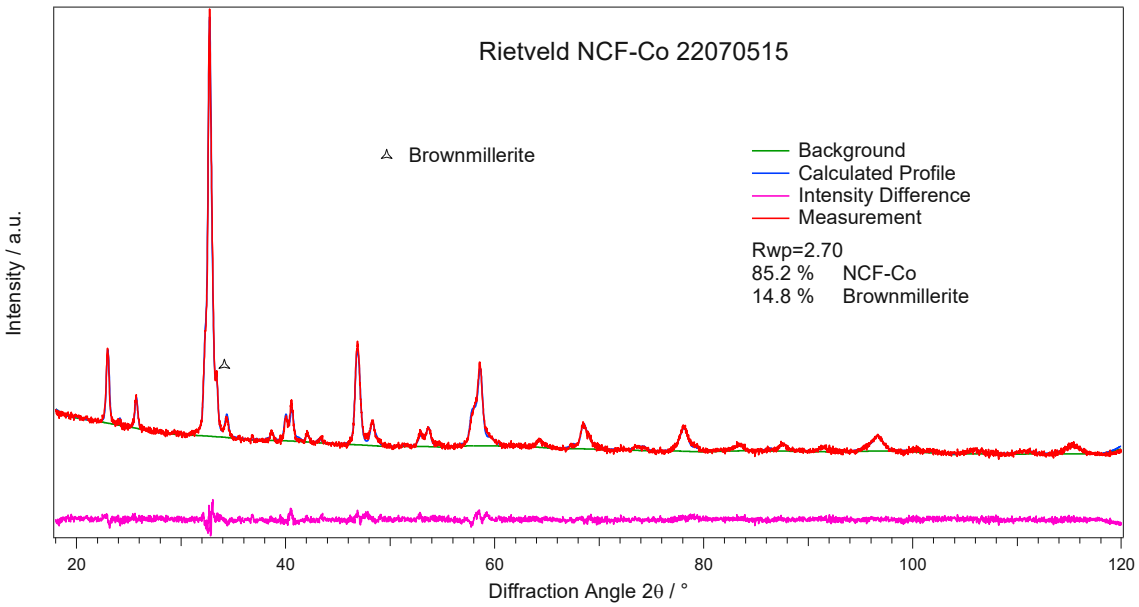

Figure 13: XRD & Rietveld fit of combined batch 05-15.07.2022, reflexes other than from NCF-Co are indicated

4 Pellets

4.1 Preparation

For the preparation of a shaped material that can be used in reactors of larger scale, pelleting and subsequent sintering was employed. To enhance the porosity, which means increased surface area, the porogens graphite and starch were used. It was tried to use Al_2O_3 as a carrier for the catalyst. The mixture used for pelleting was ground in a mortar. For pressing the pellets $300\ \mathrm{mg}$ material was used in total and the pellets were compressed with 0.5 tons for 10 minutes. The diameter of the matrix was $8.9\ \mathrm{mm}$. Before sintering the pellets were split into smaller pieces with a blade so that the split pellet pieces could fit in the tube of the reactor. The pellet presses that were used can be seen in Figure 14, the matrix used for tableting in Figure 15.

Figure 14: used presses for the preparation of the pellets

Figure 15: used matrix for the preparation of the pellets

The reagents used for the preparation of the pellets can be seen in Table 9.

Table 9: reagents used for preparation of the pellets

Reagent	Description	Supplier
Al_2O_3	PURALOX SBa200	Sasol
Al_2O_3	Aluminumoxide 90 active Acid (activity level I) Grain size 0.063-0.200 mm 70-230 mesh for column chromatography	Merck
Starch	Starch soluble A.R.	Riedel de haën
Graphite	Graphite, powder 1-2 microns, synthetic	Sigma Aldrich

The non-organic educts were characterized with XRD before and after sintering at 1150 °C, the organic educts just before sintering and it was checked if they are present after calcining.

In Figure 16 the XRDs of Al_2O_3 "PURALOX SBa200" before and after heat treatment can be seen. This reagent was only used for one pellet, because previous work of a colleague on pellet preparation was done with a different Al_2O_3 and for reasons of comparability another reagent was used instead (see below). Before heat treatment the Al_2O_3 was identified to be in the γ-phase with apparently small particle size, hence the broad reflexes. The Al_2O_3 phase after heat treatment could be identified as Θ-Al_2O_3.

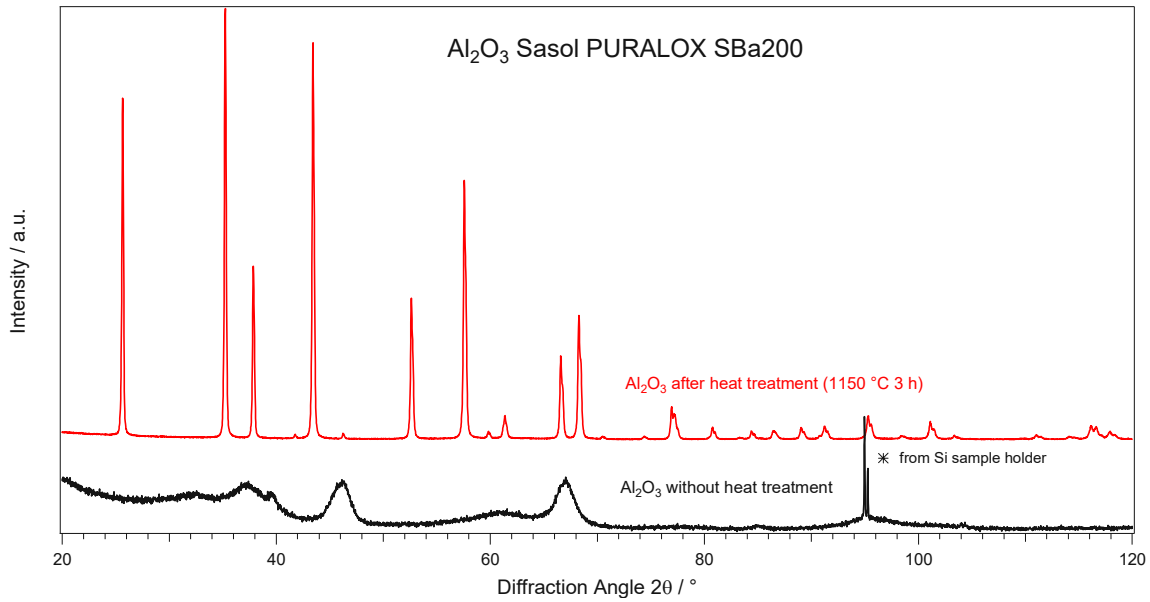

Figure 16: XRDs of Al_2O_3 "Sasol PURALOX SBa200" before and after heat treatment

In Figure 17 the XRDs of Al_2O_3 "90 active" before and after heat treatment can be seen. Before heat treatment the Al_2O_3 was identified as a mixture of γ-phase with apparently small particle size, hence the broad reflexes, and Θ-Al_2O_3 (narrow reflexes). The Al_2O_3 phase after heat treatment could be identified as Θ-Al_2O_3.

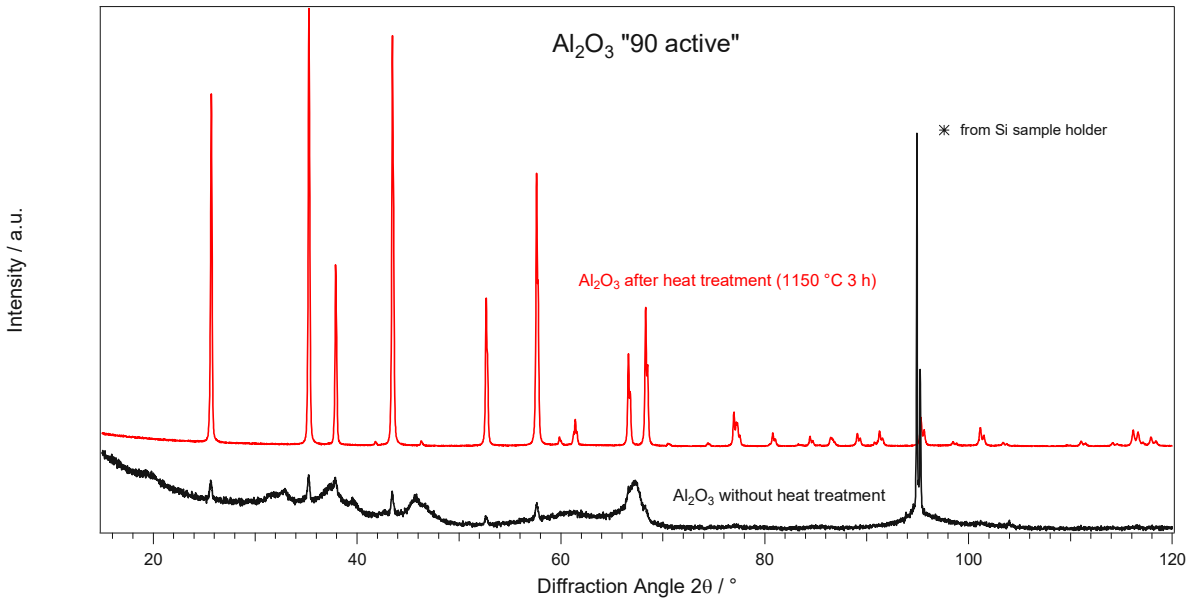

Figure 17: XRDs of Al_2O_3 "90 active" before and after heat treatment

The colors of both Al_2O_3 before heat treatment were white. After heat treatment at 1150 °C for 3 hours the color of Al_2O_3 "90 active" changed to yellow. This happened most likely due to an iron impurity.

Figure 18: left: Al_2O_3 "Sasol PURALOX SBa200" after heat treatment (1150 °C) without change of color; right: Al_2O_3 "90 active" after heat treatment (1150 °C) with clearly visible yellow coloring

In Table 10 and Table 11 an overview of all prepared pellets can be seen. The holding time at 550 °C for pellets with organic additives was always 0.5 hours and as heating and cooling rates always 5 °C/min were used.

Table 10: overview of the prepared pellets, continued on next page

Starting Date	Pellet Name	Composition	Sintering Program
11.04.2022	PEL_012	60 % NCF-Co (Batch 06.01.2022) 40 % Al_2O_3 (Sasol PURALOX SBa200)	1150 °C, 3H (11.04.2022)
14.04.2022	PEL_013	80 % NCF-Co (Batch 30.11.2021 Stelios) 20 % Graphite	1150 °C, + holding at 550 °C, 3H (14.04.2022)
20.04.2022	PEL_014	60 % NCF-Co (Batch 30.11.2021 Stelios) 40 % Al_2O_3 (90 active)	1150 °C, 3H (20.04.2022)
20.04.2022	PEL_015	60 % NCF-Co (Batch 30.11.2021 Stelios) 40 % Al_2O_3 (90 active)	1100 °C, 12H (22.04.2022)
21.04.2022	PEL_016	70 % NCF-Co (Batch 30.11.2021 Stelios) 30 % Graphite	1150 °C, + holding at 550 °C, 3H (25.04.2022)
21.04.2022	PEL_017	90 % NCF-Co (Batch 30.11.2021 Stelios) 10 % Graphite	-
29.04.2022	PEL_018	90 % NCF-Co (Batch 30.11.2021 Stelios) 10 % Graphite	1150 °C, + holding at 550 °C, 3H (02.05.2022)
02.05.2022	PEL_019	60 % NCF-Co (Batch 28.04.2022 Richard) 40 % Al_2O_3 (90 active)	1150 °C, + holding at 550 °C, 3H (02.05.2022)
03.05.2022	PEL_020	80 % NCF-Co (Batch 28.04.2022 Richard) 20 % Starch	1150 °C, + holding at 550 °C, 3H (04.05.2022)
03.05.2022	PEL_021	70 % NCF-Co (Batch 28.04.2022 Richard) 30 % Starch	1150 °C, + holding at 550 °C, 3H (05.05.2022)
05.05.2022	PEL_022	90 % NCF-Co (Batch 28.04.2022 Richard) 10 % Graphite	1150 °C, + holding at 550 °C, 3H (05.05.2022)
05.05.2022	PEL_023	70 % NCF-Co (Batch 28.04.2022 Richard) 30 % Graphite	1150 °C, + holding at 550 °C, 3H (05.05.2022)
09.05.2022	PEL_024	80 % NCF-Co (Batch 28.04.2022 Richard) 20 % Graphite	1150 °C, + holding at 550 °C, 3H (13.05.2022)
09.05.2022	PEL_025	90 % NCF-Co (Batch 28.04.2022 Richard) 10 % Starch	1150 °C, + holding at 550 °C, 3H (13.05.2022)
27.05.2022	PEL_026	90 % NCF-Co (Batch 23.05.2022 Richard) 10 % Graphite	700 °C, + holding at 550 °C, 3H (27.05.2022)

Table 11: overview of the prepared pellets, continuation from previous page

Starting Date	Pellet Name	Composition	Sintering Program
27.05.2022	PEL_027	90 % NCF-Co (Batch 23.05.2022 Richard) 10 % Starch	700 °C, + holding at 550 °C 3H (27.05.2022)
30.05.2022	PEL_028	80 % NCF-Co (Batch 23.05.2022 Richard) 20 % Graphite	700 °C, + holding at 550 °C 3H (02.06.2022)
31.05.2022	PEL_029	80 % NCF-Co (Batch 23.05.2022 Richard) 20 % Starch	700 °C, + holding at 550 °C 3H (02.06.2022)
15.06.2022	PEL_030	70 % NCF-Co (Batch 23.05.2022 Richard) 30 % Starch	700 °C, + holding at 550 °C 3H (17.06.2022)

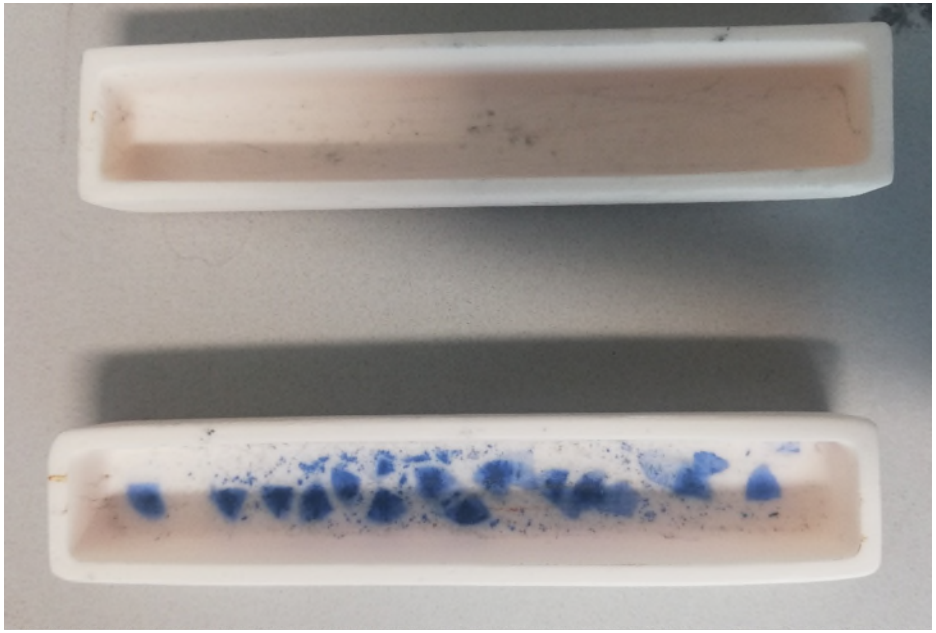

Figure 20: blue coloring of the alumina crucible after sintering pellets at 1150 °C in it

When sintering pellets in a new alumina crucible, a blue coloring of the crucible was observed (Figure 20). Since cobalt is part of the perovskite, it is most likely cobalt blue. In Figure 19 an example of a pellet can be seen.

Figure 19: example of some pieces of a pellet (PEL_027)

4.2 XRDs of the Pellets

The pellets were characterized with XRD. In Figure 21, Figure 22 and Figure 23 the XRDs of pellets 012, 013 and 014 can be seen. Reflexes of a phase that do not correspond to Al_2O_3 or the pure NCF-Co powder appeared most dominantly. This phase was identified to be $CaCO_3$, but is not part of the pellets. This phase comes from the kneading mass used for the sample preparation in XRD. The XRD samples for these three pellets were prepared by putting the pellets into the kneading mass. As it was found out later, $CaCO_3$ is used as a filler in the kneading mass and is thus visible in the XRDs.

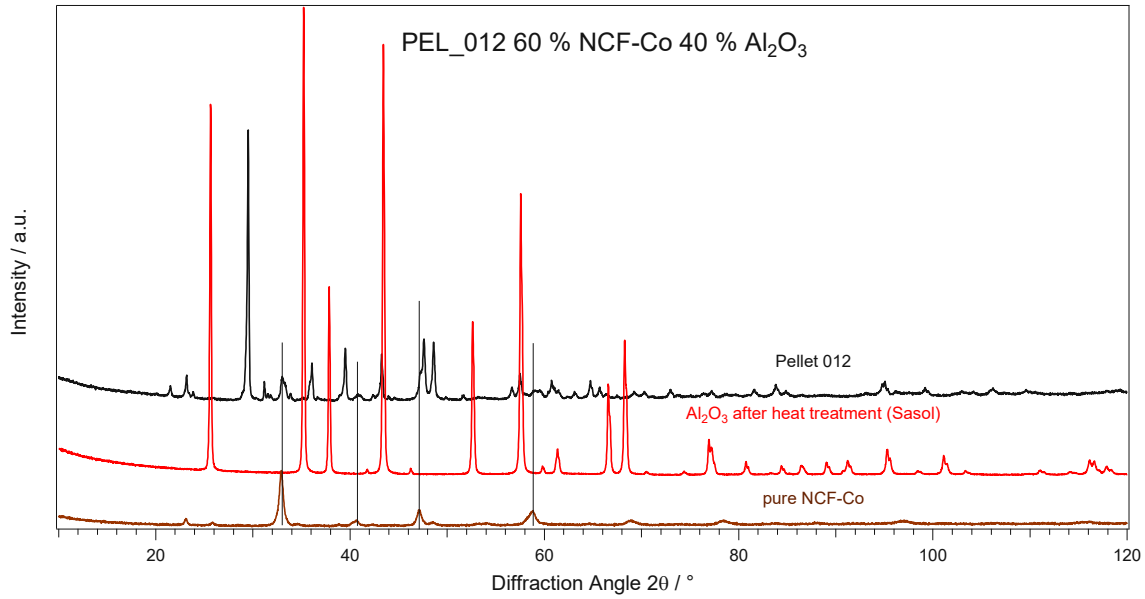

Figure 21: XRD of Pellet 012, besides NCF-Co and Al_2O_3 reflexes all reflexes of the pellet correspond to $CaCO_3$

In the XRD of Pellet 013, additionally to the Al_2O_3 reflexes another small reflex at 26.8° appears which could be from graphite or some impurity of the kneading mass.

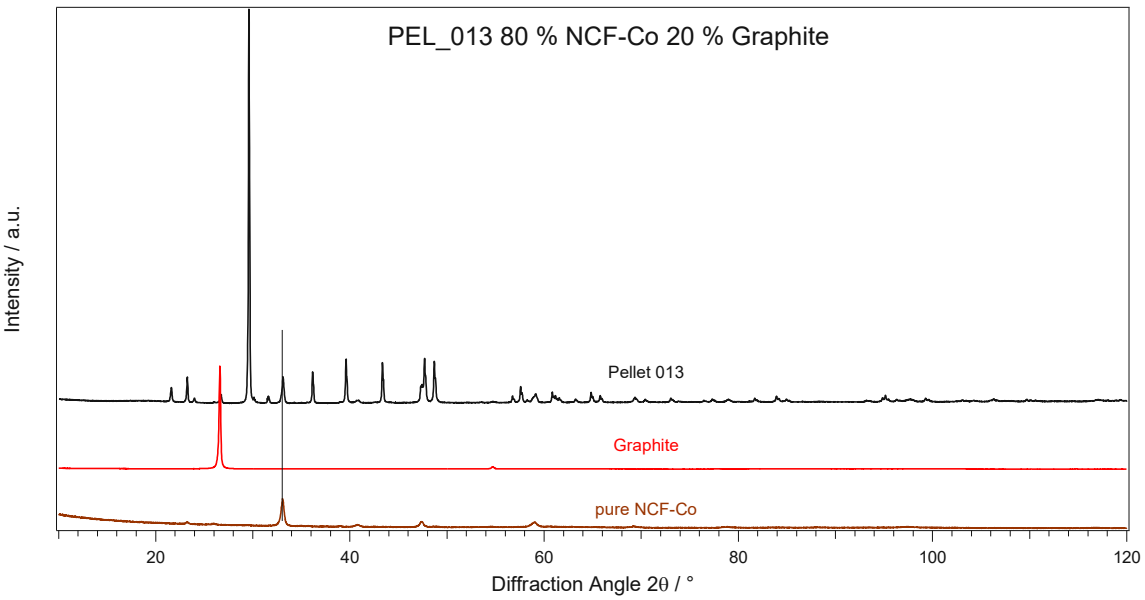

Figure 22: XRD of Pellet 013, besides NCF-Co and graphite reflexes all reflexes of the pellet correspond to $CaCO_3$

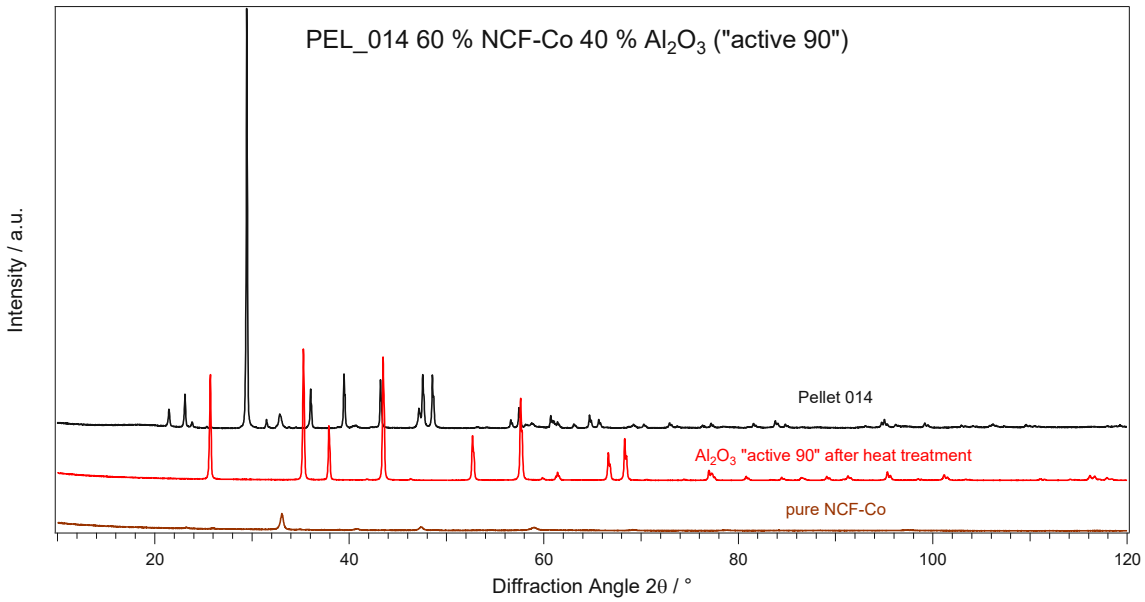

Figure 23: XRD of Pellet 014, besides NCF-Co reflexes all reflexes of the pellet correspond to $CaCO_3$

Because of the dominant presence of $CaCO_3$ in the XRDs the sample preparation was changed. With a spatula some small particles were scratched off the pellet and put on the Si single crystal sample holder. In Figure 24 the XRD of Pellet 013 can be seen. Only reflexes of NCF-Co are visible, graphite is not visible. It must be kept in mind, that only small signals were obtained by scratching some small particles off the pellet. As it can be seen in Figure 22 a small reflex from graphite may still be left.

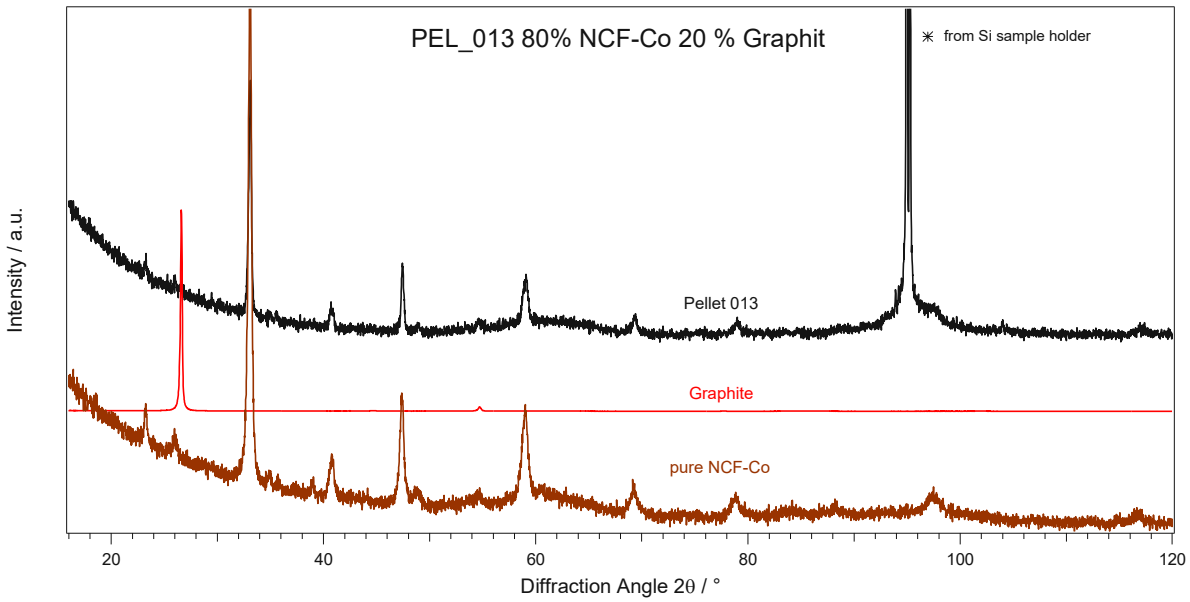

Figure 24: XRD of Pellet 013, all reflexes correspond to the phase as designated, Pellet 013 consists only of the NCF-Co phase

In Figure 25 XRDs of pellets 014, 015 and 019 can be seen. The most dominant reflexes come from NCF-Co, besides these reflexes, there are reflexes of another phase, but not the same as the ones of Al_2O_3 after heat treatment. Since later it was decided not to continue the work on pellets like this, the identification of this phase has not been done.

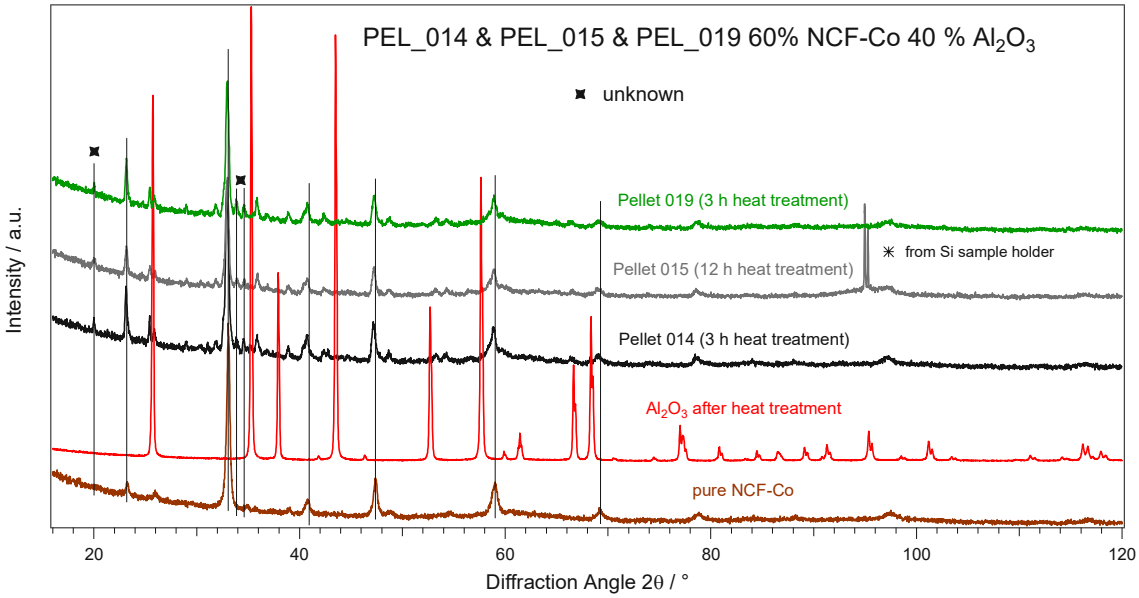

Figure 25: XRDs of pellets 014, 015 and 019, reflexes correspond to the phase as denoted, pellets consist of NCF-Co and other unidentified phases

In Figure 26 the XRD of Pellet 016 can be seen. Only reflexes of NCF-Co are visible, graphite, as expected, is not present anymore.

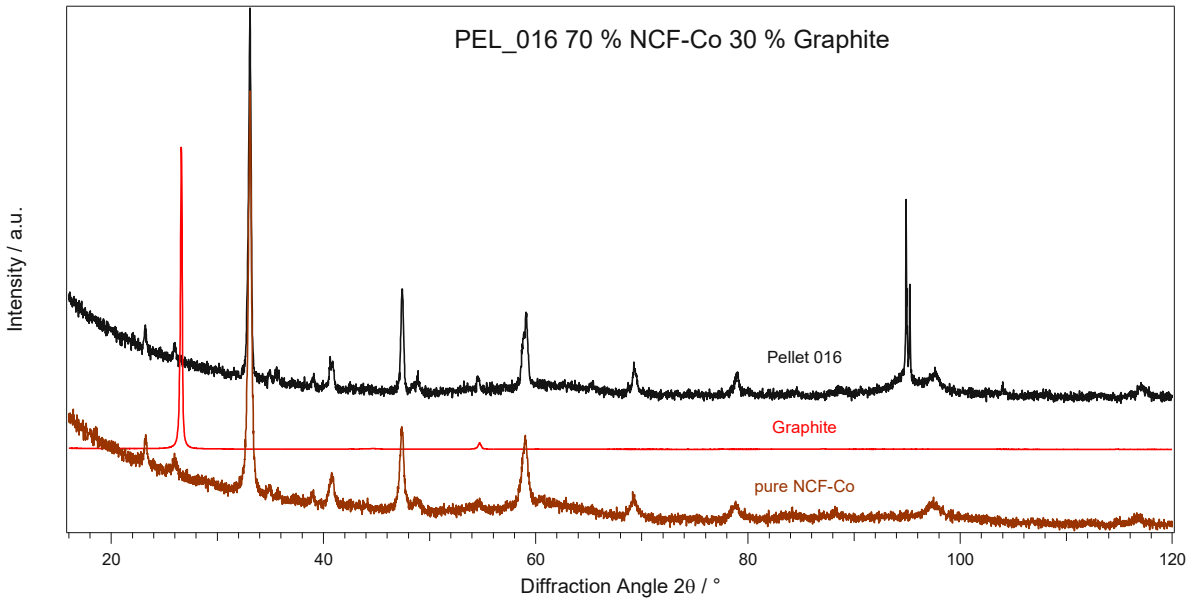

Figure 26: XRD of pellet 016, reflexes correspond to the phase as denoted, pellet 016 consists only of NCF-Co

In Figure 27 the XRDs of pellets 020, 021 and 025 can be seen. Reflexes of NCF-Co are visible, graphite, as expected, is not present anymore, however for pellet PEL_023 (80 % NCF-Co 20 % Graphite) $CaCO_3$ is visible at 29.5°. The reflexes of the pellets are shifted a bit to the left. This indicates smaller lattice parameters which could be a result of less oxygen vacancies and more Fe^{4+}.

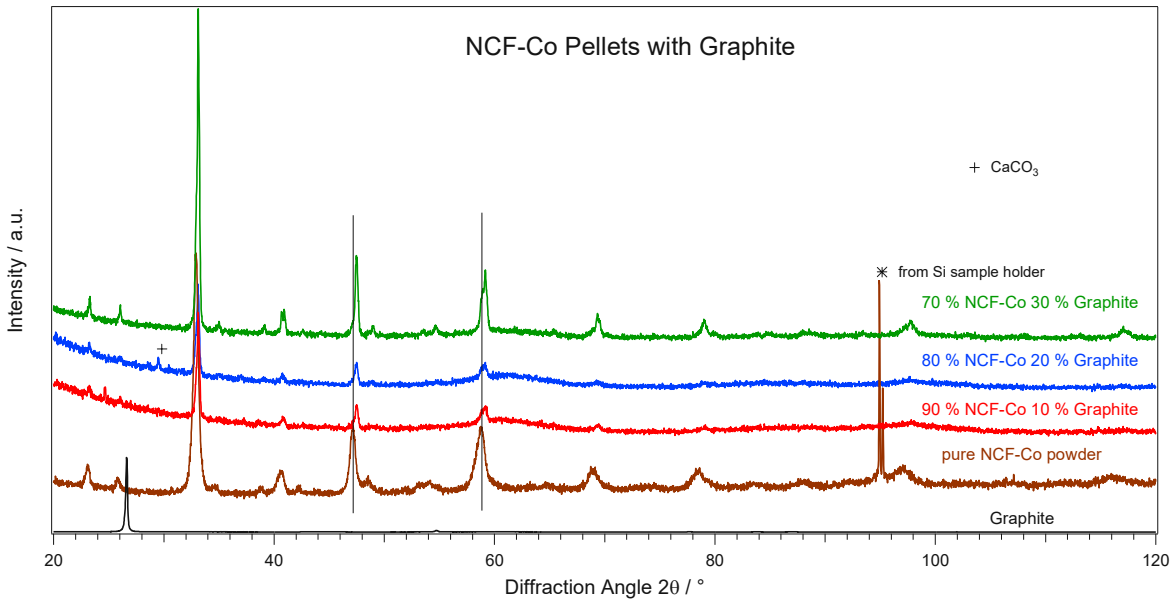

Figure 27: XRDs of pellets 022, 023 and 024, reflexes correspond to the phase as denoted, pellets consist only of NCF-Co if not indicated differently

In Figure 28 the XRDs of pellets 020, 021 and 025 can be seen. Reflexes of starch are not visible. Hence full decomposition of starch can be assumed. For pellets with 30 % starch also CaO and Fe are visible which means that Fe of NCF-Co is reduced to its metallic form and Ca is eliminated from the structure and can be seen as CaO in the diffractogram.

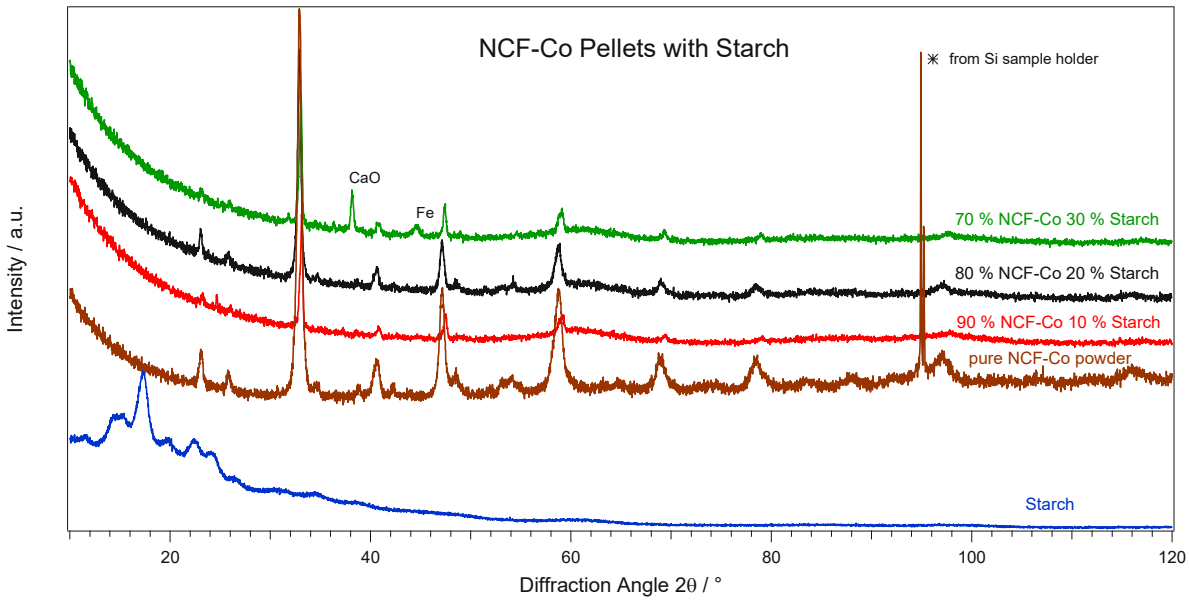

Figure 28: XRDs of pellets 020, 021 and 025, reflexes correspond to the phase as denoted, reflexes of the pellets correspond to NCF-Co if not indicated differently

4.3 BET Measurements

Measurements of the BET surface area of the pellets were tried but not successful due to the lack of a turbo pump, the lack of proper maintenance of the BET-device and probably low surface area of the pellets. Since it was decided not to continue the work with this type of pellets, measurements were not repeated and as normalization in the catalytic tests just the mass of the catalyst was used.

4.4 Mechanical Stability

A proper device for testing the mechanical stability of the pellets was not available. Nevertheless, when testing the hardness of the pellets with a spatula it was found that higher content of NCF-Co and higher sintering temperatures increased the stability. Generally speaking, the mechanical stability was very low without the use of a binder, whereas pellets with Al_2O_3 were generally of higher hardness.

4.5 Catalytic Measurements

Catalytic measurements were carried out with the equipment as described in the method section.

4.5.1 Experimental Parameters

About 20-40 mg of a catalyst pellet were used for the catalytic experiments (exact values can be seen in the appendix). Prior to the catalytic test itself, an oxygen pretreatment was conducted.

4.5.1.1 Temperature Program

For the oxidation prior to the catalytic experiment a temperature of 600 °C was used (30 min holding time). For the catalytic experiment a ramp from 400-700 °C with a heating rate of 1 °C/min was applied.

4.5.1.2 Volumetric Flows

During the oxidation, a flow of $10\ \mathrm{NmL \cdot min^{-1}}$ of O_2 was used.

The following volumetric flows of the gases were used during the reactions:

- CO_2: $6\ \mathrm{NmL \cdot min^{-1}}$
- H_2: $6\ \mathrm{NmL \cdot min^{-1}}$
- Ar: $12\ \mathrm{NmL \cdot min^{-1}}$

For flushing the reactor, a flow of $10\ \mathrm{NmL \cdot min^{-1}}$ of Ar was used.

4.5.2 Results and Discussion

In order to compare the results, the specific activity was used. The specific activity was calculated according to formula 4. As normalization the mass of weighed in catalyst was used. The results of all measured pellets can be seen in Figure 29.

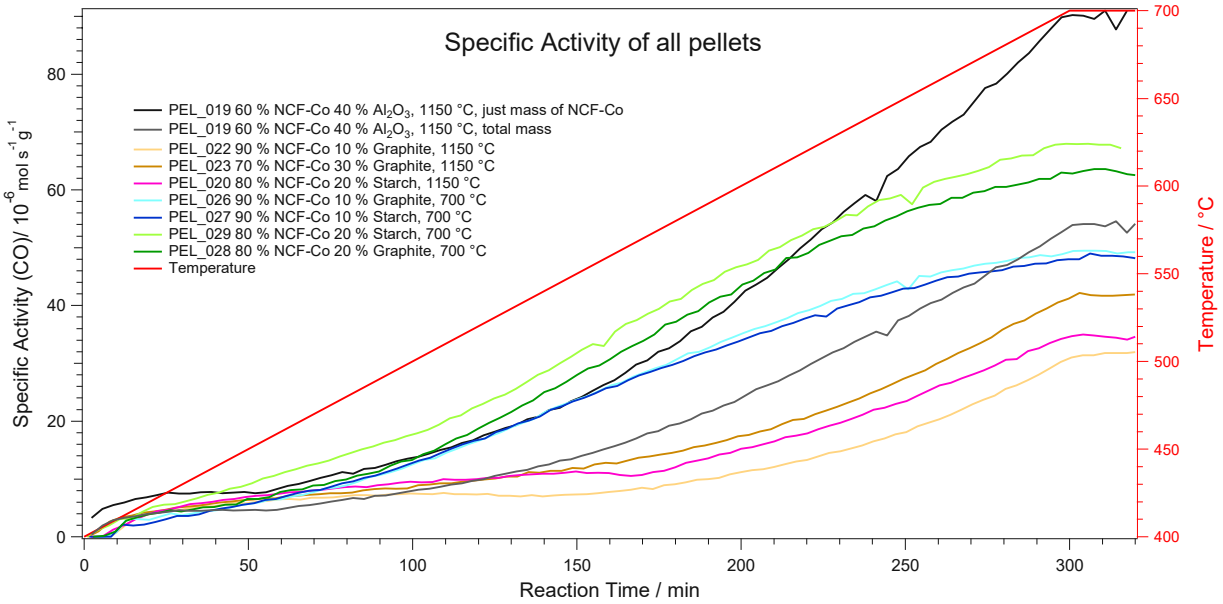

Figure 29: results of the catalytic experiments, specific activity and temperature versus reaction time, the specific activity was calculated from produced CO

As expected, with increasing temperature the specific activity also increases. This is due to better kinetics and better thermodynamics at higher temperatures. Furthermore, it was revealed that a higher content of organic material in the starting material used for the preparation of the pellets and a lower sintering temperature increase the activity. The reason for both trends might be the surface area. A lower sintering temperature as well as a higher content of organic material lead to higher surface areas. The activity of the pellet with Al_2O_3 seems to be better than the one of pellets without this binder (but sintered at the same temperature) even when the total mass was used as normalization. If only the mass of NCF-Co is used as normalization for the alumina pellet then it performs even better than the pellets sintered at 700 °C.

5 Pellets with Alumina Hydrates

For the preparation of pellets with alumina hydrates, the alumina hydrates boehmite and bayerite, which were provided from Sasol, were used. Technical details of these reagents can be seen in Table 12.

Table 12: chemical and physical properties of the used alumina hydrates [13]

Typical chemical and physical properties	PURAL SB (Boehmite)	PURAL BT (Bayerite)
Al_2O_3 (%)	74	64
Na_2O (%)	0.002	0.002
Loose bulk density (g/l)	600-850	500-700
Packed bulk density (g/l)	800-1100	600-800
Particle size (d50) (µm)	45	5-10
Surface area (BET)[1] (m^2/g)	250	360[2]
Pore volume[1] (ml/g)	0.50	0.30[2]
Crystallite size (120) (nm)	5.0	40[3]

5.1 Preliminary experiments

At first experiments with pure alumina precursors were made. XRDs of the precursors were measured. The results and performed Rietveld refinements can be seen in Figure 30 and Figure 31 for bayerite and boehmite respectively. Measured and calculated diffractograms do not coincide so well. A better agreement could be obtained by using more fitting parameters, but the intention here was only the identification of the phase itself. The following phases were used as a starting point for the Rietveld refinement:

- Boehmite (PDF-Code: 01-074-2898)
- Bayerite (PDF-Code: 01-074-1119)

The parameters that were fitted in the Rietveld refinement are:

Global Parameters:

- Specimen Displacement

Alumina hydrate phase:

- Scale Factor
- B overall
- Cell Parameter: a, b, c
- B isotropic of all atoms
- Profile Variables: Cagliotti u, Cagliotti v, Cagliotti w, Peak Shape 1, Peak Shape 2, Peak Shape 3

[1] After activation at 550 °C for 3 hours
[2] After activation at 350 °C for 3 hours
[3] (331) reflection

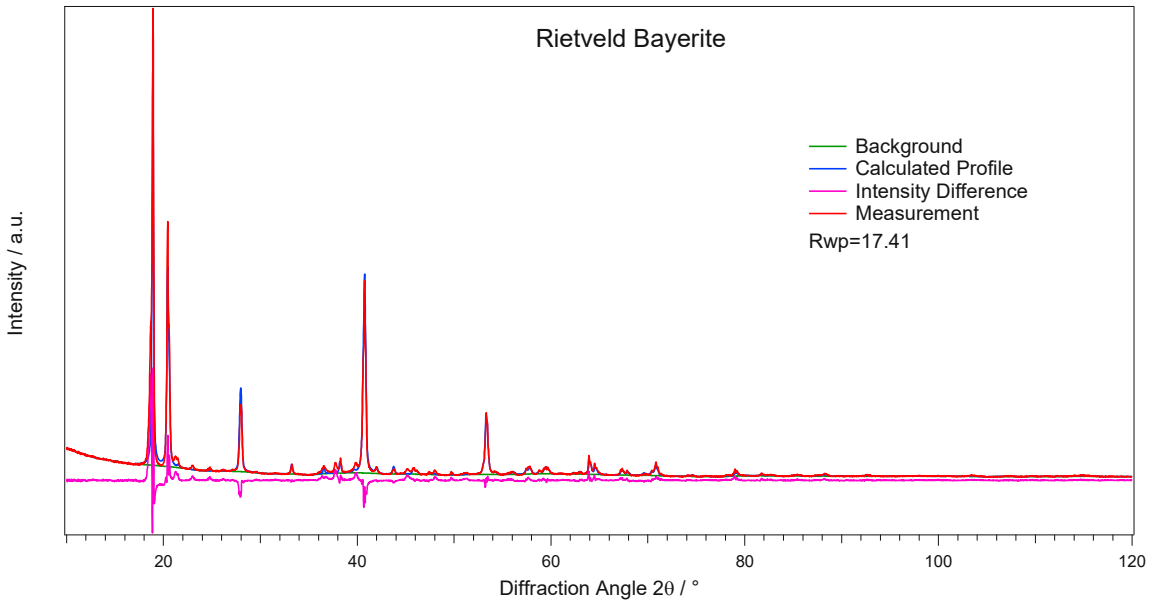

Figure 30: XRD with Rietveld refinement of bayerite

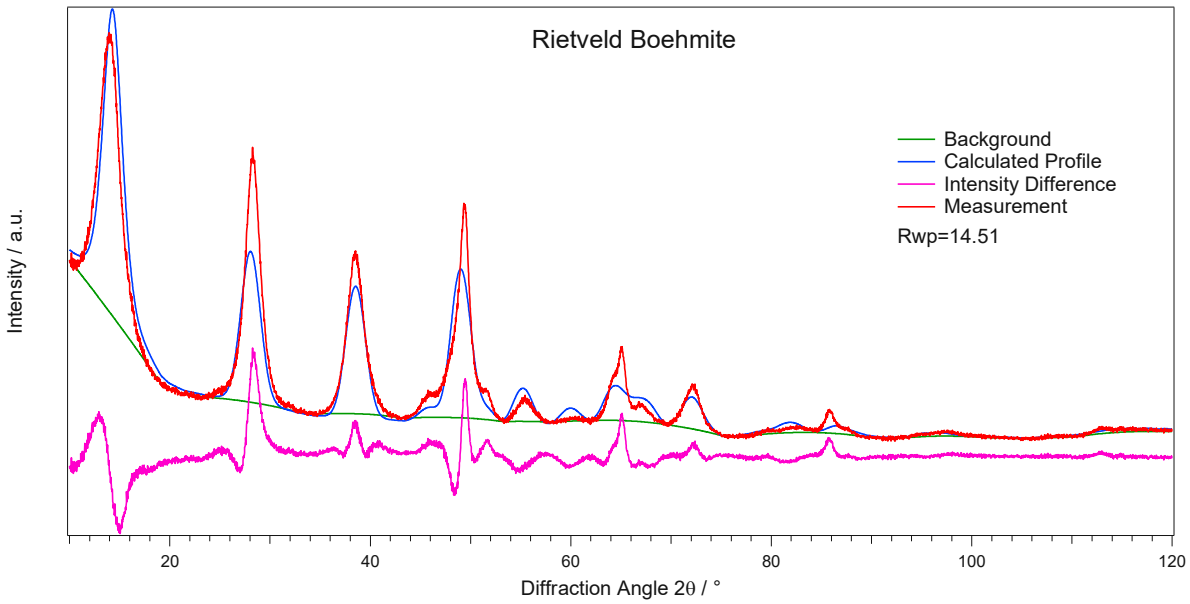

Figure 31: XRD with Rietveld refinement of boehmite

For pelleting, the same matrix as before with a diameter of $8.9\ \mathrm{mm}$ was used. The pellets were only pressed for $20\text{-}30\ \mathrm{seconds}$ this time. The thickness of the pellets was measured in dependence of the pressure and the mass. The results can be seen in Figure 32 and Figure 33. In general, lower pressure leads to thicker pellets. This is especially pronounced for boehmite pellets pelleted with $0.125\ \mathrm{tons}$. Furthermore it can be said that from 100 up to $400\ \mathrm{mg}$ the thickness correlates linearly with mass except for $0.125\ \mathrm{tons}$ with bayerite, here the $400\ \mathrm{mg}$ pellets are thicker. The reason for that might be an inhomogeneous pressure distribution in the material.

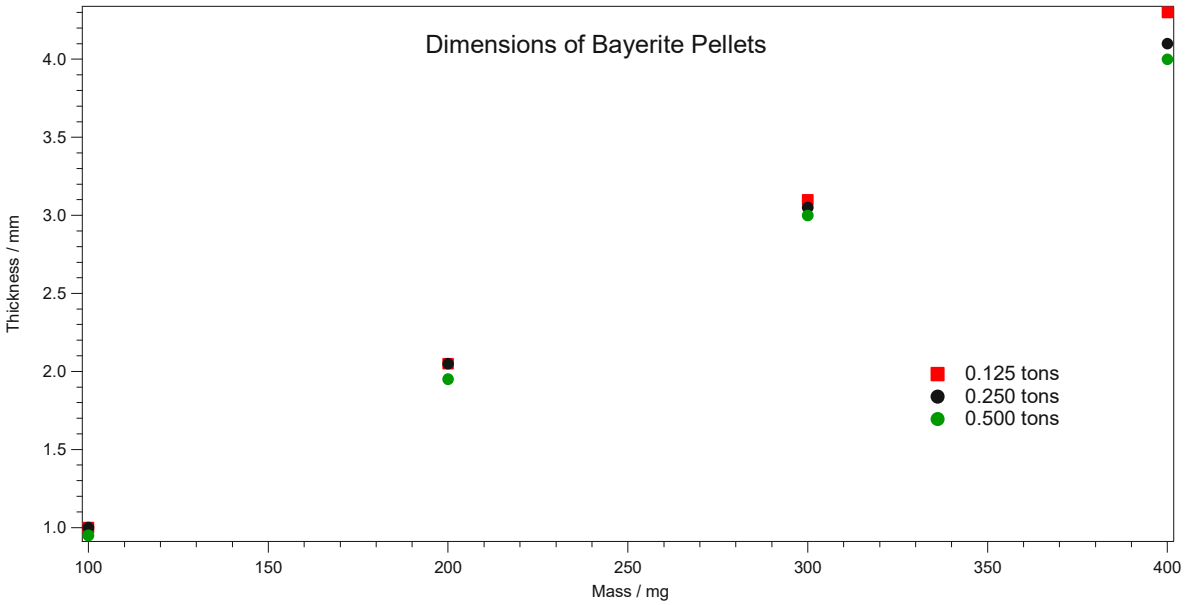

Figure 32: dimensions of bayerite pellets for different pressures

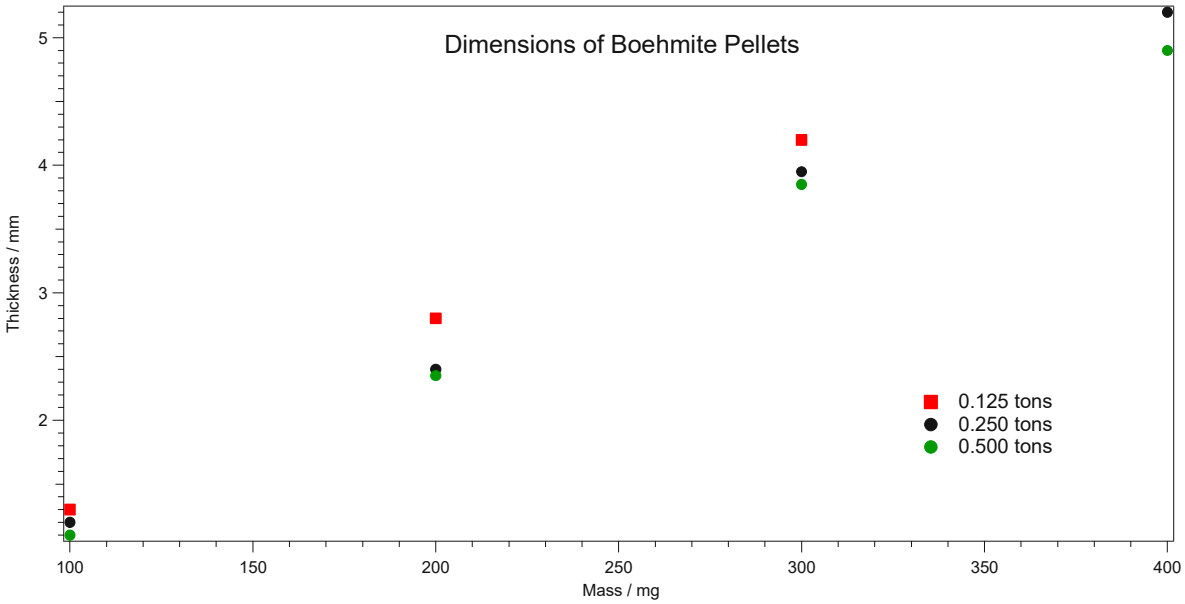

Figure 33: dimensions of boehmite pellets for different pressures

For the further pelleting always a pressure corresponding to 0.5 tons and a mass of 400 mg was used. Due to reasons of the time-consuming pelleting process and not infinite availability of NCF-Co only 3-5 pellets were prepared, which does not give a very good statistic. With the device depicted in Figure 34 the hardness of the pellets was tested for the green pellets (no sintering, 25 °C) as well as for pellets sintered at different temperatures.

Figure 34: tablet hardness tester type: „Pfizer"

In Figure 35 and Figure 36 the results of the hardness tests are graphically depicted in the way of minimum and maximum value that was measured. Only the pellets made from boehmite gave reasonable strength (Figure 35). The strength after sintering was higher, with the best values at sintering temperatures of 700 °C. Bayerite pellets on the other hand were even weaker after sintering (Figure 36). This is probably because for these pellets more water is eliminated from the structure hence more shrinkage and not sufficient contact between the particles. Higher pelleting pressures, which would probably lead to better contact between particles, than 0.5 tons were not possible due to safety reasons but would have probably given higher strengths of the pellets.

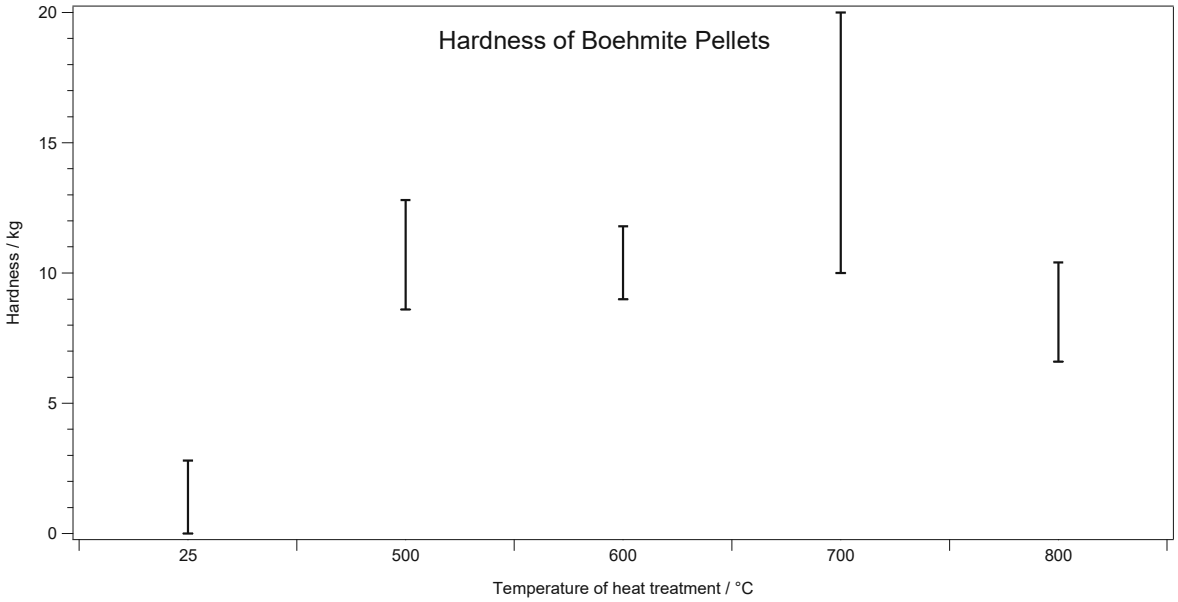

Figure 35: hardness of boehmite pellets after sintering at different temperatures

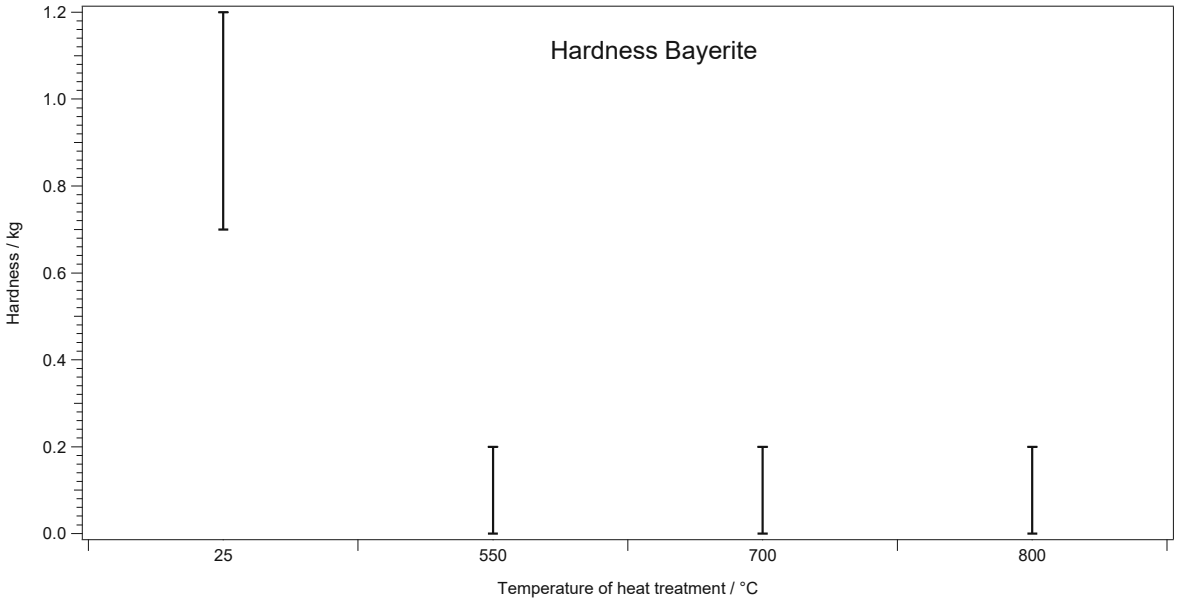

Figure 36: hardness of bayerite pellets after sintering at different temperatures

After testing with pure alumina hydrates it was tried to mix boehmite with NCF-Co and again test the hardness of the pellets before and after sintering. As sintering temperature 700 °C was chosen. Pellets with weight ratios boehmite/NCF-Co of 0/100, 20/80, 50/50, 80/20 and 100/0 were prepared for the hardness tests. The results of the hardness tests can be seen in Figure 37. It was found that higher boehmite content increases the strength of the green as well as the strength of the sintered pellets. Some green pellets 100/0 also showed minor strength.

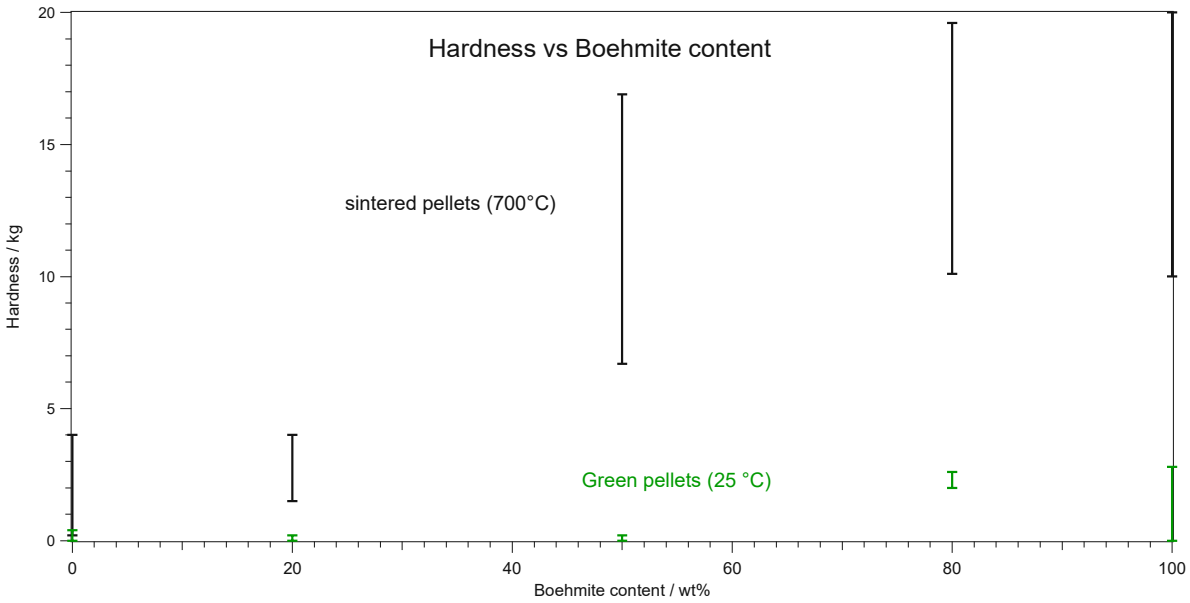

Figure 37: hardness of boehmite/NCF-Co pellets versus boehmite content for green pellets and sintered pellets (700 °C)

5.2 Preparation of Pellets for Catalytic Testing

For catalytic testing, sieve fractions (212-425 µm) of pellets with weight ratios boehmite/NCF-Co of 0/100, 50/50, 80/20 and 100/0 were prepared via crushing the pellets with a pistill in a mortar before sintering and subsequent sieving with a sieve tower (Figure 37). Some examples of how the sieve fractions look like can be seen in Figure 39 and Figure 40.

Figure 38: sieve tower used for preparation of the sieve fractions

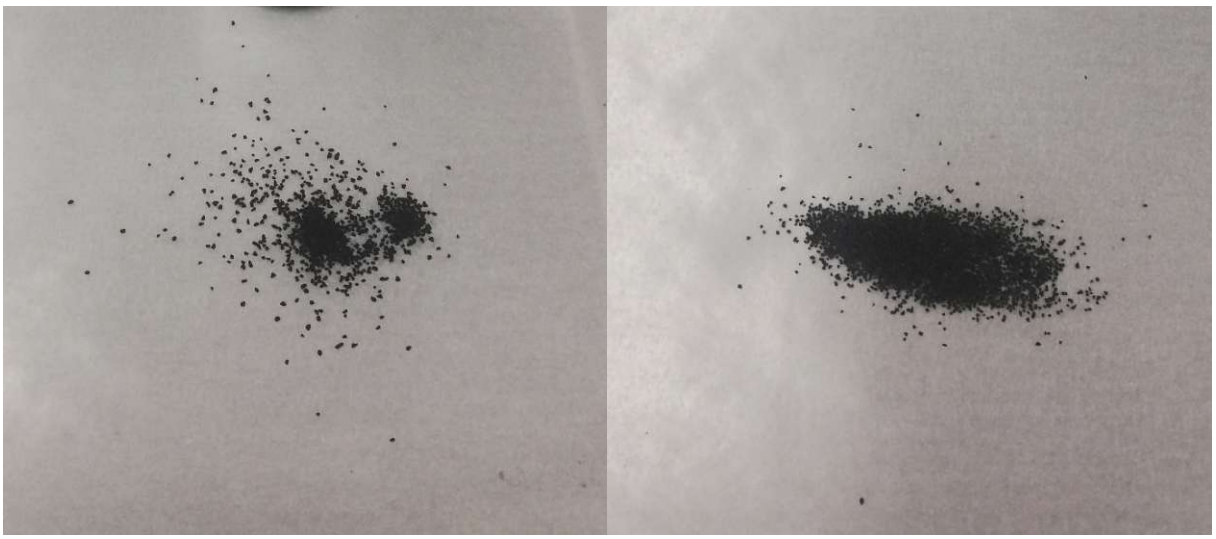

Figure 39: sieve fraction 212-425 µm; left: 0/100 boehmite/NCF-Co; right: 80/20 boehmite/NCF-Co

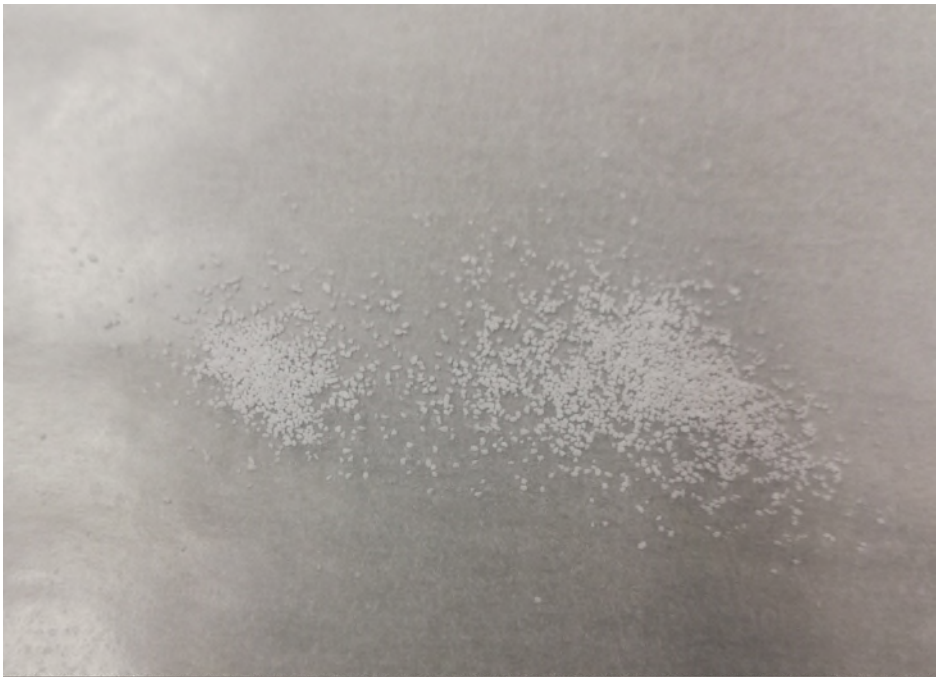

Figure 40: sieve fraction 212-425 µm of 100/0 boehmite/NCF-Co

The specific surface area was determined via BET. The results of the BET-measurents can be seen in Table 13 and in Figure 41. It is clearly visible, that with increasing boehmite content also the surface area increases.

Table 13: BET surface area of the prepared sieve fractions

Date	Composition (boehmite/NCF-Co; wt-ratio)	BET surface area ($m^2 \cdot g^{-1}$)
17.08.2022	0/100	4.7
11.08.2022	50/50	92.4
18.08.2022	80/20	158.8
18.08.2022	100/0	207.8

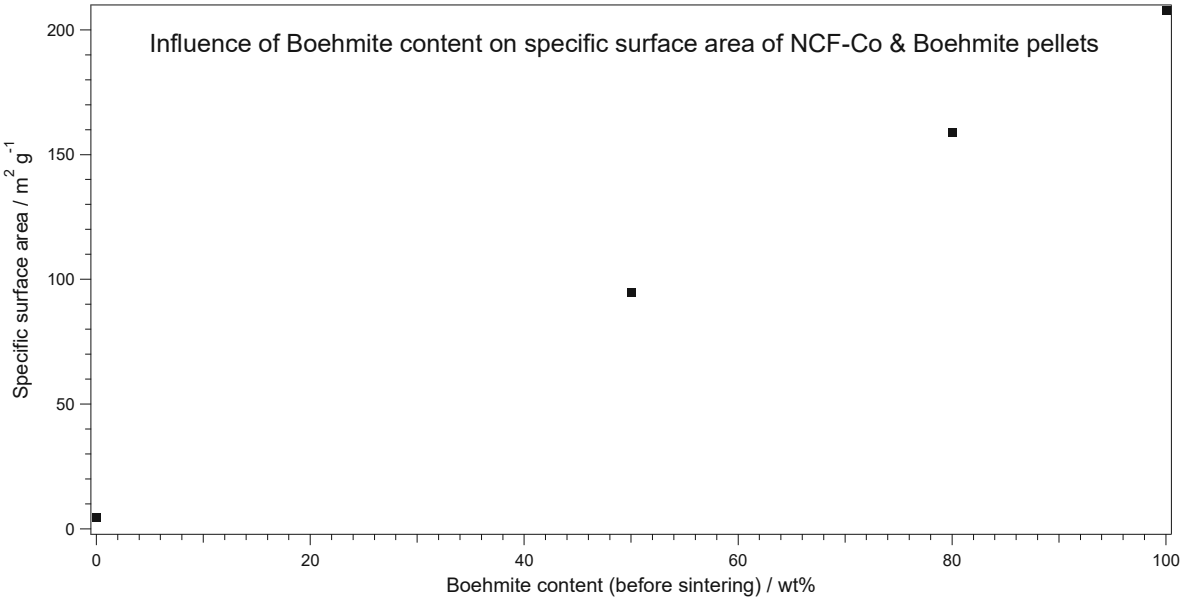

Figure 41: influence of the boehmite content on the specific surface areas of boehmite/NCF-Co pellets

In Figure 42 the XRDs of the prepared sieve fractions can be seen. For pure boehmite pellets a Rietveld refinement that is depicted in Figure 43 was prepared. As expected from the reference of the supplier, the boehmite transformed into γ-Al_2O_3. Pure NCF-Co pellets only show reflexes of this phase. For the 50/50 and 80/20 the NCF-Co reflexes can be seen clearly, the γ-Al_2O_3 slightly.

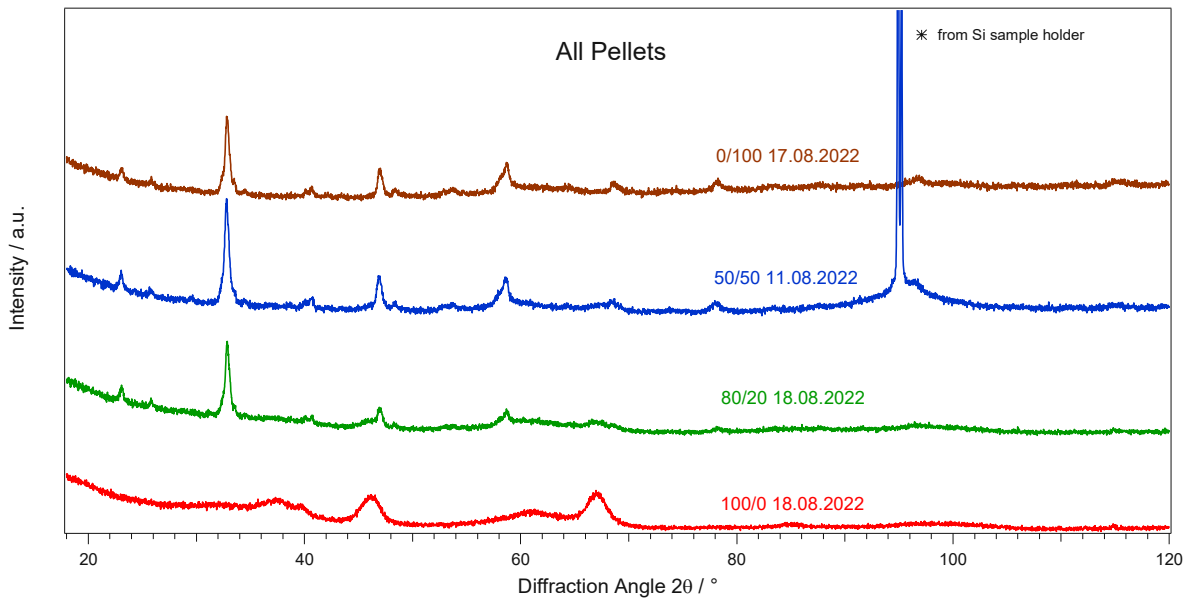

Figure 42: XRDs of the prepared sieve fractions

The parameters that were fitted in the Rietveld refinement are:

Global Parameters:

- Specimen Displacement

Alumina phase (00-010-0425):

- Scale Factor
- B overall

- Cell Parameter: a, b, c
- B isotropic of all atoms
- Profile Variables: Cagliotti u, Cagliotti v, Cagliotti w, Peak Shape 1, Peak Shape 2, Peak Shape 3

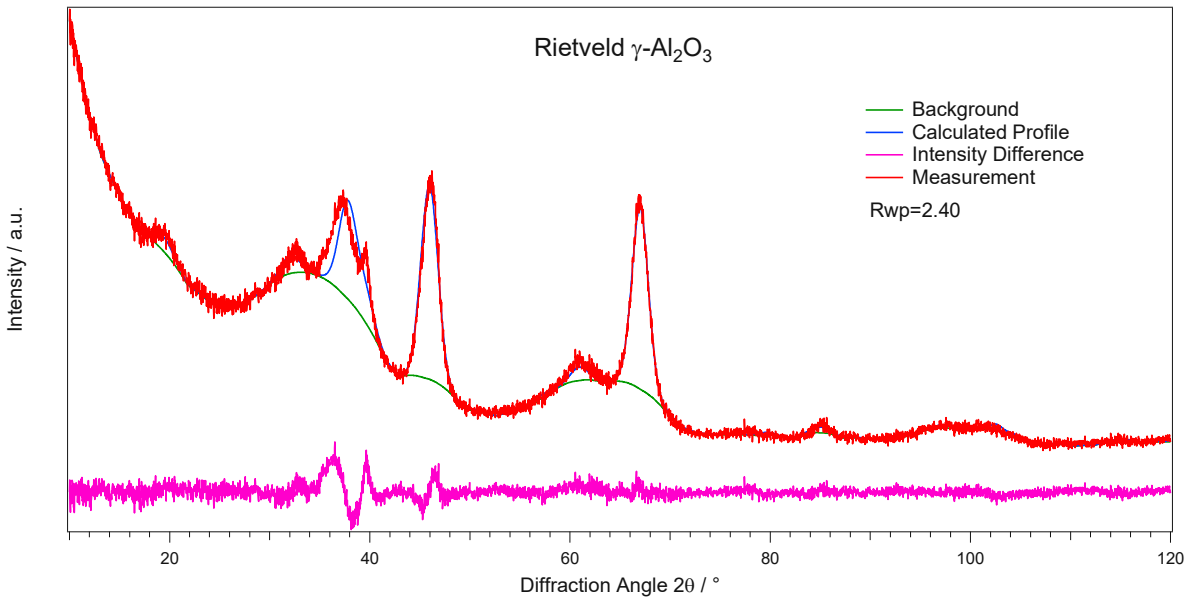

Figure 43: XRD and Rietveld refinement of pellet 100/0 boehmite/NCF-Co after calcining at 700 °C

5.3 Catalytic Tests

5.3.1 Experimental Parameters

The catalytic tests of the pellets with alumina hydrates were performed together with Hedda Drexler. The amount of sieve fraction was chosen such that 20 mg of pure NCF-Co were in the reactor (exact values can be seen in the appendix). For the alumina reference 80 mg were used. During sintering the pellets lose weight due to the elimination of water. To account for that, the theoretical relative mass loss of 15 % was assumed when calculating the amount of catalyst that should be weighed in. As dilutant of the catalyst, a sieve fraction in the range from 212-425 µm of quartz glass was used. The catalyst was filled up with quartz glass to 250 mg (catalyst + quartz glass). Prior to the catalytic test itself, an oxygen pretreatment was conducted. The condensation of the water formed during the reaction was tried to avoid with heated gas lines. However, this could not be achieved fully. After the catalytic test XRDs of the catalysts were recorded.

5.3.1.1 Temperature Program

For the oxidation prior to the catalytic experiment, it was heated to 400 °C in oxygen flow. For the catalytic experiment a ramp from 400-800 °C with a heating rate of 2 °C/min was applied. At 800 °C the temperature was held for 15 min. Furthermore, to the heating ramp also a cooling ramp from 800-400 °C with a cooling rate of 2 °C/min was used for some catalytic tests.

5.3.1.2 Volumetric Flows

During the oxidation, a flow of 20 $NmL \cdot min^{-1}$ of O_2 was used.

The following volumetric flows of the gases were used during the reactions:

- CO_2: 20 $NmL \cdot min^{-1}$
- H_2: 50 $NmL \cdot min^{-1}$

For flushing the reactor, a flow of 50 $\mathrm{NmL \cdot min^{-1}}$ of Ar was used.

5.3.2 Results & Discussion

In Figure 44 the results of the catalytic measurements can be seen. For all experiments an increase of the yield for increasing temperature can be seen. This is as expected from literature due to reasons of kinetics and thermodynamics. A clear difference of the catalysts to the blank measurement (glass wool and quartz glass) and pure boehmite pellets can be seen. Very interestingly the 1. catalytic test with pure NCF-Co performed significantly better than the 2. and 3. test even though the same, but fresh, catalyst was used. A reason might be that for the 1. test there was to too much water condensing in the gas lines hence a higher CO concentration in the gasphase and hence the higher activity, but it cannot be explained completely so far. In Figure 45 it can be seen how differently the water peaks appeared in the chromatograms for the three runs. Besides that, all the catalysts show similar behavior. The reason for the similarities of the catalysts might be because the test was performed close to the thermodynamic equilibrium. For the ramp down, smaller yields at the same temperature were observed, so apparently deactivation processes take place.

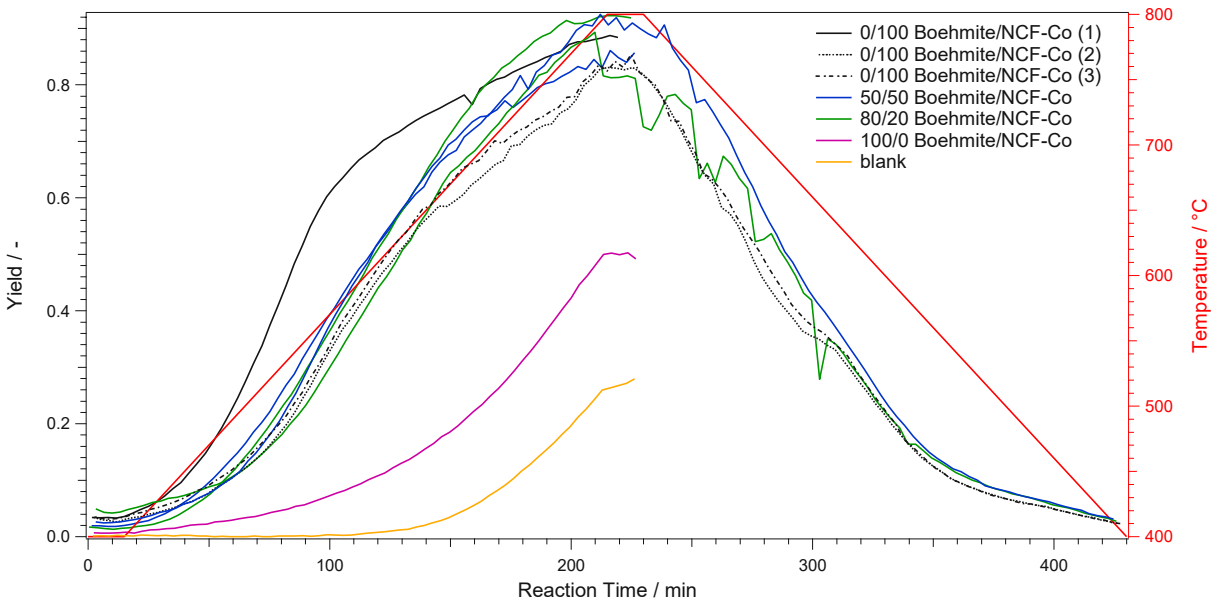

Figure 44: yields of the catalytic tests of all catalysts; yield of CO with respect to CO_2, calculated according to formula 3

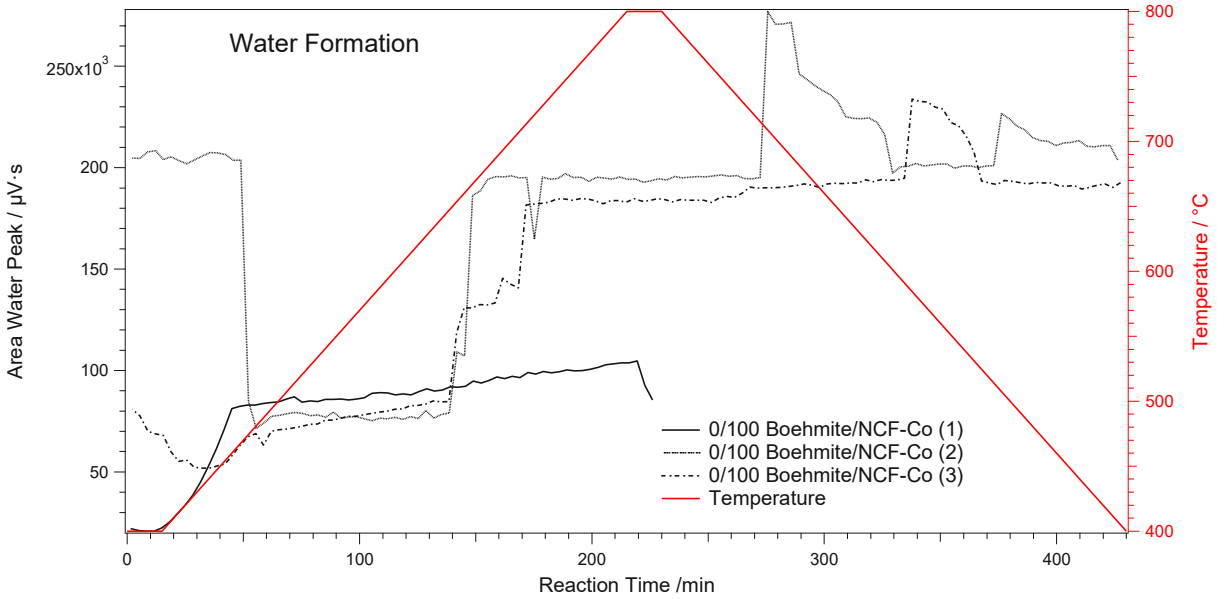

Figure 45: water formation during catalytic tests of catalyst 0/100 boehmite/NCF-Co

As a byproduct only CH_4 was detected by the GC and taken into account for the calculation of the selectivity (see formula 5). The selectivities towards CO, especially at higher temperatures where rWGS should be performed, of all catalysts are very high as it can be seen in Figure 46. It remains unclear why the runs with only ramps up performed much better at low temperatures in the selectivity.

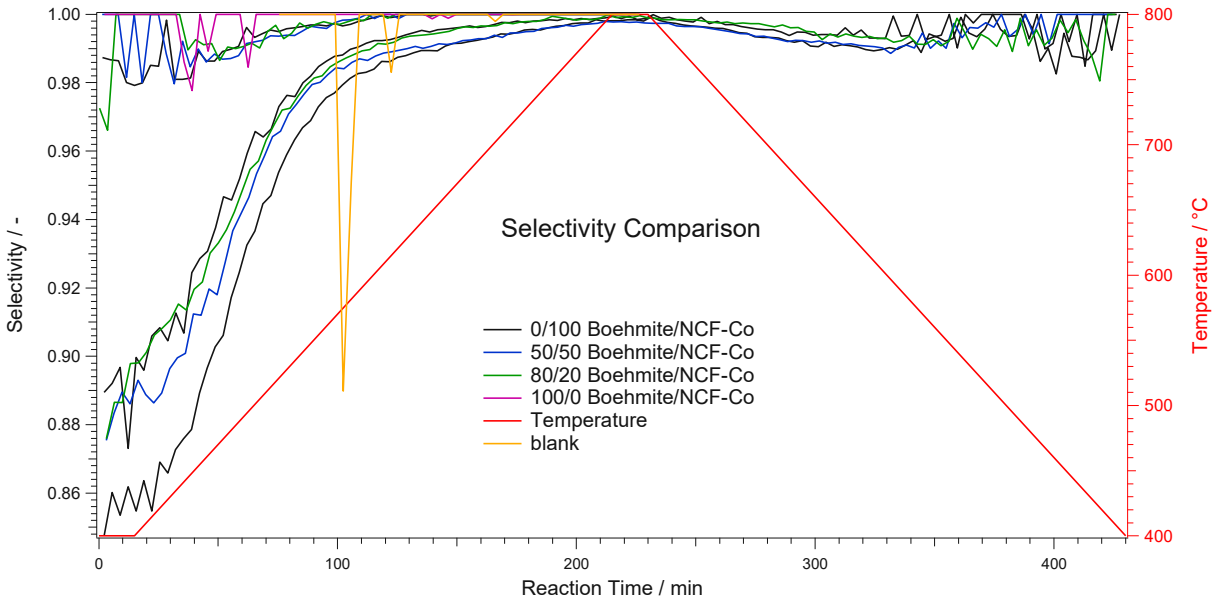

Figure 46: selectivities of the catalytic tests of all catalysts; selectivity towards CO, byproduct was CH_4

After the reaction exemplarily XRDs were measured. The SiO_2 sieve fraction used as a dilutant could not be properly separated because it was the same sieve fraction as the catalyst hence the large SiO_2 reflex, but for just a qualitative assessment of the occurrence of the iron reflex this should be enough. For both, the pure NCF-Co sieve fraction (Figure 47) and for the sieve fraction with NCF-Co with the highest alumina content (Figure 48) iron reflexes appear. They are shifted slightly to the left. This hints that an alloy between iron and cobalt (reflex of pure cobalt would be at a lower diffraction angle) is exsolved. For pellet $80/20$ it was found that four new reflexes were formed. These reflexes cannot be

interpreted so far. XRD of pellet $100/0$ did not show these four reflexes hence these four reflexes probably correspond to a new phase formed between elements from NCF-Co and alumina or SiO_2.

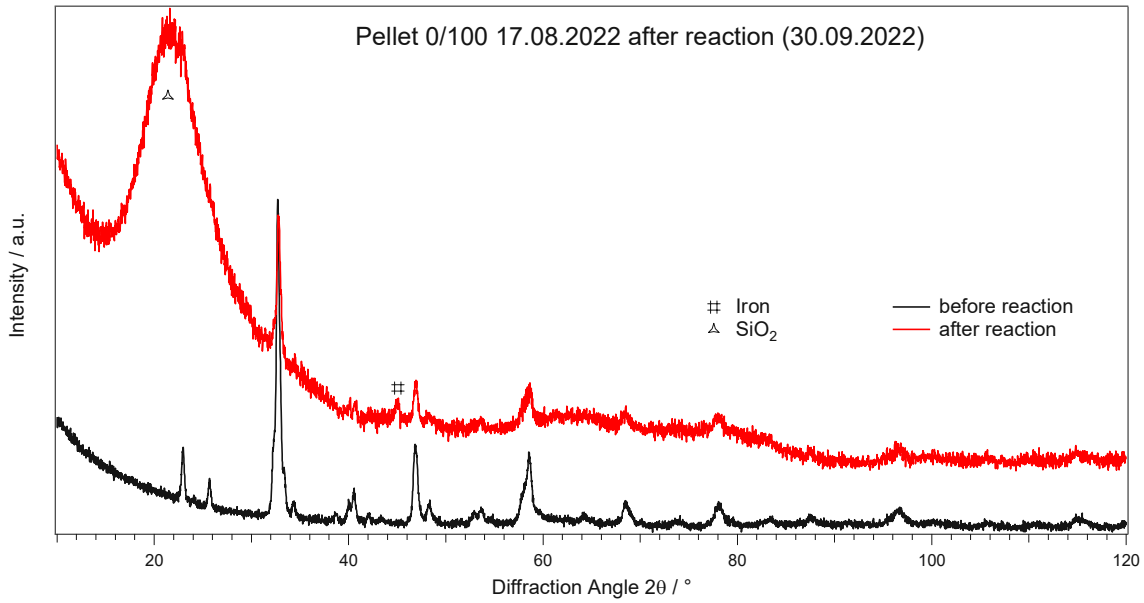

Figure 47: XRD of pellet 0/100 boehmite/NCF-Co after reaction (30.09.2022), not indicated reflexes are discussed above

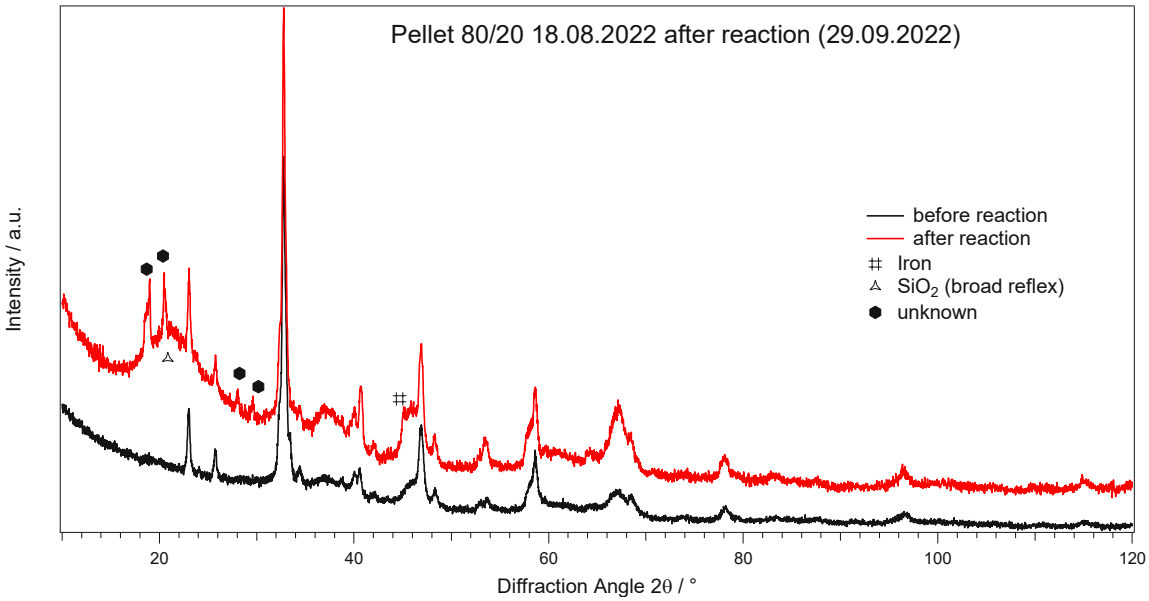

Figure 48: XRD of pellet 80/20 boehmite/NCF-Co after reaction (29.09.2022), not indicated reflexes are discussed above

For pellets without NCF-Co no significant changes could be observed via ex-situ XRD (Figure 49).

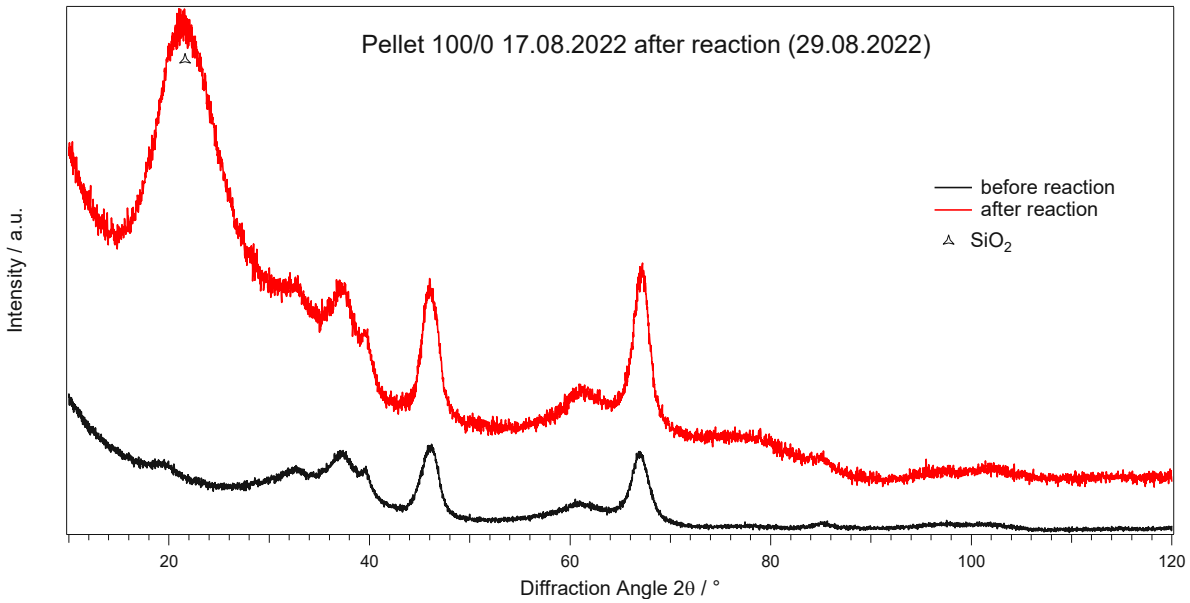

Figure 49: XRD of pellet 100/0 boehmite/NCF-Co after reaction (29.08.2022), not indicated reflexes are discussed above

5.4 Material Preparation for Catalytic Tests at Pilot Scale

The preparation of the catalyst for the pilot scale reactor was done with the tableting press depicted in Figure 50. The pressure at which the tablets were pressed could not be measured.

Figure 50: picture of tablet press TPD O [17]

A mixture according to Table 14 was prepared and tableted. Calcination was performed for 12 hours at 700 °C, heating and cooling was done with rates of 5 °C/min.

Table 14: weighed in amounts for mixture used for tableting, for graphite and boehmite the reagents according to Table 9 and 12 were used

Reagent	Mass (g)	Content (wt%)
NCF-Co 22070515	99.2	77.5
Graphite	4.0	3.1
Boehmite	24.8	19.4

The tablets after calcination can be seen in Figure 51.

Figure 51: tabletted material after calcination

6 Zeolites

As another approach it should be tried to prepare composites between zeolites and NCF-Co to combine the properties of both phases (e.g. high surface area of zeolites) and get to catalyst bodies with good properties. The zeolites MCM-22 (because of its high surface area) and ZSM-5 (due to its common use in industry) should be used.

6.1 Synthesis of pure Zeolites

At first the syntheses of pure zeolites were tried. The maximum value of the Si/Al ratio at which MCM-22 is still stable is 35 [18]. The water steam stability of zeolites is better for higher Si/Al ratios, hence a Si/Al ratio of 35 was chosen. ZSM-5 would also be stable completely without Al, but due to reasons of comparability with MCM-22 the Si/Al ratio was chosen to be 35 too.

In Table 15 the reagents used for the zeolite syntheses can be seen.

Table 15: reagents used for preparation of zeolites

Reagent	Description	Supplier
Distilled water	18.2 MΩ·cm^{-1} resistance	In-house
NaOH	Puriss 98-100.5 %	Sigma Aldrich
KOH	≥85 % flakes	Roth
$Al(OH)_3$	Aluminium hydroxide hydrate, powder, Dried gel 50-57.5 % as Al_2O_3	Sigma Aldrich
Hexamethylenimine (HMI)	≥98 %	TCI
Fumed Silica	Silicon(IV) oxide, amorphous fumed, S.A. 85-115 m^2/g 325 Mesh Powder SiO_2	Alfa Aesar
Ethanol	96 %	In-house
Tetrapropylammoniumhydroxide solution (TPAOH)	20-25 % in solution	TCI
Tetraethylorthosilicate (TEOS)	98 %	Sigma Aldrich
N-Cetyl-N,N,N-trimethylammoniumbromide (CTAB)	pro analysi	Merck
$NaAlO_2$	Technical, anhydrous	Sigma Aldrich

6.1.1 MCM-22

The general course of the synthesis was always the same and is described below. Details about the batches like weighed in amounts can be seen in the appendix.

The synthesis of MCM-22 was done following the recipe of Quintela et al. [19] with the modification of the Si/Al ratio to 35. At first distilled water was filled in a beaker. Then NaOH and KOH were added and dissolved during 15 min. After the addition of $Al(OH)_3$ 15 min were waited. Then HMI was added dropwise. After adding fumed silica, the gel was aged under magnetic stirring for 24 hours at room temperature. Then the gel was transferred into a teflon-lined autoclave and it was crystallized at 150 °C for 10 days. The product was vacuum filtrated and washed with distilled water until pH was below 8. The product was dried in an oven at 60 °C overnight. After that, the white product was ground to powder and heat-treated at 550 °C for 6 hours in a muffle furnace.

Since the first prepared batch (MCM-22 220412) failed (see XRD in Figure 52), another batch (MCM-22 220519) was prepared with more water to allow better stirring of the gel.

The XRD of batch MCM-22 220519 clearly showed reflexes in the XRD (Figure 52). In a Rietveld refinement the phase was matched with good agreement with MCM-22 (see Figure 53).

The following parameters were refined in the Rietveld refinement:

Global Parameters:

- Specimen Displacement

MCM-22 (PDF-Code: 00-049-0627):

- Scale Factor
- B-overall
- Cell Parameter: a, b, c
- Profile Variables: Cagliotti u, Cagliotti v, Cagliotti w, Peak Shape 1, Peak Shape 2, Peak Shape 3

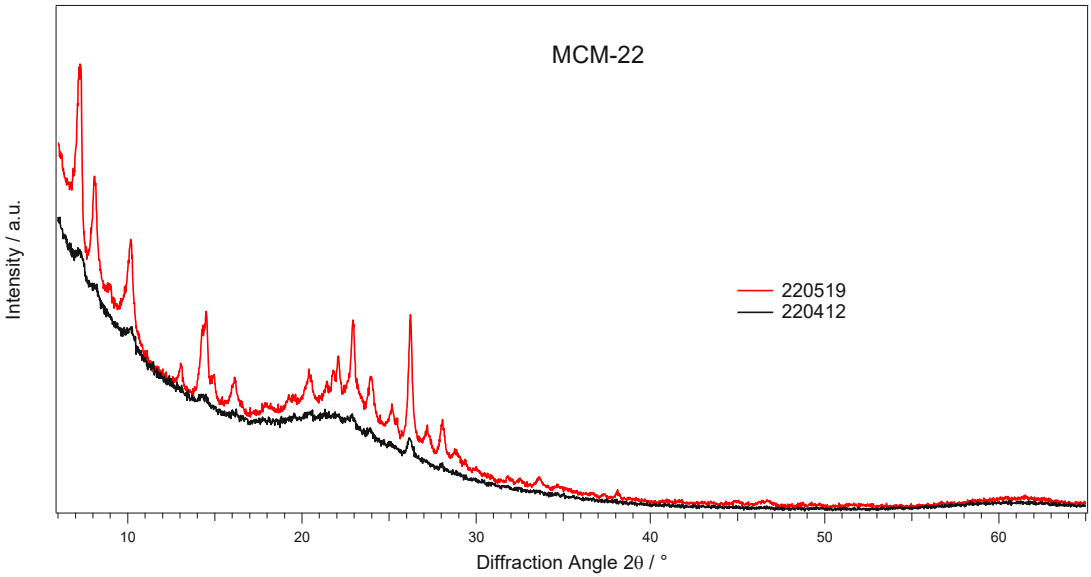

Figure 52: XRDs of the prepared MCM-22 batches, reflexes are matched below in a Rietveld refinement

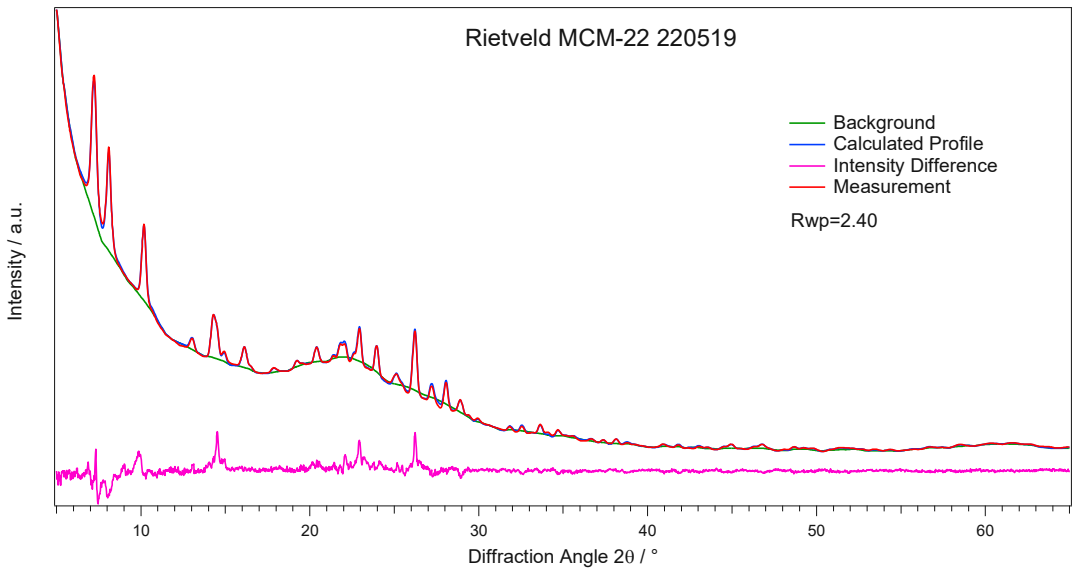

Figure 53: XRD and Rietveld refinement of batch MCM-22 220519

Because MCM-22 is not so commonly used in industry compared to ZSM-5 no attempts for synthesizing composites with NCF-Co were tried. Instead composites with ZSM-5 should be tried.

6.1.2 ZSM-5

At first again a pure zeolite was prepared. The general course of the synthesis was always the same and is described below. Details about the batches like weighed in amounts can be seen in the appendix.

The synthesis of ZSM-5 was done following the recipe of Chen et al. [20] except that fumed silica mixed with water was used instead of silica sol bought as a whole, that in general more water was used and that the Si/Al ratio was adjusted to 35. For the preparation of the seeding solution, distilled water, ethanol, TPAOH solution and dropwise added TEOS were stirred for 2 hours and subsequently hydrothermally treated for 96 hours at 100 °C in a teflon-lined autoclave.

The gel was prepared by filling water into a beaker and adding NaOH, $NaAlO_2$ and CTAB. After that it was stirred for 0.5 hours. Then the seeding solution, fumed silica and water were added dropwise. After stirring for 2 hours (see Figure 54) the gel was aged for 12-14 hours at 120 °C in a teflon-lined autoclave with subsequent crystallization at 170 °C for 24 hours. The product was centrifuged and washed with distilled water until pH was about 7. The product was dried in an oven at 60-100 °C, ground to powder and calcined at 550 °C for 6 hours in a muffle furnace. The product was a white powder. In Figure 55 an example of a prepared zeolite is shown.

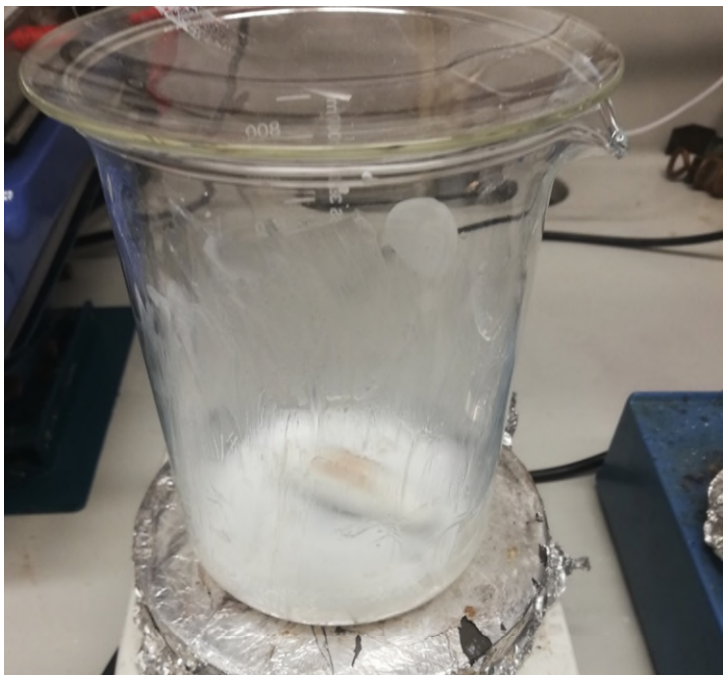

Figure 54: typical appearance of the gel from which ZSM-5 is crystallized

Figure 55: appearance of ZSM-5 batch 220609

"L" and "R" in the names of batches 220429L and 220429R only denote that different heating plates were used for crystallization (the same gel was used). After measuring XRD, Rietveld refinements were prepared of the products. The agreement with the reference is good except for smaller reflexes, but all intense reflexes can be explained. The following parameters were refined:

Global Parameters:

- Specimen Displacement

ZSM-5 (PDF: 01-080-4532):

- Scale Factor
- B-overall
- Cell Parameter: a, b, c
- Profile Variables: Cagliotti u, Cagliotti v, Cagliotti w, S/L Asymmetry, D/L Asymmetry, Peak Shape 1, Peak Shape 2, Peak Shape 3
- Occupancy of O27-O38

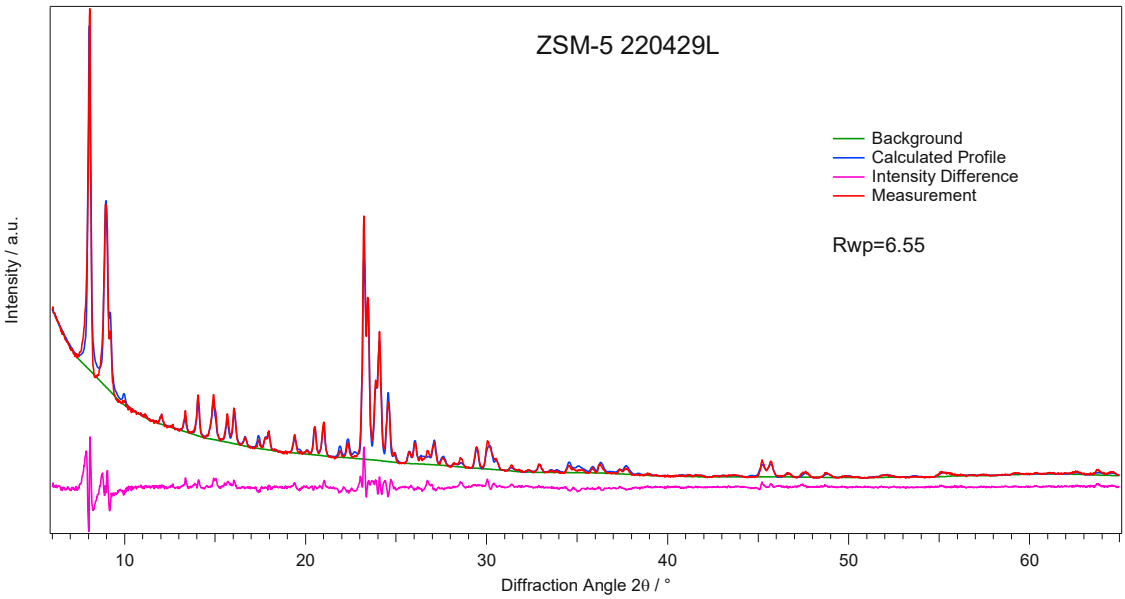

Figure 56: Rietveld refinement of ZSM-5 220429L

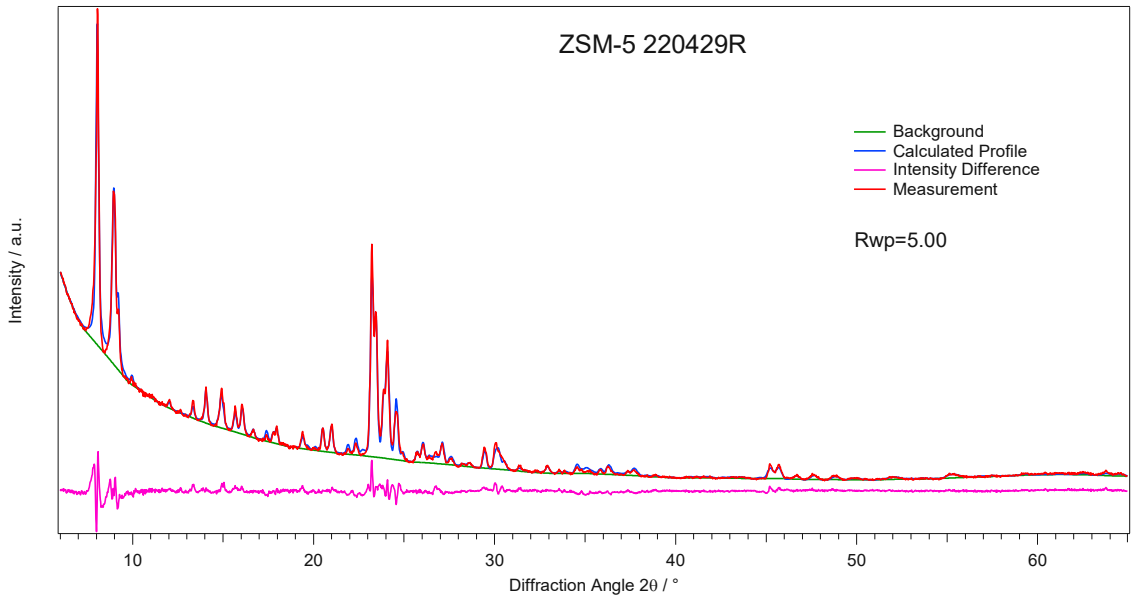

Figure 57: Rietveld refinement of ZSM-5 220429R

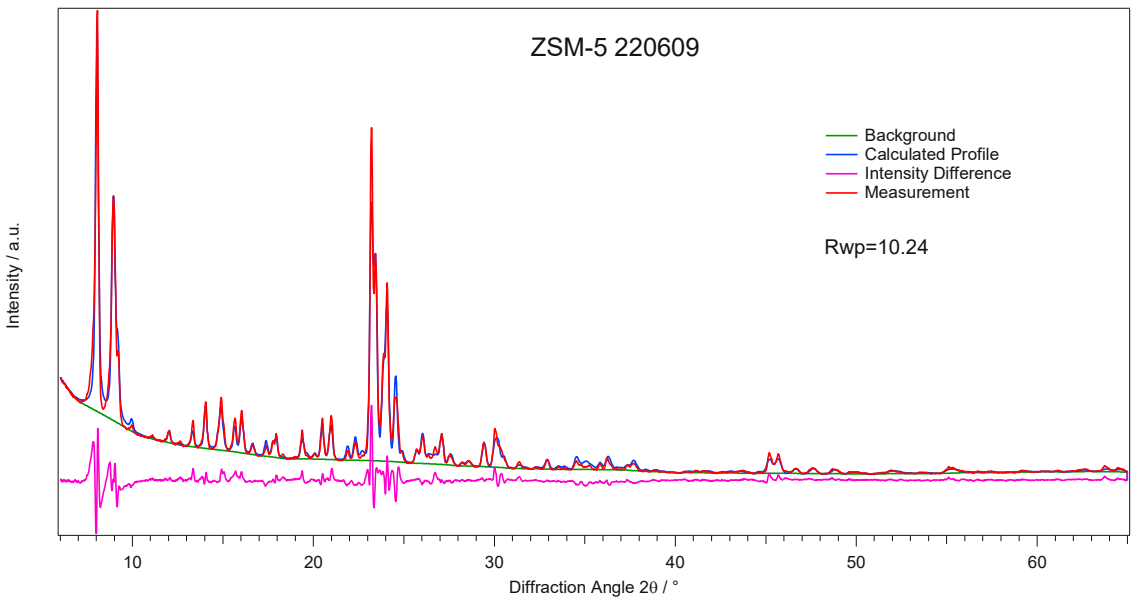

Figure 58: Rietveld refinement of ZSM-5 220609

As result from a BET surface area measurement a value of $443\ m^2 \cdot g^{-1}$ was received for batch 220429L, but it must be noted that the C parameter from the BET equation which should always be positive was negative. Hence this is only a rough value, but the order of the surface area is a reasonable value for a zeolite.

Besides the self-prepared samples also samples gotten from colleagues of Noelia Barrabés were characterized via XRD. These samples are:

- ZSM-5 “pure Si (Zeocat PZ-2 1000Na)”
- ZSM-5 “Si/Al=140 (Zeolyst CBV28014)”; NH_4^+ cation

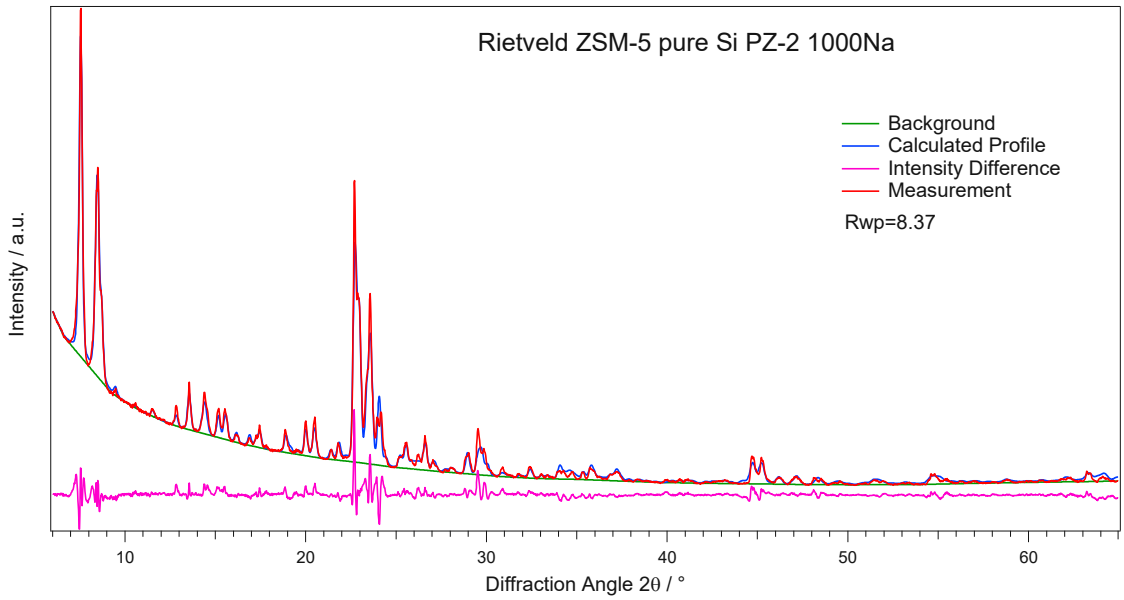

Figure 59: Rietveld refinement of ZSM-5 "pure Si PZ-2 1000Na"

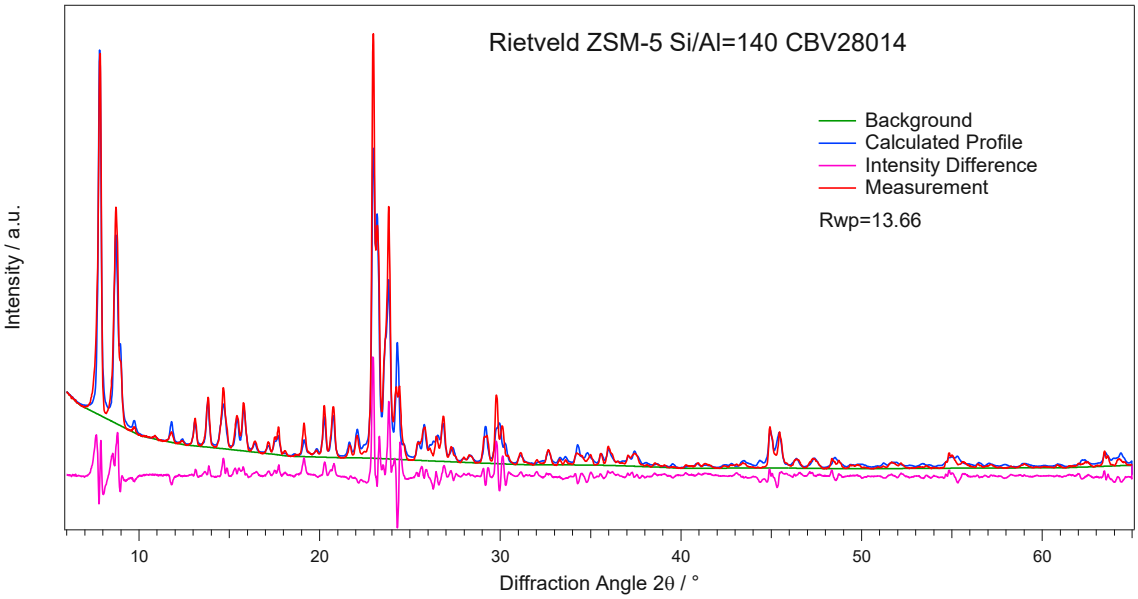

Figure 60: Rietveld refinement of ZSM-5 "Si/Al=140 CBV28014"

Additionally, to XRD also ICP-OES measurements were conducted by Laura Kronlachner to determine the Si/Al ratio of the self-prepared zeolites. As it can be seen in Table 16 the Si/Al ratio was too low for MCM-22 and too high for the ZSM-5 batches, but the values for batches 220609 and 220429 are similar. Reasons for the deviations in the Si/Al ratio might arise from hygroscopic reagents and thus the right amount was not weighed in.

Table 16: results of the ICP-OES measurements of zeolites

Batch name	Na (mol)	K (mol)	Al (mol)	Si (mol)	Si/Al (-)
MCM-22 220519	0.010	0.024	0.045	1.309	28.9
ZSM-5 220609	0.036	-	0.033	1.320	39.6
ZSM-5220429R	0.028	-	0.028	1.137	40.9
ZSM-5 220429L	0.041	-	0.036	1.425	39.2

6.2 Stability Tests of pure Zeolites

The stabilities of the zeolites were tested via in-situ XRD. Different temperature programs up to 700 °C were used. At each temperature three XRDs were recorded. As gas atmosphere hot water vapor (3 % humidity) in inert gases like He or Ar was chosen. The humidity of the gas was achieved via bubbling inert gases through a water filled bubbler.

As samples the self-prepared zeolite ZSM-5 220429L as well as the zeolites gotten from Noelia Barrabés´ colleagues from Spain were investigated. If only one XRD at a certain temperature is shown, then the other two XRDs recorded at the same temperature do not differ significantly from the first one.

6.2.1 ZSM-5 "Si/Al=140"

The results of the first conducted in-situ measurement from 25-700 °C can be seen in Figure 61. For this experiment it was forgotten to conduct a measurement at 25 °C in He atmosphere. Nevertheless, some observations can be made. Due to the different atmospheres (temperature and gas composition) the signal-to-noise ratio can be different, hence reflexes might appear less intense at different atmospheres. Another observation was the transition from two reflexes to one at about 24.1° which changed back to two when it was cooled down. Also a small reflex at 26.2° was formed beginning at a temperature of 500 °C. If the curves before and after heating are compared, only minor changes in the intensities and broadness of reflexes can be seen, hence the zeolite is stable. For this zeolite the positions of the reflexes seem to remain more or less unshifted when heating up.

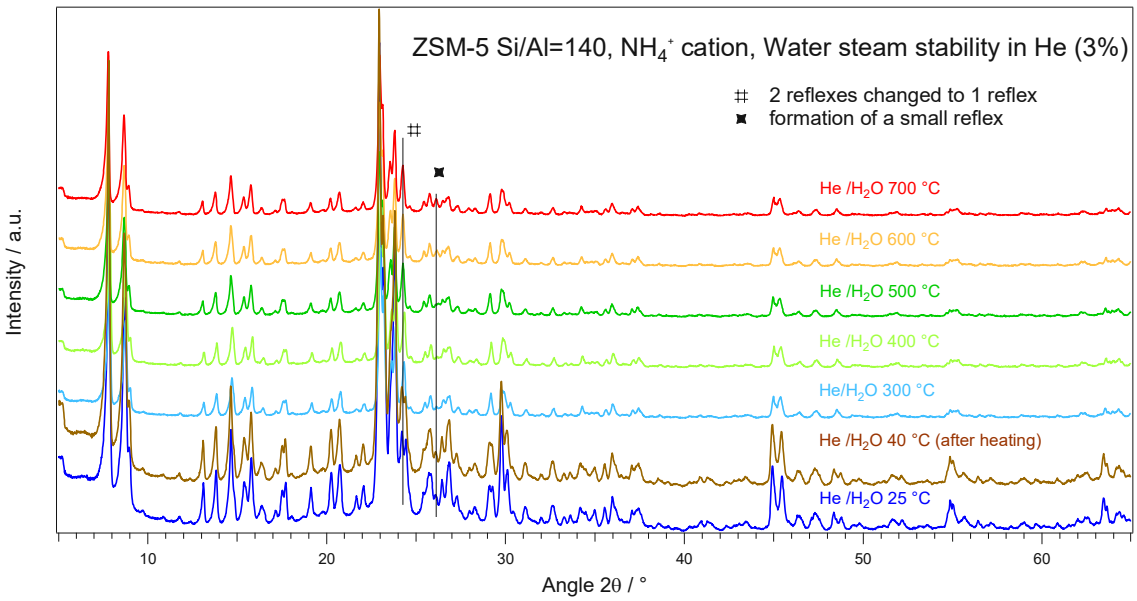

Figure 61: results of in-situ XRD for ZSM-5 "Si/Al=140 CBV28014" in the temperature range from 25-700 °C

Because in the experiment before it was forgotten to measure in He atmosphere at 25 °C another in-situ experiment was conducted (Figure 62). But in this experiment another problem of unknown origin arose, namely that there was a big change in reflex positions and intensities just when it was switched to He/H_2O. One explanation might be that the sample did not stay in place. The change from two reflexes to one was observed again. Interestingly it did not change back to two reflexes after cooling down. Regarding the still missing proper comparison between inert gas atmosphere and water vapor atmosphere two more measurements were performed anyway.

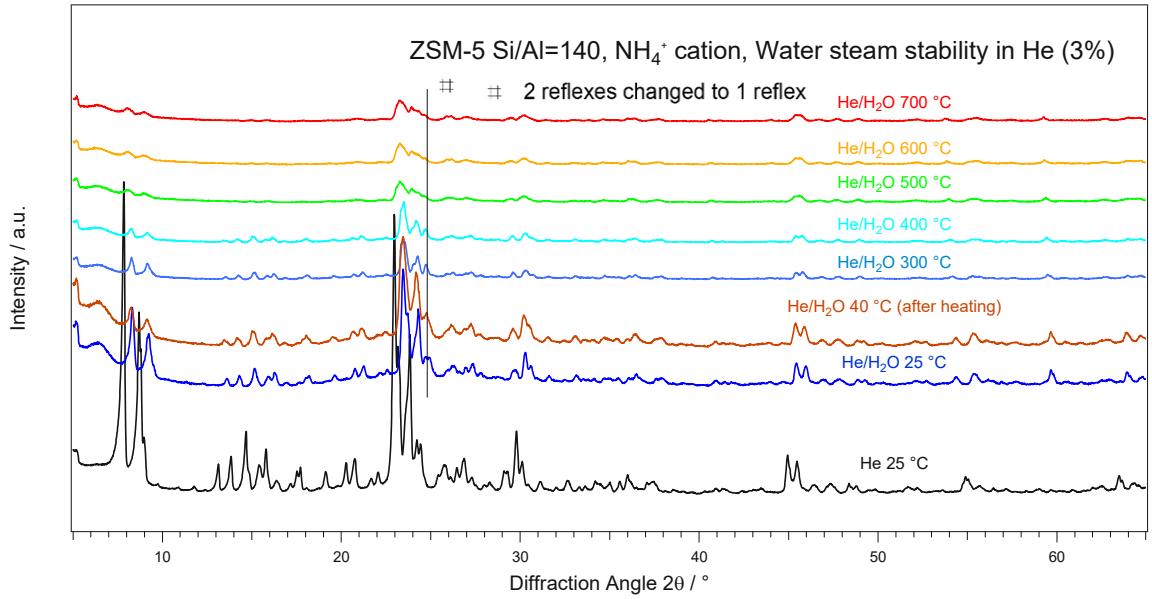

Figure 62: results of in-situ XRD for ZSM-5 "Si/Al=140 CBV28014" in the temperature range from 25-700 °C

In a further experiment (Figure 63) the change from two reflexes to one also occurred but a change back could also be observed. To closer check when this change happens also measurements at lower temperatures were performed. It was confirmed that the change even happened before 100 °C.

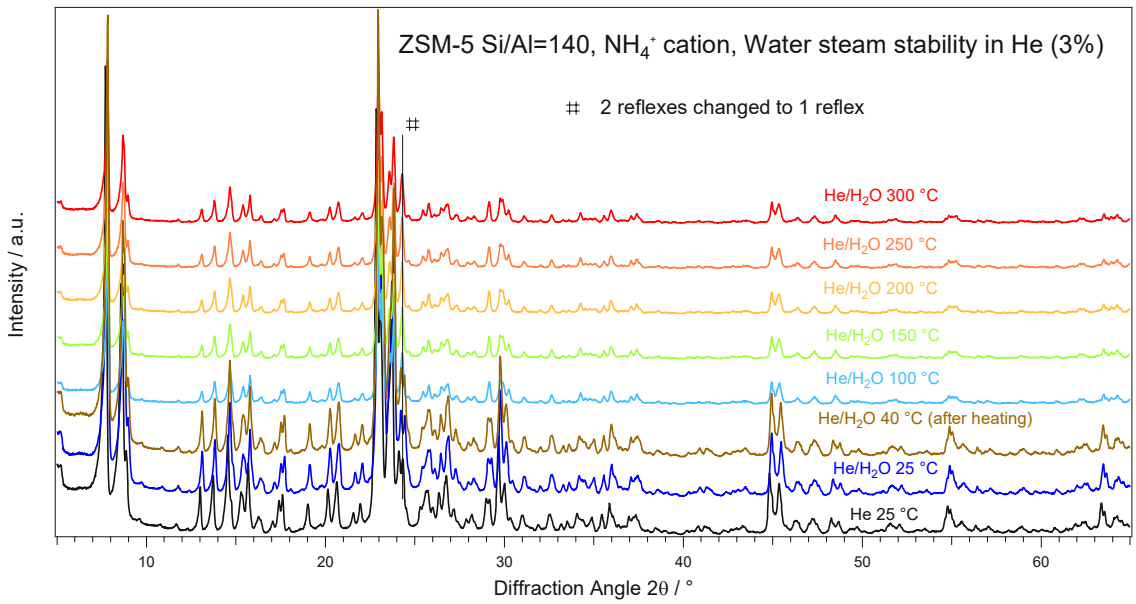

Figure 63: results of in-situ XRD for ZSM-5 "Si/Al=140 CBV28014" in the temperature range from 25-300 °C

To check when the formation of a new reflex at 26.2° happens the following measurements (Figure 64) were performed. Since it was run out of He, Ar was used instead as inert gas. It can be seen that the signal-to-noise ratio is not very good hence not much assessments of what happened can be made except that the two peaks here changed again to one and changed back after heating.

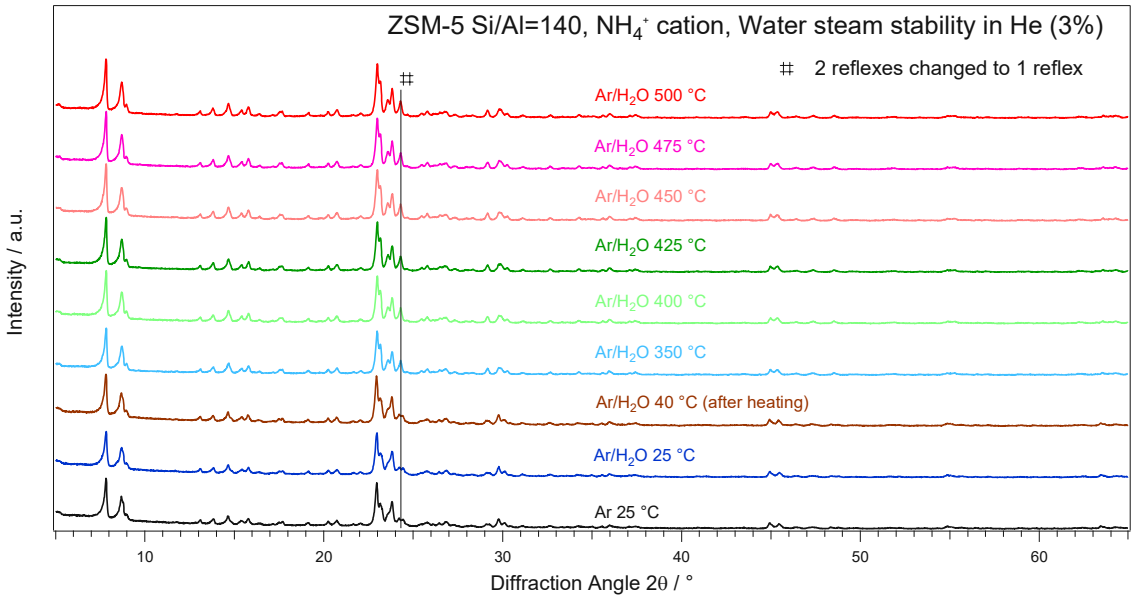

Figure 64: results of in-situ XRD for ZSM-5 "Si/Al=140 CBV28014" in the temperature range from 25-500 °C

6.2.2 ZSM-5 homemade

In Figure 65 the XRDs of the self-prepared zeolite ZSM-5 220429L can be seen. When heating up there are no big changes in the structure. Only small difficile changes like the reflex at 30.5° that appears more dominant can be seen. The positions of the reflexes seem to remain unshifted when heating up.

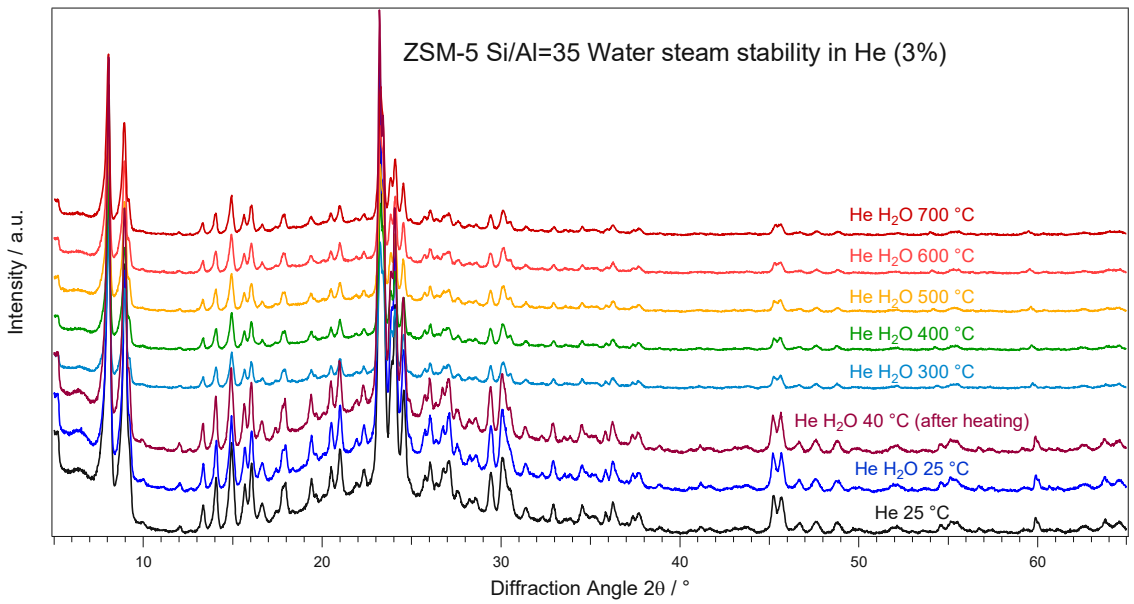

Figure 65: results of in-situ XRD for ZSM-5 "Si/Al=35 (220429L)" in the temperature range from 25-700 °C

6.2.3 ZSM-5 “pure Si”

In Figure 66, Figure 67, Figure 68 and Figure 69 the XRDs of sample ZSM-5 “pure Si (Zeocat PZ-2 1000Na)” can be seen. The formation of a new Si-O-phase (β-cristobalite) was observed when reaching a temperature of 700 °C in the first experiment (Figure 66). A drastic change in the reflex positions can be observed. In the next experiments (Figure 67 and Figure 69) this was not observed. Since the first steps are the same for each experiment, this change was probably not a result of any changes of the material itself, but from the alignment of the sample stage. Another change in the XRD was the change from two reflexes at 24.0° and 24.2° to one at 24.4° when changing to He/H_2O atmosphere. After heating this change remained. It is interesting to note that β-cristobalite is normally not formed at such low temperatures and is not stable down to room temperature. The reason these phenomena happened is probably due to the special structure of the zeolite. For a better overview here only one XRD of each temperature is shown, but as described in the next experiment the β-cristobalite reflex was getting more intense with time.

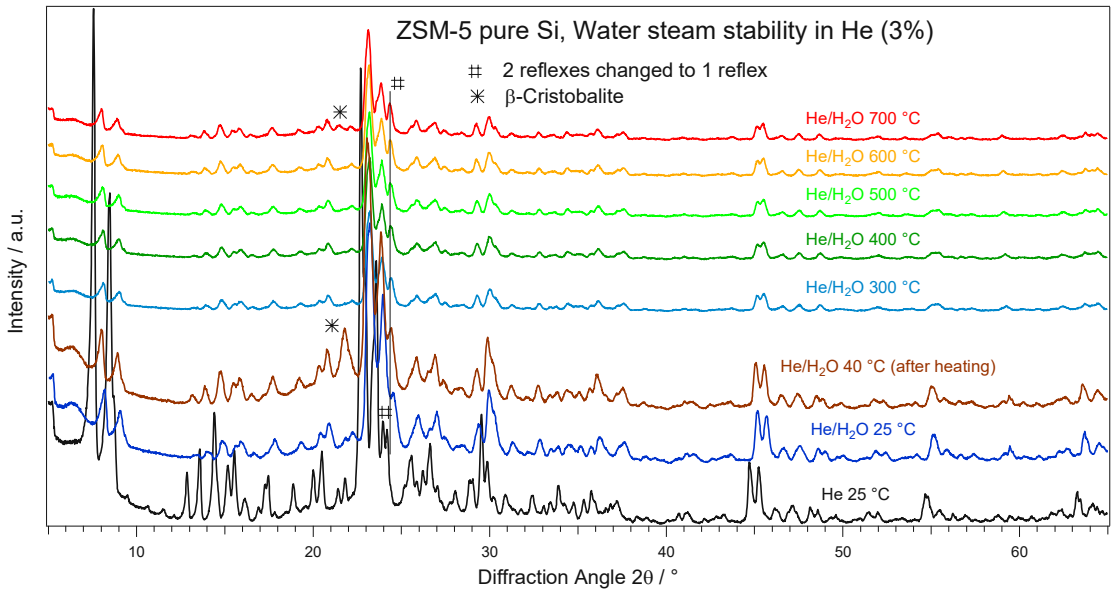

Figure 66: results of in-situ XRD for ZSM-5 “pure Si (Zeocat PZ-2 1000Na)” in the temperature range from 25-700 °C

An experiment with a smaller step size (Figure 67) in the temperature revealed that the formation of cristobalite starts at 650 °C. It was found that the main reflex of β-cristobalite appears at a smaller angle at higher temperatures. This can be explained with the Bragg Equation and the thermal expansion of β-cristobalite. Very interestingly the change from two reflexes to one happened only when it was heated up compared to the experiment before. When cooling down to 40 °C, a split into two reflexes was observed. For this experiment also the temporal appearance of a reflex at 26° was observed when reaching a temperature of 600 °C. For this zeolite the positions of the reflexes seem slightly shifted towards smaller angles when heating up. The reason might be the thermal expansion of the zeolite.

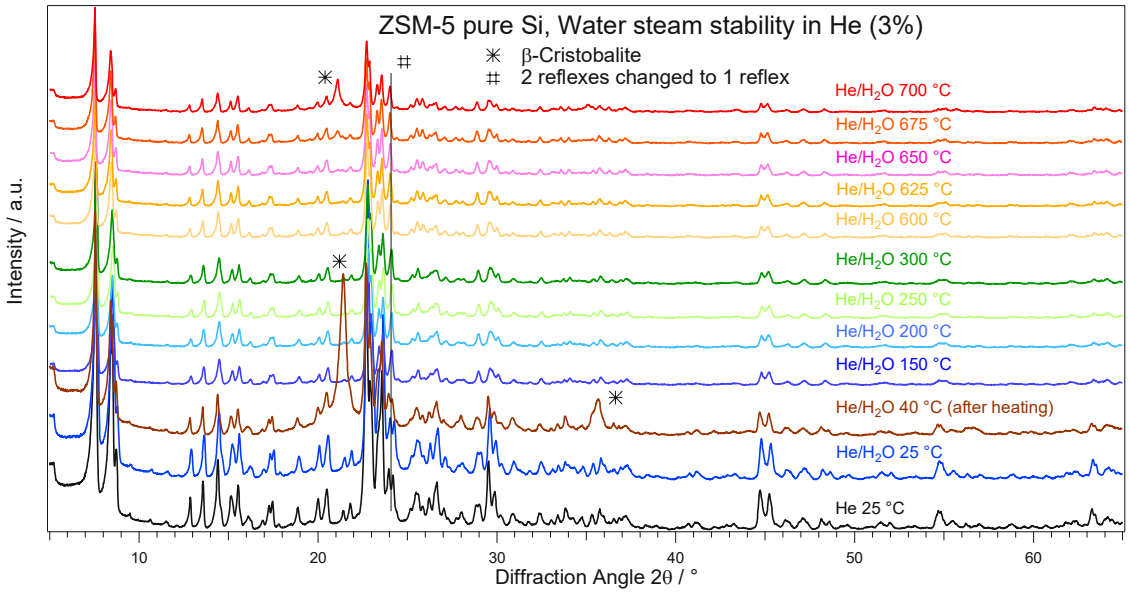

Figure 67: results of in-situ XRD for ZSM-5 "pure Si (Zeocat PZ-2 1000Na)" in the temperature range from 25-700 °C

If all three measurements that were conducted for each temperature from 650-700 °C are depicted, it can be seen, that the reflex corresponding to β-cristobalite is getting more intense over time (Figure 68).

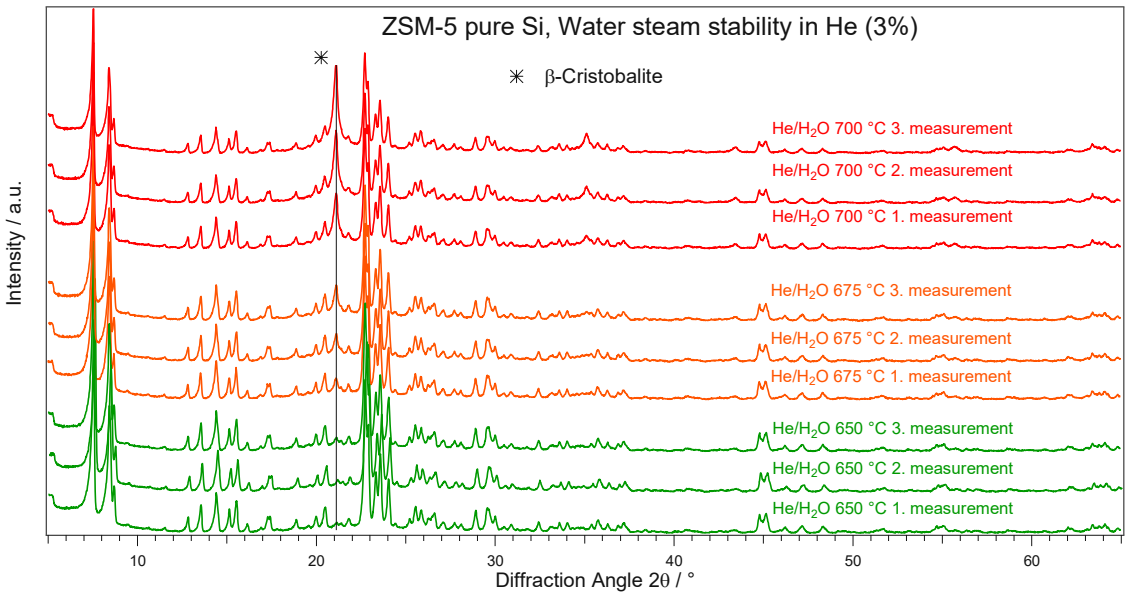

Figure 68: results of in-situ XRD for ZSM-5 "pure Si (Zeocat PZ-2 1000Na)" in the temperature range from 650-700 °C; time dependence

To check, when the two reflexes become one, lower temperatures were tested as it can be seen in Figure 69. It seems that this transition starts to occur at 50 °C and is finished at 100 °C.

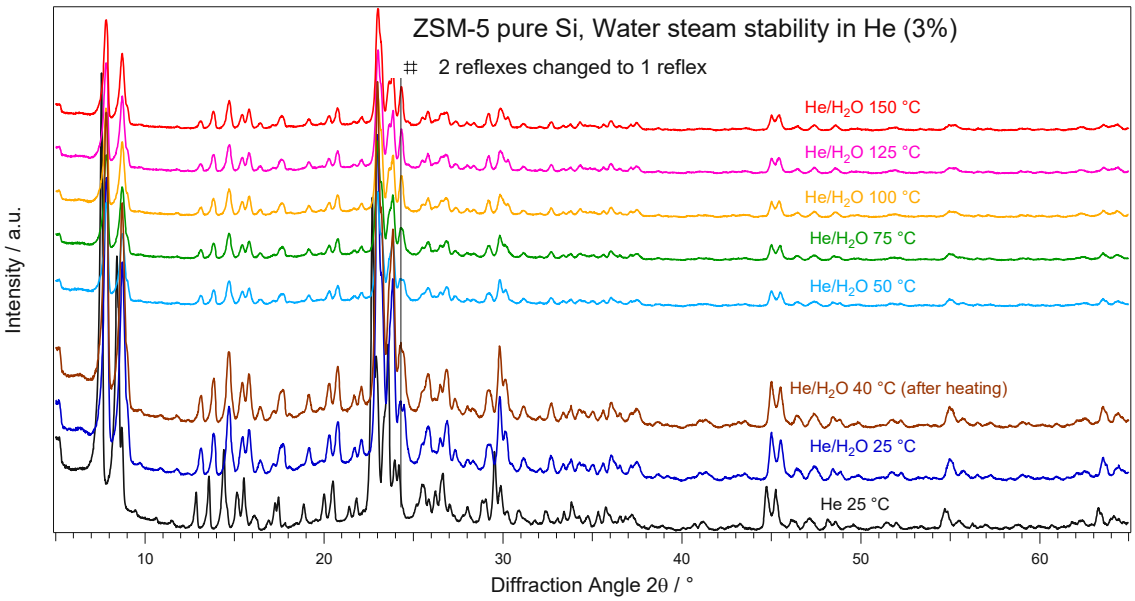

Figure 69: results of in-situ XRD for ZSM-5 "pure Si (Zeocat PZ-2 1000Na)" in the temperature range from 25-150 °C

6.3 Zeolites added to Pechini Synthesis

As first approach for composite preparation it was tried to add zeolites to a classical Pechini synthesis (as described above in "3 Pechini Syntheses"). This was tried with the zeolites ZSM-5 "pure Si (PZ-2 1000Na)" and ZSM-5 "Si/Al=140 (CBV28014)". The composites were prepared using a weight ratio of 50/50 zeolite/NCF-Co. Details about the synthesized batches can be seen in Table 17, the reagents that were used refer to Table 2 and Table 3. As products, grey powders were obtained.

Table 17: synthesis details of the batches where zeolites were added to the Pechini synthesis

Batch name	**Amount Nd_2O_3 (g)**	**Amount $CaCO_3$ (g)**	**Amount Fe (g)**	**Amount $Co(NO_3)_2{\cdot}6H_2O$ (g)**	**Amount citric acid (g)**	**Amount zeolite (g)**	**Used reagent for: Nd_2O_3; $CaCO_3$, Fe; $Co(NO_3)_2{\cdot}6H_2O$; citric acid; HNO_3**	**Sintering program (heating rate in °C/min – holding temperature in °C – holding time in h – heating rate in °C/min – holding temperature in °C – holding time in h – cooling rate in °C/min)**	**Yield (g)**
18.05.2022 ZSM-5 "pure Si PZ-2/1000Na"	1.0840	0.3874	0.4862	0.2818	4.95	2.0004	B;A;B;B,B;B	5-350-0,5-5-800-5-5	3.82
18.05.2022 ZSM-5 "Si/Al=140 CBV28014"	1.0842	0.3875	0.4863	0.2816	4.99	2.0006	B;A;B;B,B;B	5-350-0,5-5-800-5-5	3.27

6.3.1 XRD of zeolites added to Pechini Synthesis

As characterization of the products XRDs were measured. For ZSM-5 "Si/Al=140" it was found that the zeolite structure is partly destroyed as it can be seen in the XRD (Figure 70), but still ZSM-5 and NCF-Co phases can be seen. The minor details are discussed next, when a Rietveld refinement was prepared.

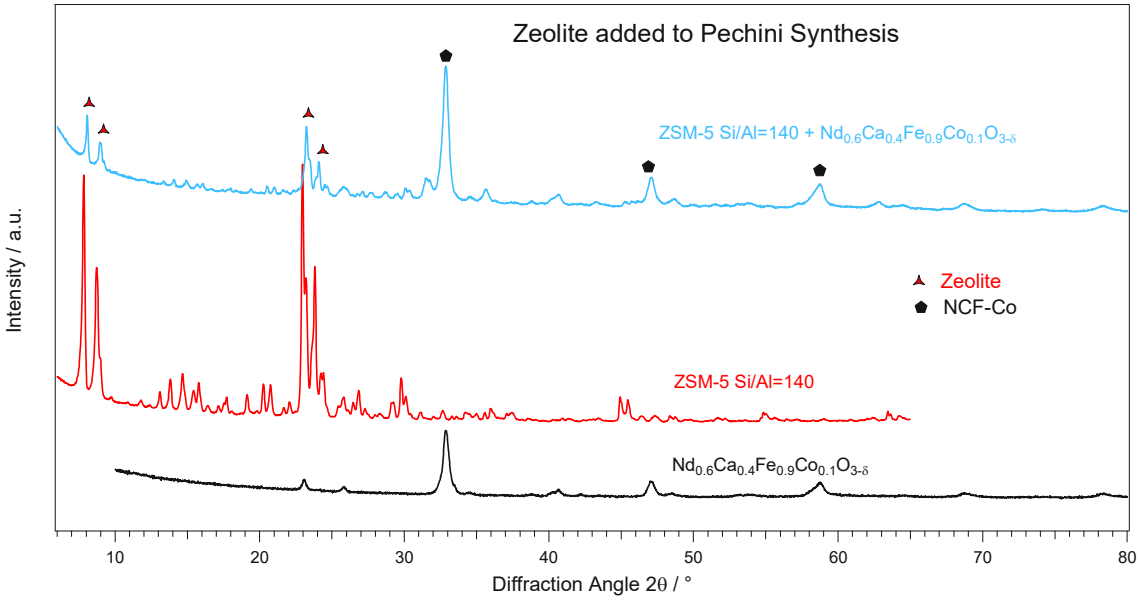

Figure 70: XRD of composite with zeolite ZSM-5 "CBV28014 (Si/Al=140)" added to a Pechini synthesis

Except for some very small reflexes, phases corresponding to the intense reflexes could be found and with these phases a Rietveld refinement was prepared of the product. The following parameters were refined:

Global Parameters:

- Specimen Displacement

ZSM-5 (PDF: 01-080-4532):

- Scale Factor
- B-overall
- Cell Parameter: a, b, c
- Profile Variables: Cagliotti u, Cagliotti v, Cagliotti w, S/L Asymmetry, D/L Asymmetry A, Peak Shape 1, Peak Shape 2, Peak Shape 3
- Occupancy of O27-O38

NCF-Co (04-014-5430):

- Scale Factor
- B-overall
- Cell Parameter: a, b, c
- Profile Variables: Cagliotti u, Cagliotti v, Cagliotti w, Peak Shape 1, Peak Shape 2, Peak Shape 3

Calcium Oxide Silicate (04-025-8090):

- Scale Factor
- B-overall
- Cell Parameter: a, b, c
- Profile Variables: Cagliotti u, Cagliotti v, Cagliotti w, Peak Shape 1, Peak Shape 2, Peak Shape 3

Coesite (01-072-1601):

- Scale Factor
- B-overall
- Cell Parameter: a, b, c
- Profile Variables: Cagliotti u, Cagliotti v, Cagliotti w, Peak Shape 1, Peak Shape 2, Peak Shape 3

Maghemite (00-025-1402):

- Scale Factor
- B-overall
- Cell Parameter: a, b, c
- Profile Variables: Cagliotti u, Cagliotti v, Cagliotti w, Peak Shape 1, Peak Shape 2, Peak Shape 3

The wt-% of the phases are given in Table 18. Here it can be seen, that a rather big amount of the zeolite is transformed into other phases.

Table 18: composition of composite ZSM-5 "Si/Al=140" added to Pechini synthesis

Phase	Content (wt%)
ZSM-5 Silicon Oxide Hydrate	22.9
NCF-Co	47.7
Calcium Oxide Silicate	22.5
Coesite	0.0
Maghemite (Fe_2O_3)	7.0

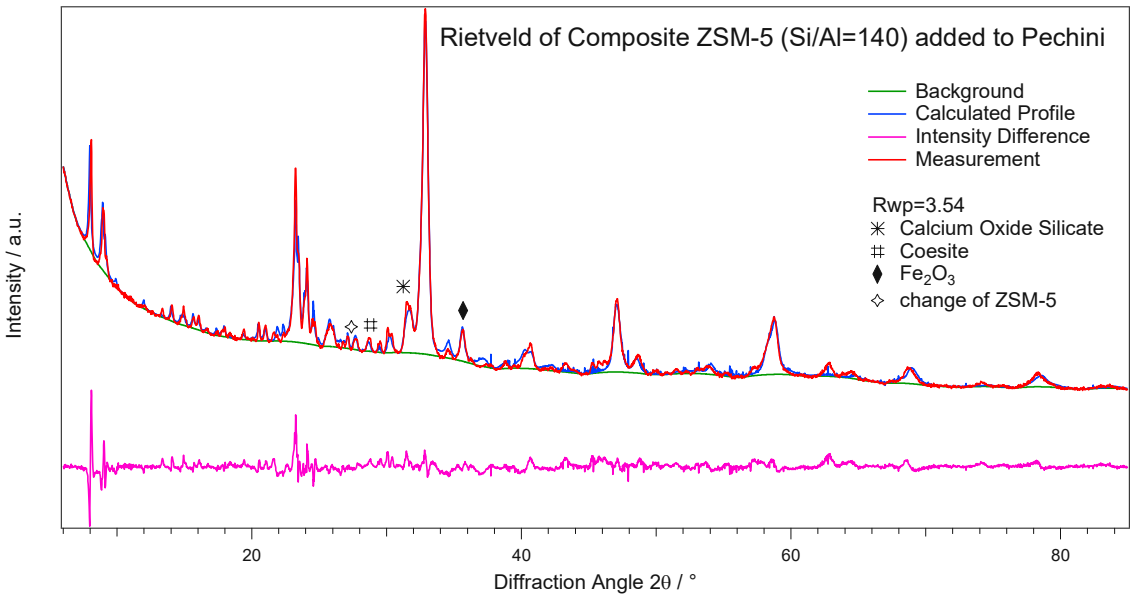

Figure 71: Rietveld refinement of XRD of composite with zeolite ZSM-5 "Si/Al=140 CBV28014" added to the Pechini synthesis, intense reflexes are discussed above

For composite preparation with ZSM-5 "pure Si" it was found that the zeolite structure is mostly destroyed and as already observed in the in-situ XRDs the formation of β-cristobalite was observed again (Figure 72). In the range from 27-29 ° changes of the zeolite or the formation of the zeolite to new phases (coesite) were observed but not further investigated.

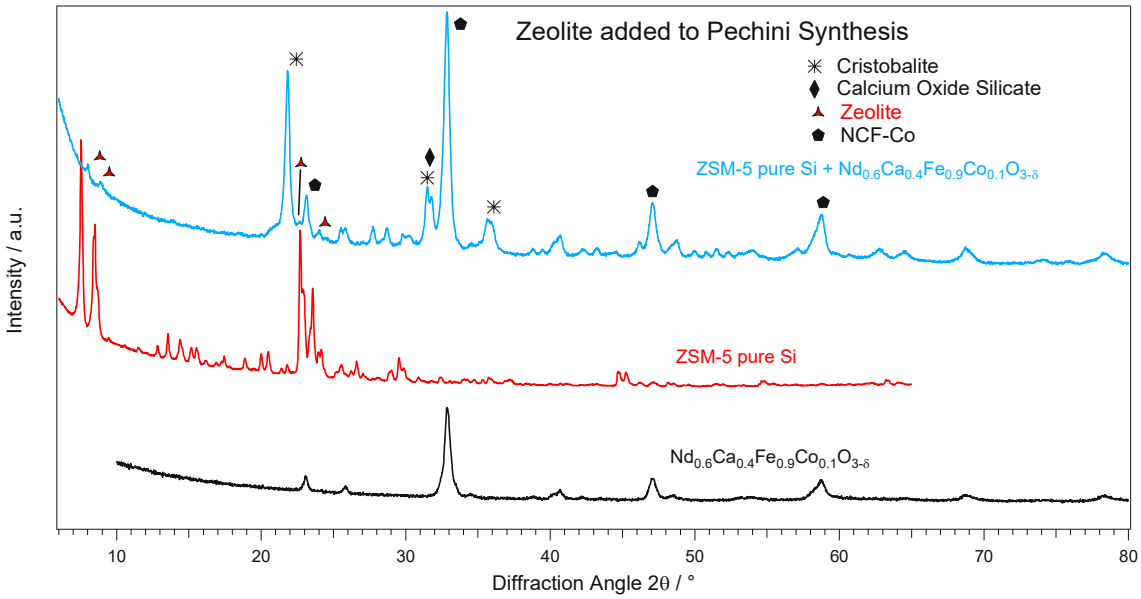

Figure 72: XRD of composite with zeolite ZSM-5 "pure Si" added to a Pechini synthesis

6.3.2 Catalytic Measurements and XRD after Reaction

Catalytic measurements with the composites were performed. The same parameters as for the pellets were used (see chapter "4.5.1 Experimental Parameters"). Again, an increase of the activity with increasing temperature due to reasons of thermodynamics and kinetics can be seen. For pure zeolites the specific activity is very low. For the composite with ZSM-5 "Si/Al=140" the specific activity is lower compared to the composite with ZSM-5 "pure Si", but it has to be kept in mind, that the measurement of ZSM-5 "Si/Al=140" was very close to the thermodynamic equilibrium. The measurement of ZSM-5 "pure Si" added to Pechini synthesis was done with a lower amount of catalyst (12.8 mg), hence farther

away from thermodynamic equilibrium and a higher specific activity was reached. Further measurements were conducted with the parameters used for catalytic measurements of the boehmite/NCF-Co sieve fractions and can be seen below.

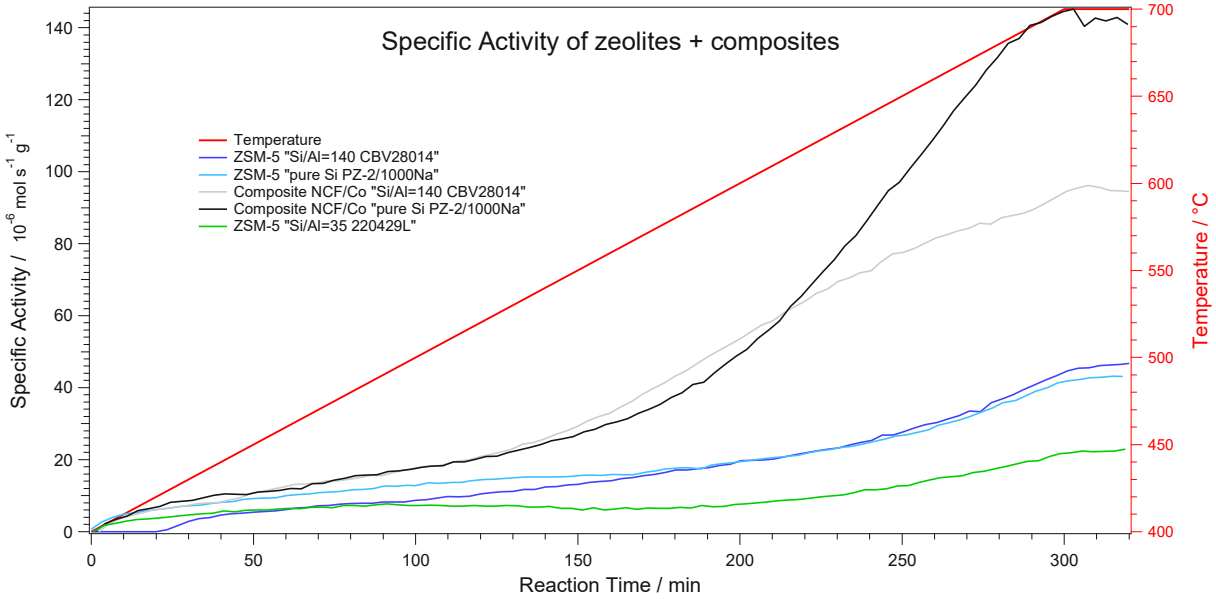

Figure 73: results of catalytic measurements, specific activity versus reaction time, the specific activity was calculated from produced CO and as normalization the mass of the catalyst (total) was used

After the reaction, XRDs of the catalysts which can be seen in Figure 74 and Figure 75 were recorded. Reflexes corresponding to iron are clearly visible for both composites. The other reflexes are already discussed above.

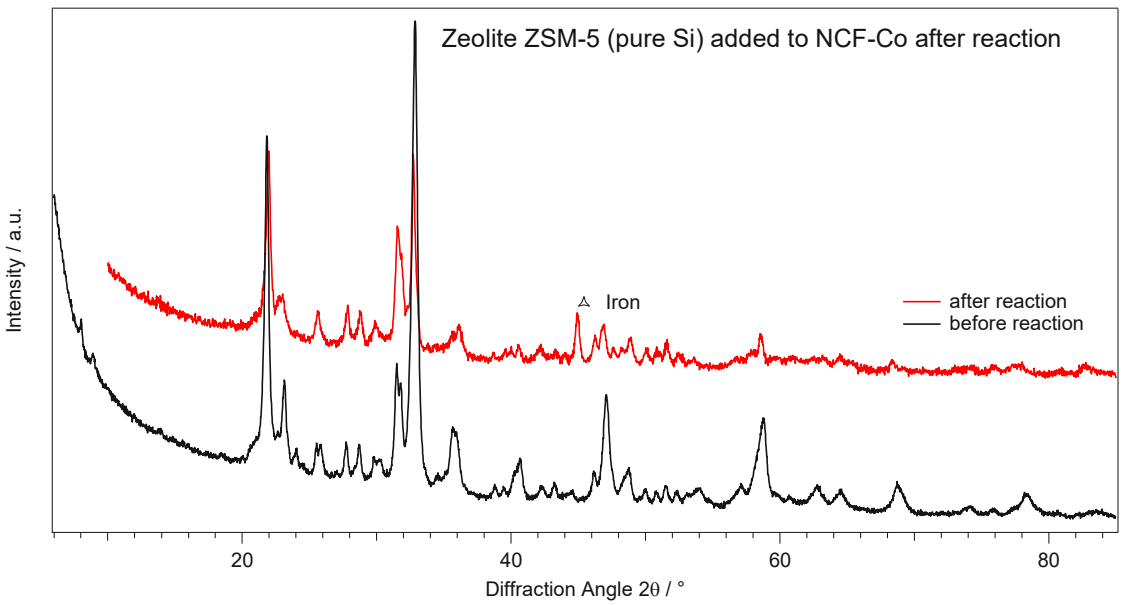

Figure 74: XRD of batch "NCF-Co/ZSM-5 pure Si 220518" after reaction

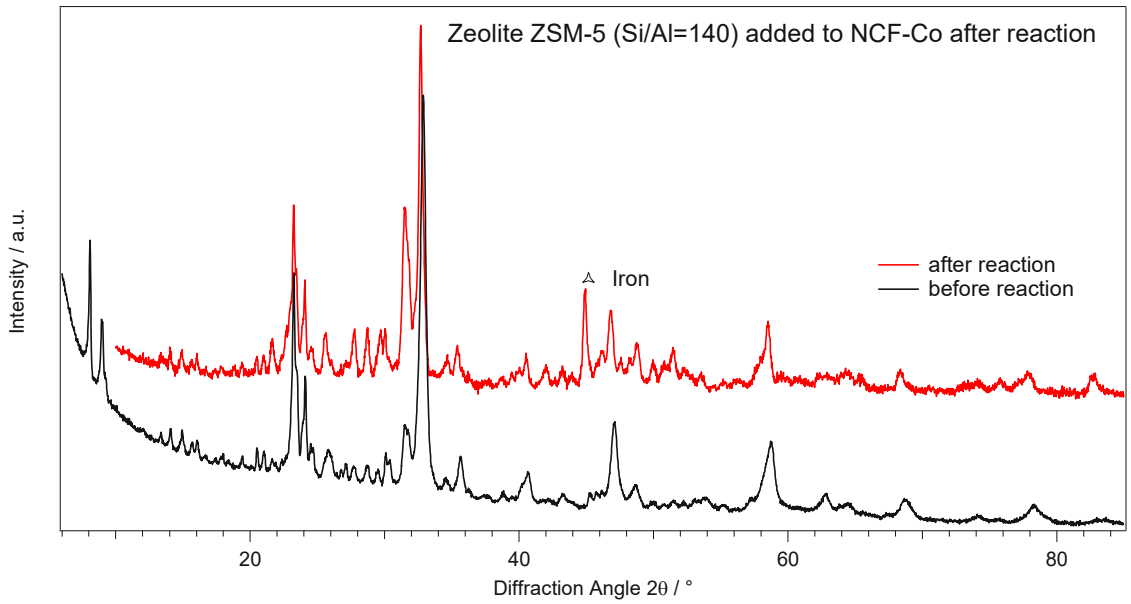

Figure 75: XRD of batch "NCF-Co/ZSM-5 CBV28014 (Si/Al=140) 220518" after reaction

6.4 NCF-Co added to Zeolite Synthesis

For the 2. approach of composite preparation it was tried adding the perovskite at different stages of the synthesis of the ZSM-5 zeolite. As a weight ratio $50/50$ for ZSM-5 (without crystal water)/NCF-Co was chosen. When adding the NCF-Co to the gel it was calculated how much solids are remaining after calcining for calculation of the amount of NCF-Co that should be added. For batch 220609A just a $50/50$ mixture of the masses of ZSM-5/NCF-Co was prepared. For batch 220922A a weight loss of 16.7 % as a result of loss of organic template and crystal water was assumed. In Figure 76 the prepared batches and when NCF-Co was added to the zeolite synthesis can be seen. In blue the typical course of the zeolite preparation as already described before can be seen. In black the different times where NCF-Co was added can be seen. The preparation of the zeolite was the same as already described before. As products grey powders, as it can be seen in Figure 77 exemplarily, were obtained.

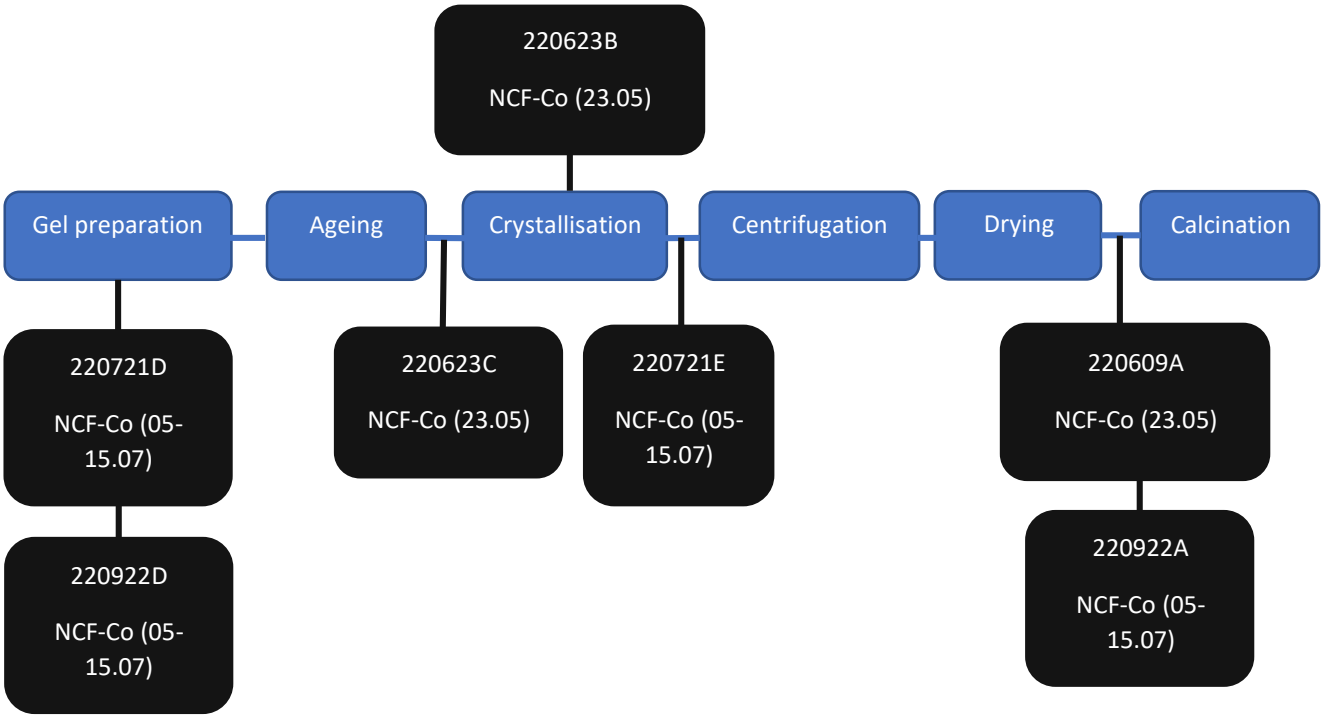

Figure 76: overview of classic zeolite preparation (blue), black boxes indicate the batches of the composites and at wich step NCF-Co was added to the zeolite synthesis

Figure 77: appearance of product of composite synthesis: batch 220623C

6.4.1 XRD of NCF-Co added to Zeolite Synthesis

XRDs of the composite materials were measured. As it can be seen in Figure 78, reflexes of both NCF-Co and zeolite appear in the diffractograms for all batches. Hence it can be concluded that the NCF-Co does not affect the zeolite formation in that manner that no zeolite would have formed at all. Furthermore, it was found that the reflex corresponding to the brownmillerite phase gets smaller when NCF-Co was added at an earlier stage in the zeolite synthesis. At a closer look one can also see, that the reflexes seem a bit shifted. To check if these shifts are random or consistently, Rietveld refinements were prepared.

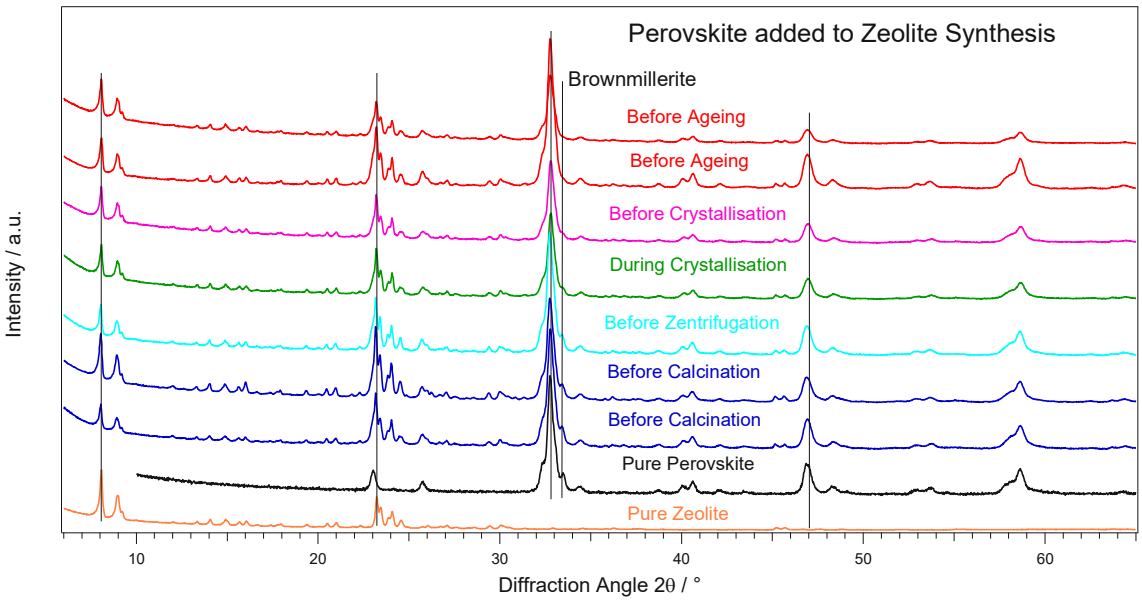

Figure 78: XRDs of different batches with NCF-Co added to the zeolite ZSM-5 synthesis, reflexes are from pure NCF-Co and ZSM-5, most intesive reflexes are indicated with vertical lines

For the Rietveld refinements the following parameters were refined:

Global Parameters:

- Specimen Displacement

NCF-Co (PDF-Code: 04-014-5430):

- Scale Factor
- B overall
- Cell Parameter: a, b, c
- Nd: occupancy (0.5-0.7), Ca: occupancy (0.2-0.3)
- B isotropic of all atoms
- Profile Variables: Cagliotti u, Cagliotti v, Cagliotti w, Peak Shape 1, Peak Shape 2, Peak Shape 3

Brownmillerite $Ca_2Fe_2O_5$ (PDF-Code: 04-008-6821):

- Scale Factor
- B overall
- Cell Parameter: a, b, c
- Profile Variables: Cagliotti u, Cagliotti v, Cagliotti w, Peak Shape 1, Peak Shape 2, Peak Shape 3

ZSM-5: (PDF-Code: 01-080-4532):

- Scale Factor
- B-overall
- Cell Parameter: a, b, c
- Profile Variables: Cagliotti u, Cagliotti v, Cagliotti w, Peak Shape 1, Peak Shape 2, Peak Shape 3
- Occupancy of O27-O38

The Rietveld refinements can be seen in Figure 79 and Figure 80 and coincide in principle well with the measurement. Deviations can be seen for the reflex of brownmillerite.

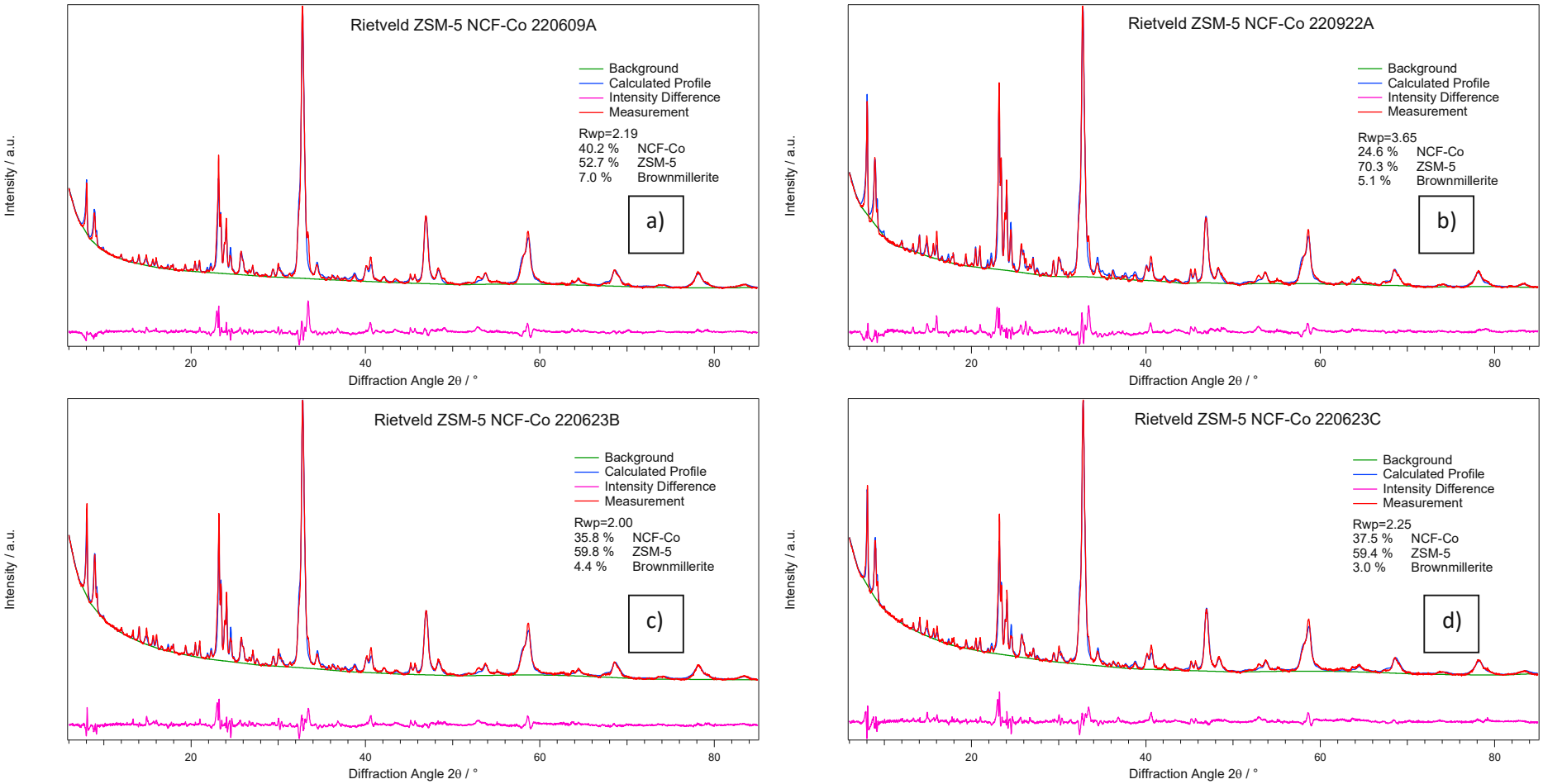

Figure 79: Rietveld refinements for batches a):220609A, b): 220922A, c): 220623B, d): 220623C

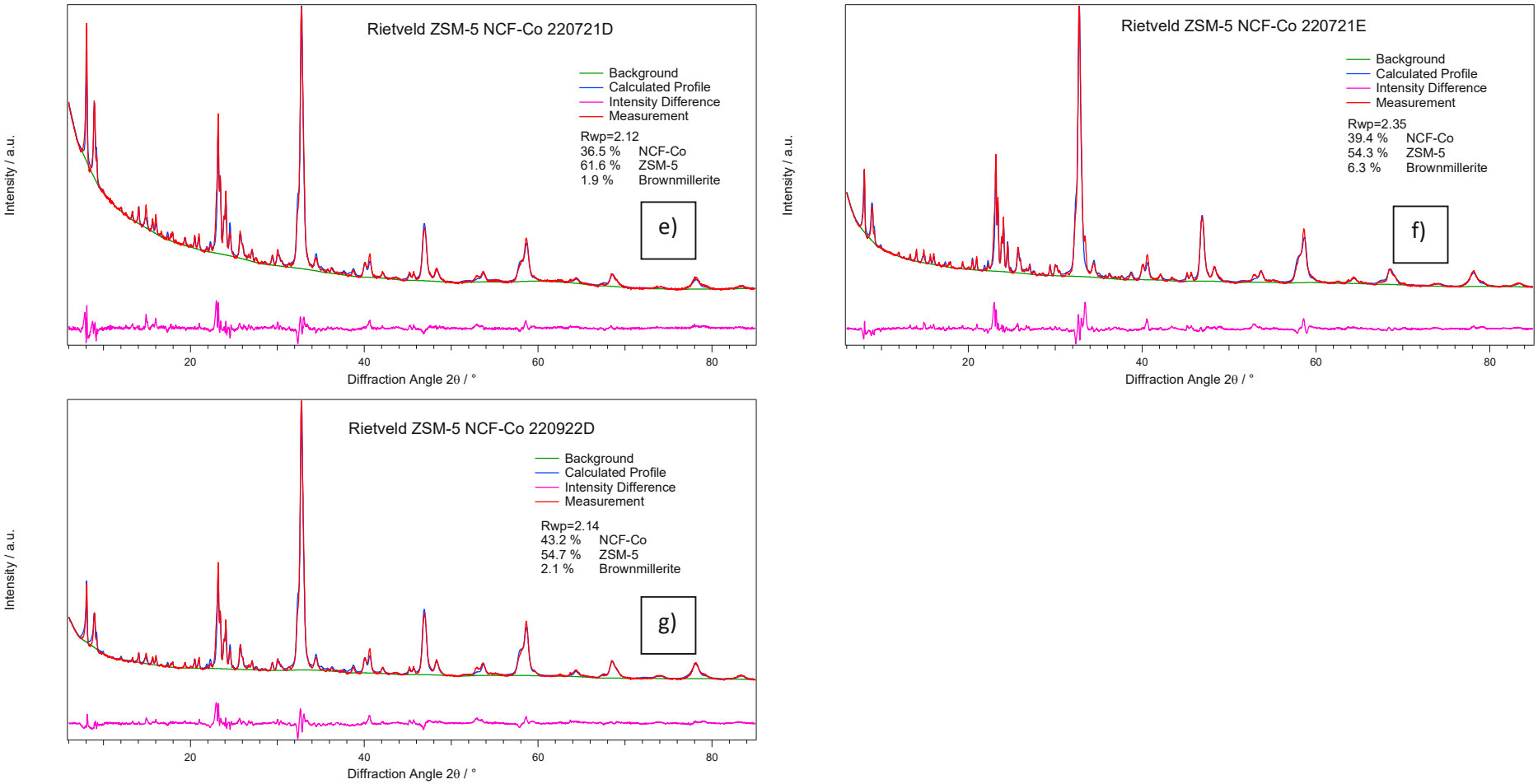

Figure 80: Rietveld refinements for batches e): 220721D, f): 220721E, g): 220922D

The cell parameters of NCF-Co gotten from the Rietveld refinement can be seen in Figure 81. The cell parameters of ZSM-5 can be seen in Figure 82. A relationship between time of NCF-Co addition to the synthesis and lattice parameter cannot be seen.

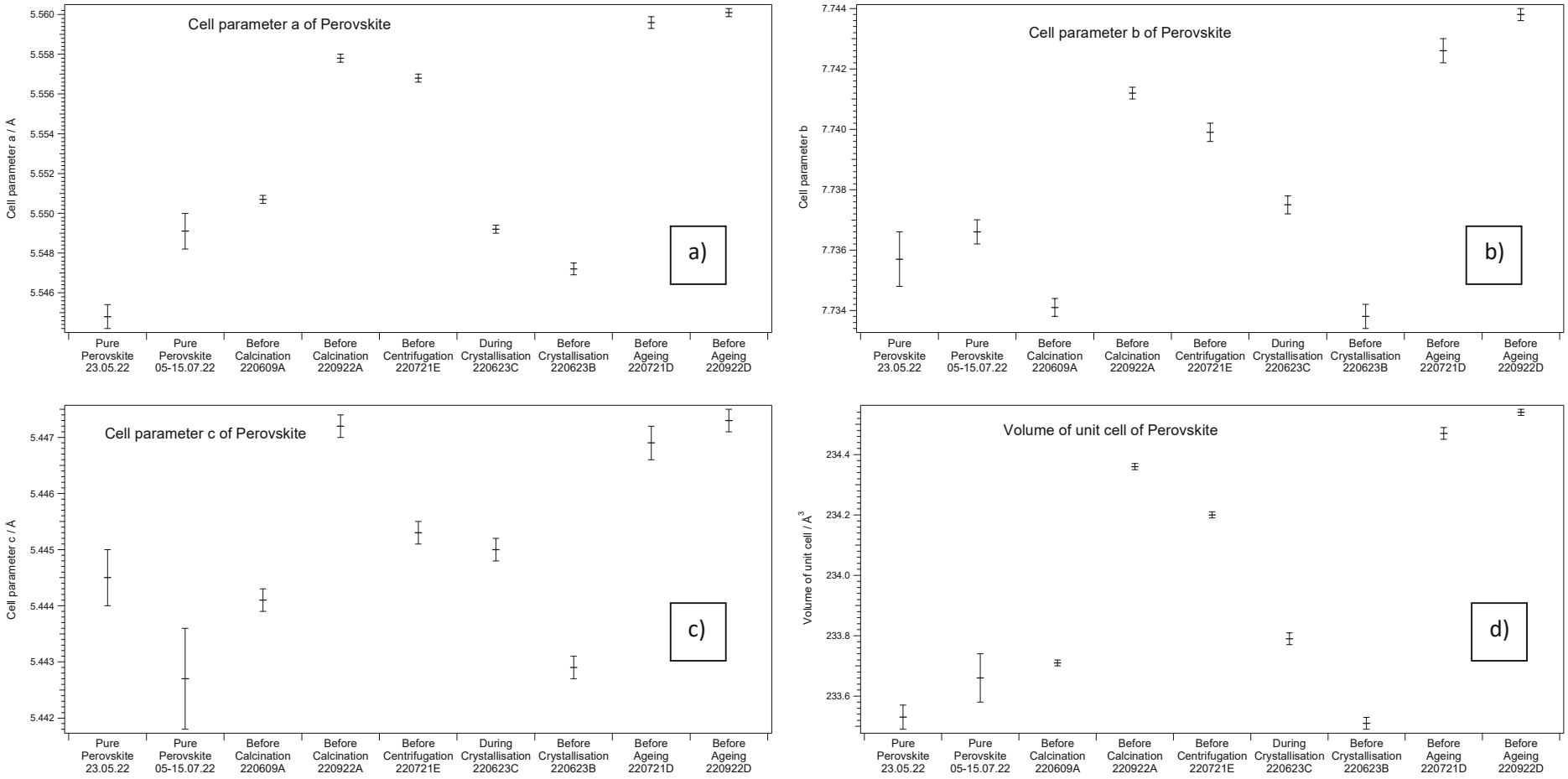

Figure 81: cell paramaters and volume of unit cell of the NCF-Co phase of the prepared batches; a): cell parameter a of NCF-Co; b): cell parameter b of NCF-Co; c): cell parameter c of NCF-Co; d): volume of the unit cell of NCF-Co; error bars from Rietveld refinement

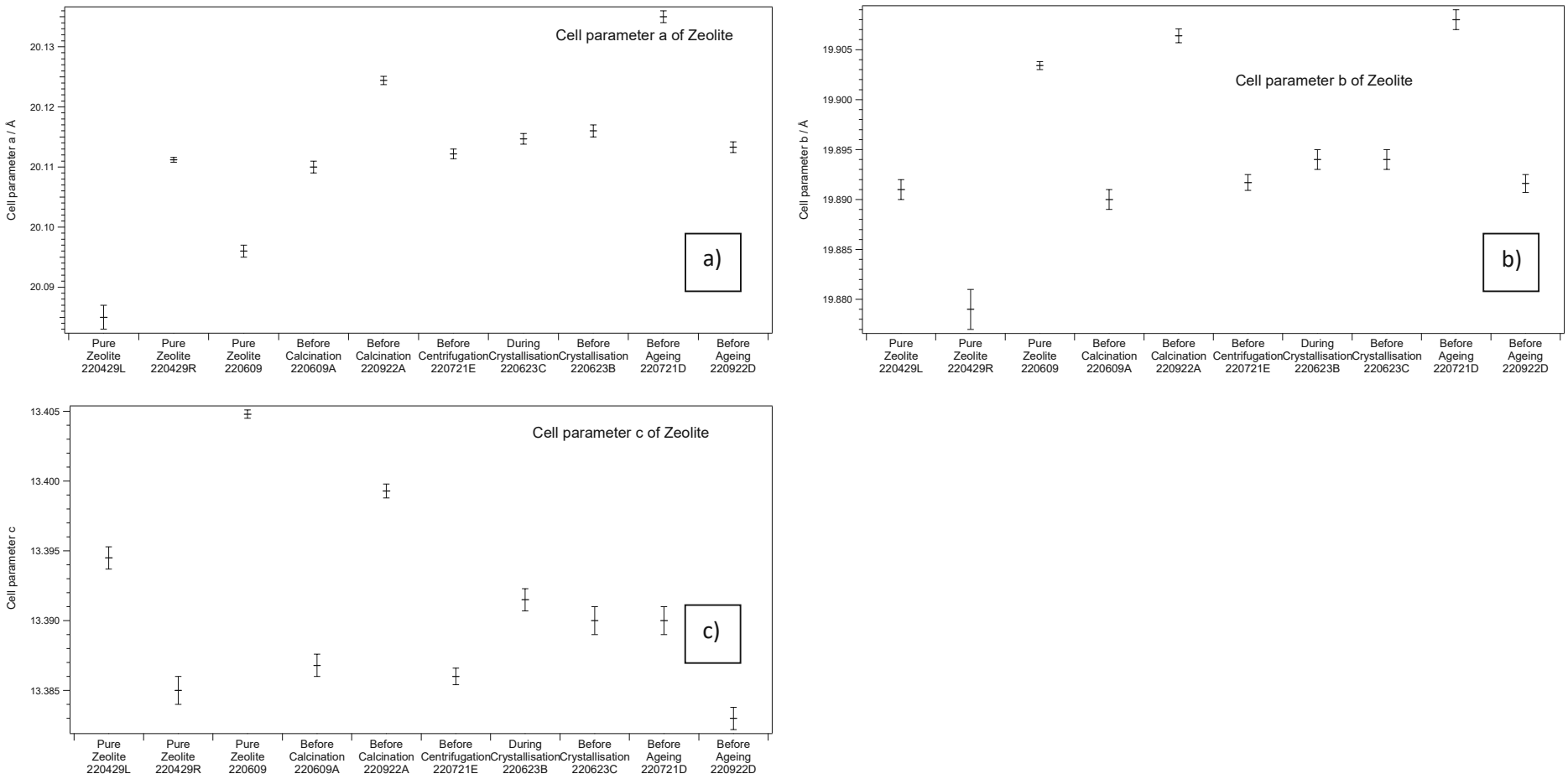

Figure 82: cell paramaters of the ZSM-5 phase of the prepared batches; a): cell parameter a of ZSM-5; b): cell parameter b of ZSM-5; c): cell parameter c of ZSM-5; error bars from Rietveld refinement

In Figure 83 the volume of the unit cell and the additional oxygen atoms per unit cell can be seen. Additional oxygen atoms mean, that crystal water is refined, but since H does not contribute much to the diffraction anyway only O were in the model used for the refinement. The volume of the unit cell seems random. Regarding the water content it might be the case, that the composites contain more crystal water compared to the pure zeolites.

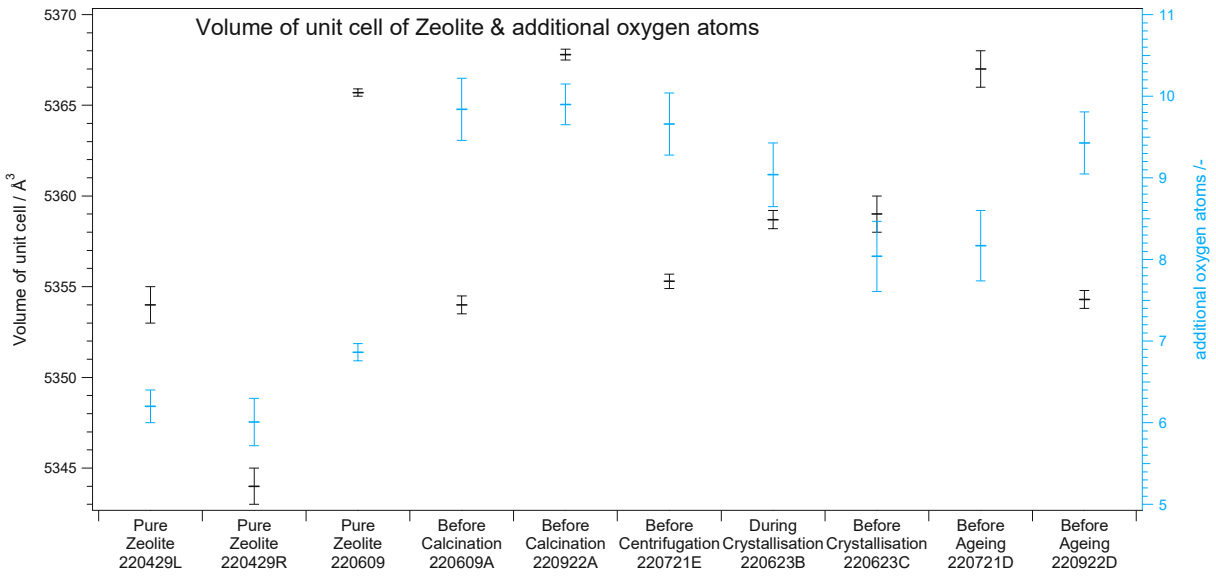

Figure 83: volume of unit cell of the zeolite and additional oxygen atoms per unit cell of the prepared batches; error bars from Rietveld refinement

For quantification of the brownmillerite content, the wt% brownmillerite were normalized to the wt% of NCF-Co phase to account for changes in different wt% between zeolite and the non-silica phases NCF-Co + brownmillerite. The results can be seen in Figure 84. As expected a decline of the brownmillerite content can be seen the earlier NCF-Co was added to the zeolite synthesis. Especially a big difference can be seen for the batches where NCF-Co was added during crystallization or earlier to the three batches where NCF-Co was added later. If NCF-Co was added before crystallization or even before ageing seems not to make a difference.

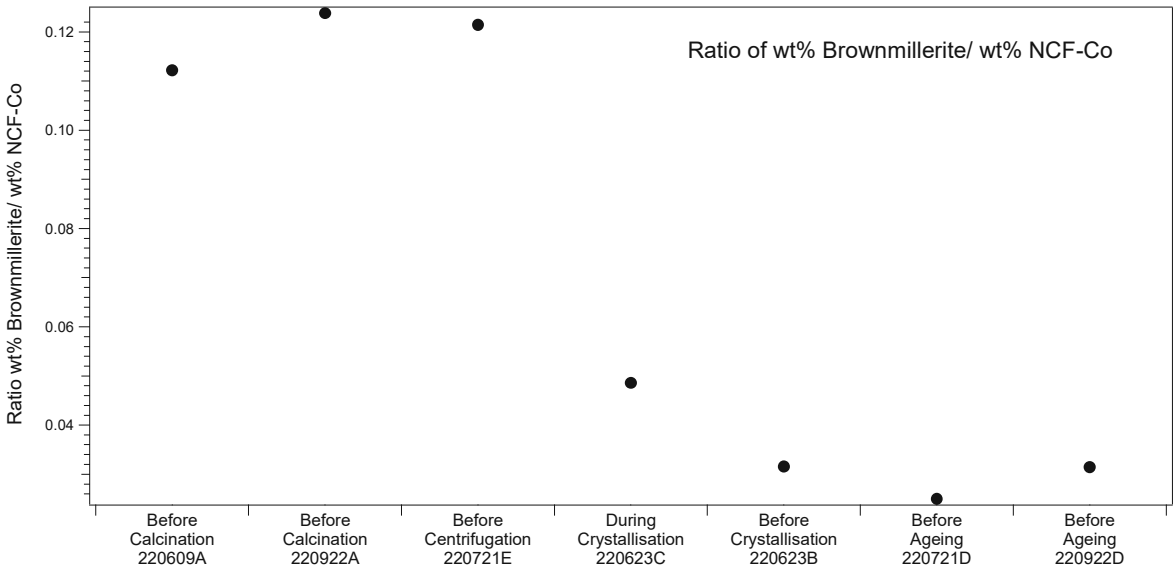

Figure 84: ratio of brownmillerite/NCF-Co for the different batches

6.4.2 SEM Measurements

The SEM images were recorded by Florian Schrenk. In Figure 85 SEM images of composites 220609A and 220922D can be seen. A NCF-Co phase (bigger particles) as well as a zeolite phase (small spherical particles) can be seen. The zeolite phase is also on top of the NCF-Co particles. Conclusions on the strength of interaction between both phases cannot be drawn.

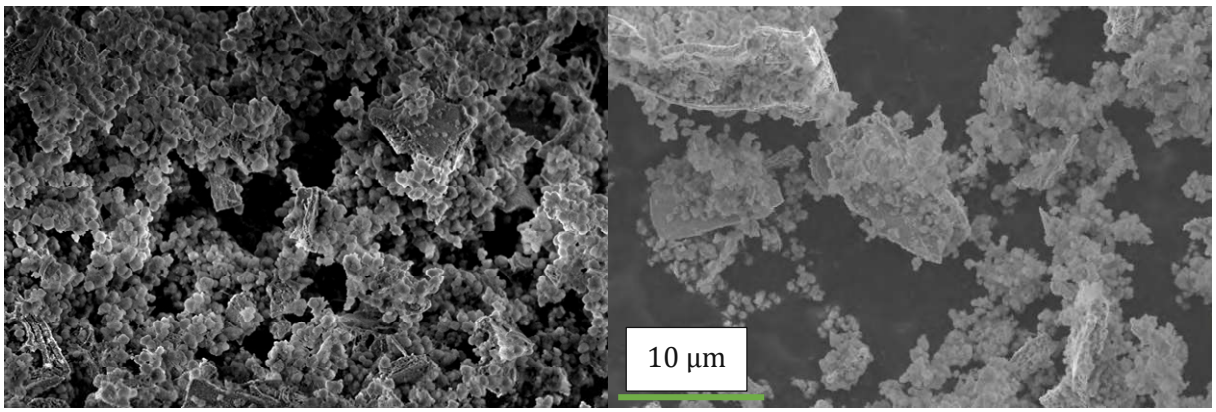

Figure 85: SEM images of: left: composite 220609A parameters: HV: 5 kV, mag 10k, WD 7.6 mm; right: composite 220922D, parameters: HV: 5 kV, mag 10k, WD 7.7 mm

6.4.3 X-ray Fluorescence of NCF-Co added to Zeolite Synthesis

The composition of the composites was determined by performing a borate pulp and subsequent X-ray fluorescence (XRF) analysis by Johannes Zbiral.

The results of the XRF measurements were given in wt% oxides normalized to $100\ \%$ for all elements that could be measured with XRF (raw data are given in the appendix).

Since the composite also contains elements that cannot be measured with XRF this has to be corrected. To do that at first the wt% were transformed into mol% for the metal oxides Me_nO_m that are part of the composite:

$$mol\%_i = \frac{\frac{wt\%_i}{M_i} \cdot n_i}{\sum_i \frac{wt\%_i}{M_i} \cdot n_i} \tag{7}$$

$wt\%_i$ .....weight percent of component i $(-)$

$mol\%_i$ .....molar percent of component i $(-)$

M_i .....molar weight of component i $(\frac{\mathrm{g}}{\mathrm{mol}})$

n_i.....subscript of metal i in formula Me_nO_m $(-)$

Then the following assumptions were made:

$$mol\%_{Nd} = (mol\%_{Ca} + mol\%_{Fe} + mol\%_{Co}) \cdot \frac{0.6}{1.4} \quad (8)$$

$$mol\%_{O,Zeo} = (mol\%_{Si} + mol\%_{Al}) \cdot \frac{13}{6} \quad (9)$$

$$mol\%_{O,Zeo\ cw} = (mol\%_{Si} + mol\%_{Al}) \cdot \frac{n_{H_2O}}{12} \quad (10)$$

$$mol\%_{O,NCF-Co} = (mol\%_{Nd} + mol\%_{Ca} + mol\%_{Fe} + mol\%_{Co}) \cdot \frac{2.8}{2} \quad (11)$$

$$mol\%_{H,Zeo} = (mol\%_{H,Zeo} + mol\%_{H,Zeo\ cw}) \cdot \frac{1}{3} \quad (12)$$

$$mol\%_{H,Zeo\ cw} = (mol\%_{Si} + mol\%_{Al}) \cdot \frac{n_{H_2O}}{6} \quad (13)$$

$mol\%_{O,Zeo}$ ..... molar percent of O from the zeolite structure itself including two water molecules bound as crystal water (–)

$mol\%_{O,Zeo\ cw}$ ..... molar percent of O from crystal water (–)

$mol\%_{O,NCF-Co}$ ..... molar percent of O from NCF-Co (–)

$mol\%_{H,Zeo}$ ..... molar percent of H from two water molecules bound as crystal water (–)

$mol\%_{H,Zeo\ cw}$ ..... molar percent of H from additional crystal water (–)

n_{H_2O} ..... number of additional water molecules in the zeolite structure according to XRD Rietveld refinements (–)

In the end it was again normalized:

$$mol\%_{i,new} = \frac{mol\%_i}{\sum_i mol\%_i} \tag{14}$$

$mol\%_{i,new}$ ..... molar percent of component i after consideration of elements not measured with XRF and new normalization (−)

And the wt% were calculated:

$$wt\%_{i,new} = \frac{mol\%_{i,new} \cdot M_i}{\sum_i mol\%_{i,new} \cdot M_i} \tag{15}$$

$wt\%_{i,new}$ ..... weight percent of component i after consideration of elements not measured with XRF and new normalization (−)

Then all wt% of the zeolite (Si, Al, O_{Zeo}, Na, H_{Zeo}) and NCF-Co (Nd, Ca, Fe, Co, $O_{NCF\text{-}Co}$) were summed up and the wt% of NCF-Co in the composite could be calculated. The results can be seen in Table 19. For an unknown reason batch 220721E deviates strongly from the other batches whereas the other ones seem to be in an acceptable range considering the method of preparation of the composites (evaporating water of the gel and difficulties weighing in fumed silica) and also uncertainties in the preparation of the samples for the XRF measurements and in the XRF measurement itself especially for low concentrations.

Table 19: results of XRF-measurements

Batch Name	Content NCF-Co (wt%)
220922D	43.2
220721D	39.9
220623C	39.8
220623B	42.1
220721E	46.6
220609A	44.3
220922A	40.8

6.5 Catalytic Measurements of Composites

6.5.1 Experimental parameters

The same experimental parameters as in “5.3 Experimental Parameters” were used.

6.5.2 Results and Discussion

Contrary to the measurements of the pellets with alumina hydrates, here about the same amount of the composite was used (≈ 38 mg). The exact ratio of zeolite/NCF-Co of the composites where NCF-Co was added to the zeolite synthesis was unknown at the time the reactor measurements were

conducted because no results from ICP-OES measurements were obtained due to the insolubility of the composites and the results from the XRF measurements were only gotten afterwards. It was tried to use the specific activity for comparison (Figure 86) but this deviations in the activity cannot be explained by these small differences as it can be seen in the XRDs. It was also the intention to measure at high yields and at high volumetric flows of H_2 and CO_2 which means high water production and this led to the already mentioned problems.

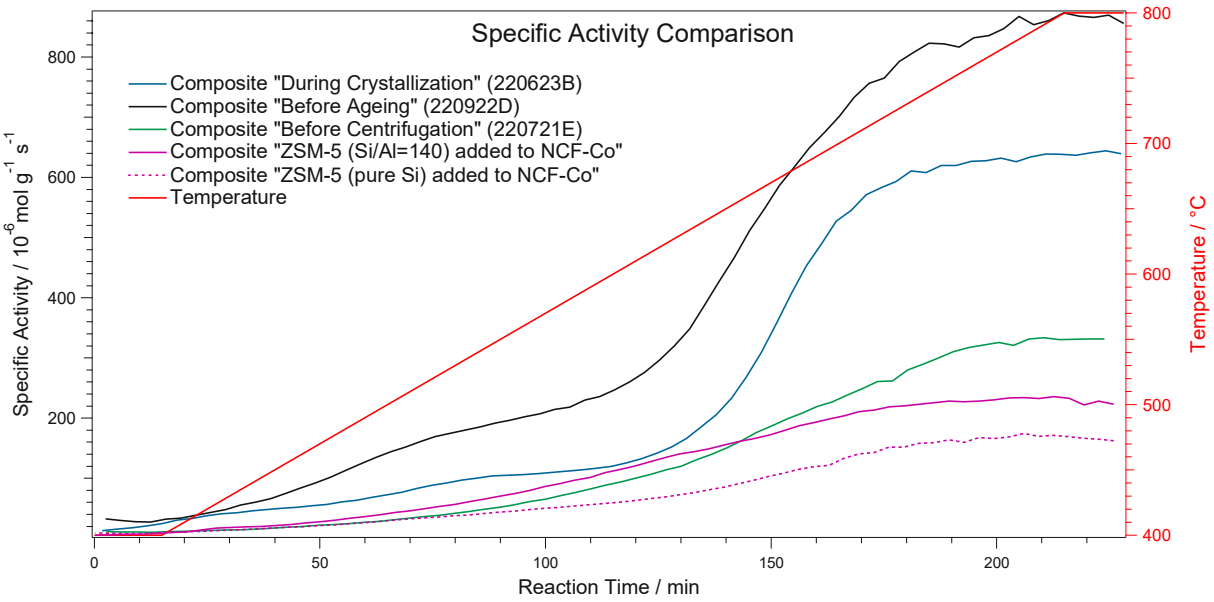

Figure 86: comparison of specific activity for composites of ZSM-5 and NCF-Co, specific activity was calculated from produced CO and normalized with the mass of the catalyst (only NCF-CO)

In Figure 87 the yields of the catalytic measurements can be seen. For the calculation of the yields no normalization is used. Due to the closeness to the thermodynamic equilibrium, the yield probably describes better how active a catalyst is. Anyhow the problems with condensing and later evaporating water was still there. Hence not much quantitative assessments can be made besides that catalyst "ZSM-5 (Si/Al=140) added to NCF-Co" is performing better than the rest in the temperature range of 550-650 °C. Other than that, only qualitative analysis can be made. It can be seen that for batches where NCF-Co was added early to the zeolite synthesis (batches 220623B and 220922D) the yields are flattened at a certain temperature (≈520 °C). Probably the zeolite blocks the NCF-Co and does not allow higher yields.

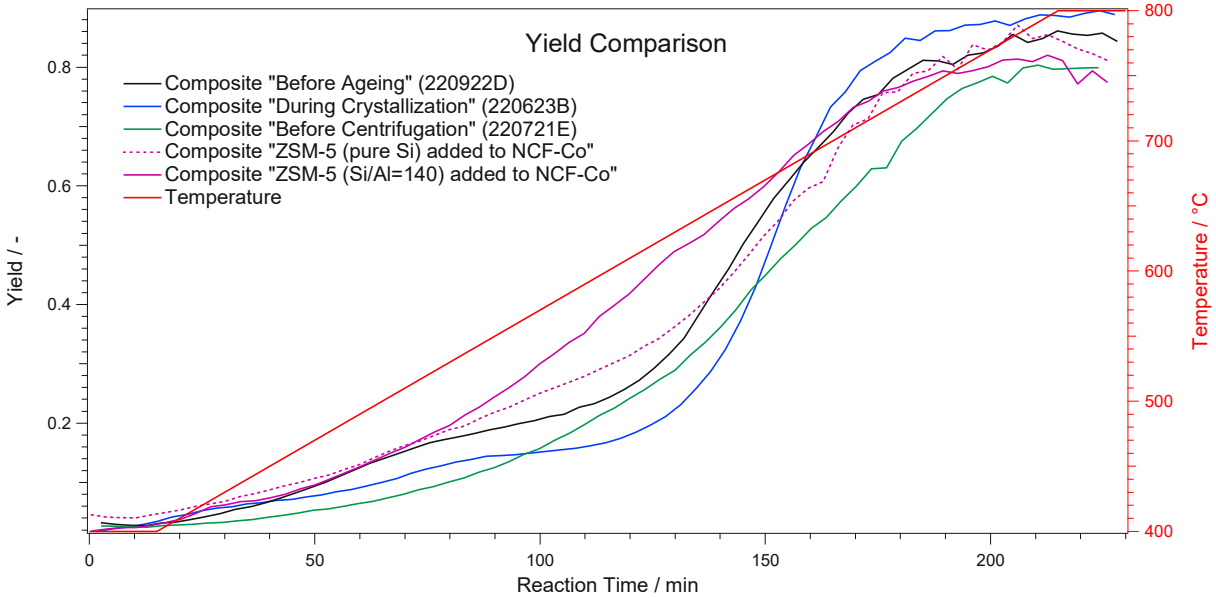

Figure 87: comparison of yields for composites of ZSM-5 and NCF-Co; yield of CO with respect to CO_2, calculated according to formula 3

Only CH_4 was detected by the GC as byproduct and considered for the calculation of the selectivity (see formula 5). In Figure 88 the selectivities towards CO of the composite batches can be seen. "ZSM-5 (pure Si) added to the Pechini synthesis" only exhibits a high selectivity at higher temperatures. Composites where NCF-Co was added to the zeolite synthesis showed high selectivities even at lower temperatures. Composite "ZSM-5 (Si/Al=140) added to NCF-Co synthesis" showed a different behavior. The selectivity is high for low temperatures decreases and reaches a minimum at about 520 °C and then rises till the end of the experiment.

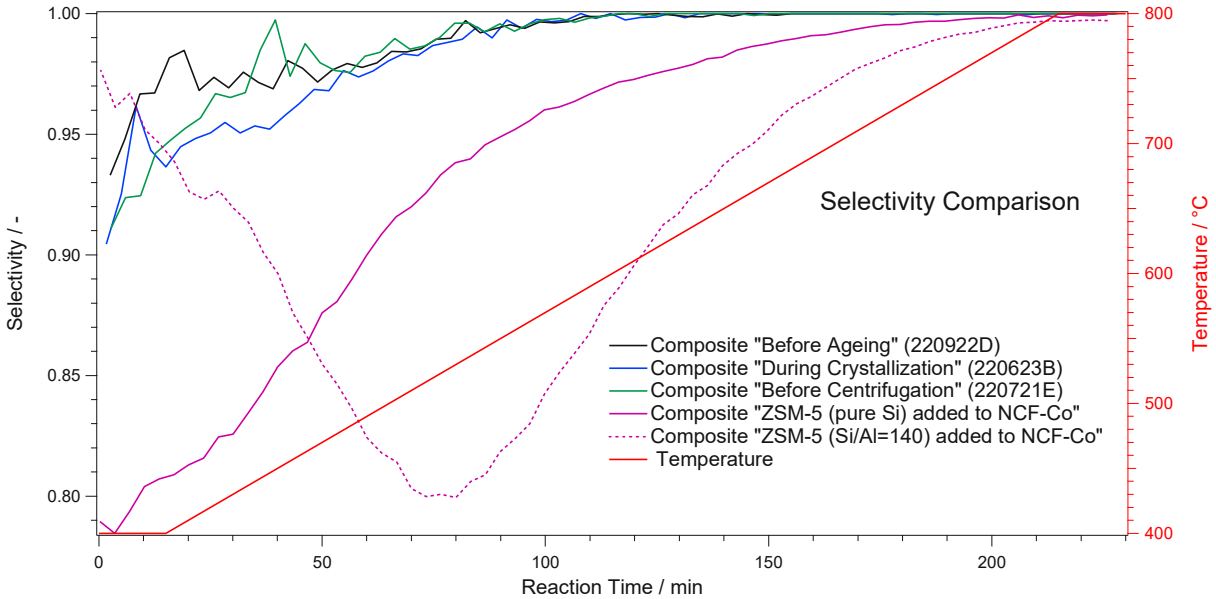

Figure 88: comparison of selectivity for composites of ZSM-5 and NCF-Co; selectivity towards CO, byproduct was CH_4

For the composites where zeolites were added to the Pechini synthesis exsolution was already confirmed (see 6.3.2). For NCF-Co added to the zeolite synthesis, XRDs after the reaction were measured (Figure 89, Figure 90 and Figure 91). This XRDs are again an overlap with SiO_2 because it was

hard to separate the two phases completely due to some smaller particles of SiO_2. A clear reflex corresponding to iron can be seen and exsolution is thus confirmed. Furthermore a calcium oxide silicate phase and in the range from 25-30° additional changes which cannot fully be explained, due to the fact that these phases only amount to low wt% and due to the general complexity of the mixture. It is probably a change of the zeolite itself but also changes to other phases like coesite for instance is a possibility. Changes in the range from 50-52° cannot be explained so far. A loss of brownmillerite phase for batches 220623B and 220721E was observed.

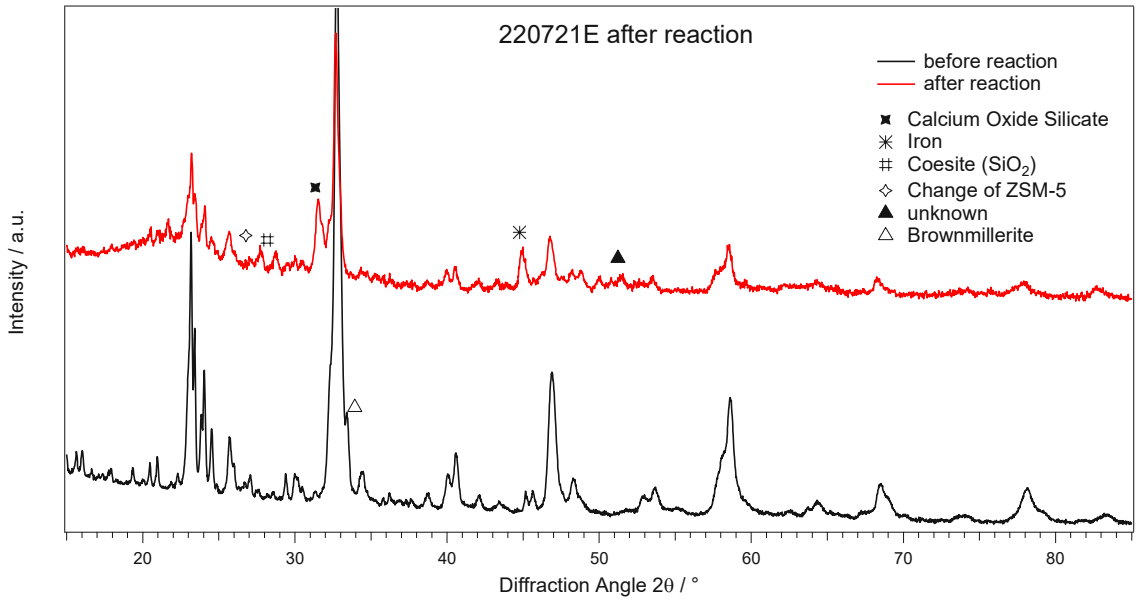

Figure 89: XRD recorded after reaction of composite 220721E

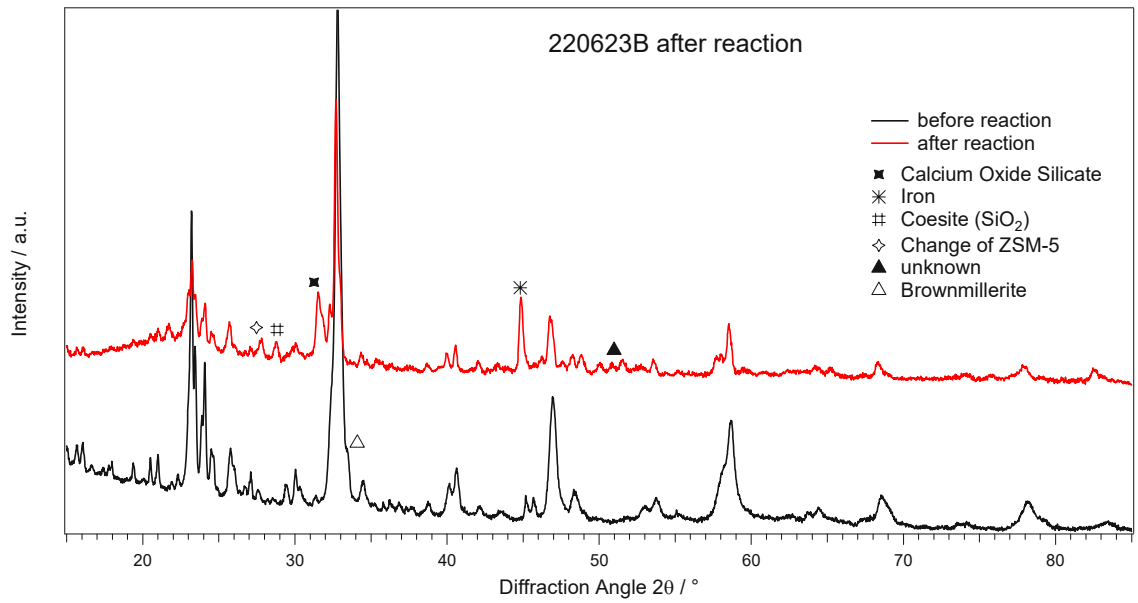

Figure 90: XRD recorded after reaction of composite 220623B

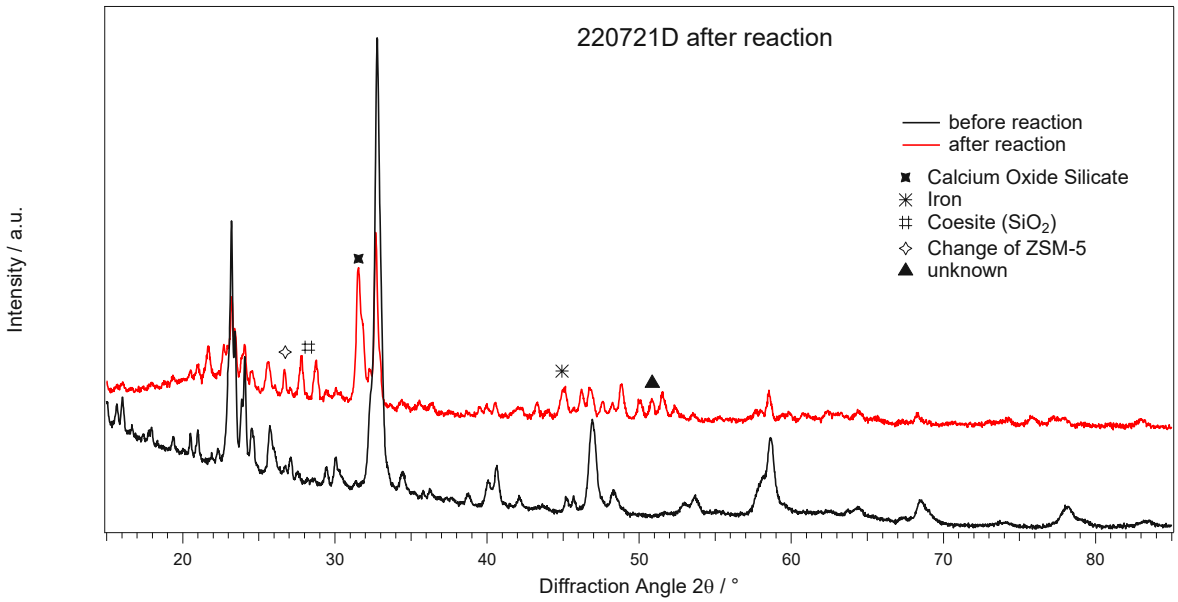

Figure 91: XRD recorded after reaction of composite 220721D

7 Summary & Discussion

For the pellets prepared with the porogens starch and graphite, which were sintered at different temperatures, it was found that higher porogen content and lower sintering temperatures increase the activity. This is a reasonable result since these pellets would be the ones for which high surface areas are expected. Pellets with Al_2O_3 as binder performed well in the catalytic tests.

For pellets produced with alumina hydrates and NCF-Co it was found that a higher boehmite content results in higher mechanical stability. A higher activity compared to pure alumina was confirmed but it was difficult to distinguish between the NCF-Co containing catalysts due to the problem of high water formation (condensing water in gas lines).

The preparation of pure MCM-22 and ZSM-5 zeolites with Si/Al=35 was successful, and the structures were confirmed with XRD. The ZSM-5 zeolite and two other ZSM-5 zeolites (ZSM-5 “pure Si” and ZSM-5 “Si/Al=140”) were tested for their stability in hot water vapor atmosphere via in-situ XRD. Two of these three zeolites were relatively stable (ZSM-5 “Si/Al=35” and ZSM-5 “Si/Al=140”) whereas for the zeolite ZSM-5 “pure Si” the formation of β-cristobalite was found. It is not fully clear why the “pure Si” zeolite is least stable because the water steam stability normally increases with higher Si/Al ratio. It is also worth to mention that it is not clear if the phase transformation happened because of the water vapor or just the temperature. One explanation for the formation might be because of different morphologies of the zeolites. Furthermore, it is interesting to note that β-cristobalite is normally not formed at these temperatures but due to the preordered structure of a zeolite it seems that its formation is possible.

For the preparation of composites two approaches were chosen:

- Zeolite added to the Pechini synthesis of NCF-Co
- NCF-Co added to zeolite synthesis

For the approach “Zeolite added to the Pechini synthesis” the formation of β-cristobalite and an almost completely destroyed zeolite was found for ZSM-5 “pure Si” whereas for ZSM-5 “Si/Al=140” a partly destruction of the ZSM-5 structure and formation of calcium oxide silicate was found. Besides these dominant phases also minor changes which cannot fully be confirmed like the formation of coesite and changes in the zeolite structure were found in the XRDs.

For the approach NCF-Co added to zeolite synthesis it was found in the XRDs that reflexes from both phases are present. A reduction of the brownmillerite phase was observed, when NCF-Co was added early in the course of the zeolite synthesis. The strength of the interaction between these two phases is still unclear.

In the catalytic tests the same problem as described above arose. Nevertheless, the qualitative assessment that an early addition of NCF-Co to the zeolite synthesis led to a flattening in the activity curve can be made. Ex-situ measurements of composites after the reaction were performed and revealed that calcium oxide silicate was formed for catalysts where NCF-Co was added to the zeolite synthesis. Furthermore minor changes in the zeolite structure and formation of other phases (like coesite) were observed.

For all catalysts which contain NCF-Co that were used in activity tests, exsolution was confirmed via ex-situ XRD.

8 Outlook

The composites must be analysed by other techniques to clarify the degree of interaction between zeolite and perovskite. Possible analysis methods would be solid-nuclear magnetic resonance (NMR) and infrared spectroscopy (IR).

In general, the approach of composite preparation where the zeolite is added to the Pechini synthesis would be more interesting in regards of getting to higher surface areas. The NCF-Co does not dissolve if added to the zeolite synthesis thus the surface area cannot really be increased. In regards of other properties like mechanical stability this preparation method still has some merit if it is possible to produce NCF-Co with higher surface area. If the composite preparation is done via adding zeolites to the NCF-Co synthesis, an increase in surface area could possibly happen if the zeolite acts as a nucleation point to the perovskite and this way of composite preparation is thus a reasonable approach if reaction conditions of the Pechini synthesis can be changed to less harshness. Possible approaches would be the synthesis using a deep eutectic solvent or in general reagents that dissolve in water could be used.

Shaping methods like extrusion or pelleting have to be performed with the composites.

Stability tests need to be performed with the composites, ideally even after the shaping process, and under humidity conditions closer to “real” rWGS conditions.

The catalytic activity has to be checked in a pilot scale reactor and very importantly the problem with condensing and later evaporating water has to be fixed.

9 Appendix

9.1 Experimental Details of Catalytic Measurements

The details about the catalytic measurements can be found in Table 20, Table 21 and Table 22.

Table 20: experimental details of catalytic experiments of pellets

Date	Sample	Amount (mg)
06.05.2022	PEL_019	27.9
11.05.2022	PEL_022	27.1
12.05.2022	PEL_023	26.7
13.05.2022	PEL_020	24.2
02.06.2022	PEL_026	33.4
07.06.2022	PEL_027	33.4
08.06.2022	PEL_029	22.1
09.06.2022	PEL_028	26.9
15.06.2022	PEL_026	37.4

Table 21: experimental details of catalytic experiments of zeolites and composites

Date	Sample	Amount (mg)
04.05.2022	ZSM-5 CBV28014	19.0
05.05.2022	ZSM-5 PZ-2/1000Na	20.6
24.05.2022	Composit NCF/Co CBV28014 (18.05.2022)	20.3
27.05.2022	Composit NCF/Co PZ-2/1000Na (18.05.2022)	12.8
13.06.2022	ZSM-5 220429	19.6

Table 22: experimental details of catalytic experiments of pellets with alumina hydrates and composites

Date	Sample	Amount Catalyst (mg)	Amount quartz glass (mg)	Total Amount (mg)
23.08.2022	blank: quartz glass	-	0.2257	0.2257
25.08.2022	0/100 Boehmite/NCF-Co	0.0204	0.2336	0.2540
26.08.2022	80/20 Boehmite/NCF-Co	0.0896	0.1602	0.2498
29.08.2022	100/0 Boehmite/NCF-Co	0.0820	0.1676	0.2496
29.08.2022	50/50 Boehmite/NCF-Co	0.0368	0.2132	0.2500
01.09.2022	Composite ZSM-5/NCF-Co 2220721E	0.0380	0.2118	0.2498
29.09.2022	80/20 Boehmite/NCF-Co	0.088	0.1623	0.2503
30.09.2022	0/100 Boehmite/NCF-Co	0.0198	0.2303	0.2501
29.11.2022	Composite ZSM-5/NCF-Co 220623B	0.0383	0.2119	0.2502
29.11.2022	Composite ZSM-5/NCF-Co 220721D	0.0383	0.212	0.2503
30.11.2022	Composite ZSM-5 (Si/Al=140)/NCF-Co (18.05.2022)	0.0379	0.2119	0.2498
01.12.2022	50/50 Boehmite/NCF-Co	0.0369	0.2131	0.25
02.12.2022	0/100 Boehmite/NCF-Co	0.0200	0.2302	0.2502
05.12.2022	Composite ZSM-5 (pure) NCF-Co (18.05.2022)	0.0396	0.2105	0.2501

9.2 Zeolite and zeolite NCF-Co synthesis

In Figure 92- Figure 111 the digitalized notes from the lab journal as weighed in amounts can be found for zeolite and composite preparation.

Recipe Zeolite MCM-22 SiO_2/Al_2O_3 = 70 V1

Start Date:	12.04.2022
Batch:	220412 MCM-22
Prepared by:	Richard Buchinger

Working Step	mass needed (g)	actual mass (g)	Start Time	End Time	Temperature (°C)	pH (-)
Fill distilled water into beaker	66.9022	66.906	12:55			-
Dissolve NaOH	0.5237	0.518	13:00			-
and/ or KOH during 15 minutes	0.4606	0.4566	13:05	13:15		
Gradually add $Al(OH)_3$	0.3205	0.334	13:15	13:20		-
Wait 15 minutes	-	-	13:20	13:35		-
Add HMI dropwise	5.3689	5.25	13:40	13:45		-
Add Fumed Silica	6.6781	6.79	13:50	13:55		-
Age at room temperatur for 24 hours under magnetic stirring	-	-	14:00	14:00		-
Transfer mixture in teflon-lined autoclave and heat to 150 °C for 10 days	-	-	13.04 15:30	25.04 7:40	150 °C	-
Vacuum filtrate the product	-	-	09:00			-
Wash with distilled water until pH below 8	-	-		11:00		7-8
Dry filtrate in an oven overnight at 60 °C	-	-	26.04		60 °C	-
Calcine in muffle furnace at 550 °C with heating rate 5 °C/min and hold for 6 hours	-	-	27.04		550 °C 6 h	-

Figure 92: digitalized notes from the lab journal of batch 220412 MCM-22

Recipe Zeolite MCM-22 SiO_2/Al_2O_3 = 70 V1

Start Date:	19.05.2022
Batch:	220519 MCM-22
Prepared by:	Richard Buchinger

Working Step	mass needed (g)	actual mass (g)	Start Time	End Time	Temperature (°C)	pH (-)
Fill distilled water into beaker	83.6278	83.71	14:20			-
Dissolve NaOH	0.6546	0.6546	14:25			-
and/ or KOH during 15 minutes	0.5757	0.560	14:27			
Gradually add $Al(OH)_3$	0.4007	0.401	14:45			-
Wait 15 minutes	-	-	14:45	15:00		-
Add HMI dropwise	6.7111	6.74	15:00			-
Add Fumed Silica	8.3476	8.3	15:10			-
add water	-	13.35				
Age at room temperatur for 24 hours under magnetic stirring	-	-	19.05 15:20	20.05 15:20		-
Transfer mixture in teflon-lined autoclave and heat to 150 °C for 10 days	-	-	20.05 16:00	30.05 16:00		-
Vacuum filtrate the product	-	-	31.05			-
Wash with distilled water until pH below 8	-	-	31.05			7-8
Dry filtrate in an oven overnight at 60 °C	-	-	31.05	2.06	120 °C	-
Calcine in muffle furnace at 550 °C with heating rate 5 °C/min and hold for 6 hours	-	-	02.06.2022		550 °C 6h	-

Figure 93: digitalized notes from the lab journal of batch 220519 MCM-22

Recipe Zeolite ZSM-5 SiO_2/Al_2O_3 = 70 V1

Start Date:	29.04.2022
Batch:	ZSM-5 220429
Prepared by:	Richard Buchinger

Working Step	mass needed (g)	actual mass (g)	Start Time	End Time	Temperature (°C)	pH (-)
Seed suspension S-1:						
Fill distilled water into beaker	4.9664	4.968	08:34			-
add EtOH	3.2149	3.2179	08:36			-
add TPAOH solution	3.4335	3.43	08:38			-
add TEOS dropwise while stirring	3.6354	3.652	08:40			-
homogenize at roomtemperature for 2 hours	-	-	08:45	10:45		-
transfer into teflon lined autoclave	-					-
treat hydrothermally at 100 °C for 96 hours	-	-	29.04 10:50	05.05 12:45	100 °C	-
cool down to room temperature	-	-				-
nano-sized ZSM-5 aggregates:						
Fill distilled water into beaker	47.8401	47.84	15:50			-
Dissolve NaOH in water	1.0815	1.085	16:10			-
dissolve NaAlO2 in water	0.3048	0.3054	16:15			
dissolve CTAB in water	1.0589	1.0588	16:20			-
stir for 0,5 hours	-	-	16:20	16:50		-

Figure 94: digitalized notes from the lab journal of batch 220429 ZSM-5 part 1

add S-1 gel dropwise	10.1668	10.17	16:50	17:05		-
Working Step	mass needed (g)	actual mass (g)	Start Time	End Time	Temperature (°C)	pH (-)
prepare silica sol: silica	7.8192	7.822	17:05			-
water and add silica sol dropwise	11.7288	20.42		17:10		
stir for 2 hours			17:10	19:10		
transfer into teflon lined autoclave and age for 12-14 hours at 120 °C			09.05 19:20	10.05 8:00	120 °C	
crystallize at 170 °C for 24 hours			10.05 9:00	11.05 9:00	170 °C	
centrifuge and wash with distilled water until pH about 7			11:00	14:00		7
dry at 60 °C for 12 hours			11.05 15:30		60 °C	
calcine at 550 °C for 6 hours			12.05		550 °C	

Figure 95: digitalized notes from the lab journal of batch 220429 ZSM-5 part 2

Recipe Zeolite ZSM-5 SiO_2/Al_2O_3 = 70 V1

Start Date:	09.06.2022
Batch:	ZSM-5 220609
Prepared by:	Richard Buchinger

Working Step	mass needed (g)	actual mass (g)	Start Time	End Time	Temperature (°C)	pH (-)
Seed suspension S-1:						
Fill distilled water into beaker	4.9664	4.97	13:13			-
add EtOH	3.2149	3.217				-
add TPAOH solution	3.4335	3.445				-
add TEOS dropwise while stirring	3.6354	3.645		13:25		-
homogenize at roomtemperature for 2 hours	-	-	13:30	15:30		-
transfer into teflon lined autoclave	-					-
treat hydrothermally at 100 °C for 96 hours	-	-	15:38	15:40 (13.06)	100 °C	-
cool down to room temperature	-	-				-
nano-sized ZSM-5 aggregates:						
Fill distilled water into beaker	47.8401	47.885	15:55			-
Dissolve NaOH in water	1.0815	1.09				-
dissolve NaAlO2 in water	0.3048	0.302				
dissolve CTAB in water	1.0589	1.063				-
stir for 0,5 hours	-	-	16:07	16:37		-
add S-1 gel dropwise	10.1668	10.179				-

Figure 96: digitalized notes from the lab journal of batch 220609 ZSM-5+NCF-Co part 1

Working Step	mass needed (g)	actual mass (g)	Start Time	End Time	Temperature (°C)	pH (-)
prepare silica sol: silica	7.8192	7.843				-
water and add silica sol dropwise	11.7288	20.53		16:49		
stir for 2 hours			16:49	18:59		
transfer into teflon lined autoclave and age for 12-14 hours at 120 °C			13.06 19:20	14.06 8:33		
crystallize at 170 °C for 24 hours			14.06 9:21	15.06 9:23		
centrifuge and wash with distilled water until pH about 7			15.06			
dry at 60 °C for 12 hours			15.06	16.06		
calcine at 550 °C for 6 hours			16.06	17.06		

Figure 97: digitalized notes from the lab journal of batch 220609 ZSM-5+NCF-Co part 2

Recipe Zeolite ZSM-5 SiO_2/Al_2O_3 = 70 V1

Start Date:	09.06.2022
Batch:	ZSM-5 220609A
Prepared by:	Richard Buchinger

Working Step	mass needed (g)	actual mass (g)	Start Time	End Time	Temperature (°C)	pH (-)
Seed suspension S-1:						
Fill distilled water into beaker	4.9664	4.97	13:13			-
add EtOH	3.2149	3.217	13:15			-
add TPAOH solution	3.4335	3.445	13:20			-
add TEOS dropwise while stirring	3.6354	3.645	13:25	13:30		-
homogenize at roomtemperature for 2 hours	-	-	13:30	15:30		-
transfer into teflon lined autoclave	-					-
treat hydrothermally at 100 °C for 96 hours	-	-	09.06 15:38	15:40 13.06	100 °C	-
cool down to room temperature	-	-				-
nano-sized ZSM-5 aggregates:						
Fill distilled water into beaker	47.8401	47.885	15:55			-
Dissolve NaOH in water	1.0815	1.09	16:00			-
dissolve NaAlO2 in water	0.3048	0.302	16:03			
dissolve CTAB in water	1.0589	1.063	16:07			-
stir for 0,5 hours	-	-	16:07	16:37		-
add S-1 gel dropwise	10.1668	10.179	16:40	16:43		-

Figure 98: digitalized notes from the lab journal of batch 220609A ZSM-5+NCF-Co part 1

Working Step	mass needed (g)	actual mass (g)	Start Time	End Time	Temperature (°C)	pH (-)
prepare silica sol: silica	7.8192	7.843				-
water and add silica sol dropwise	11.7288	20.53		16:49		
stir for 2 hours			16:49	18:59		
transfer into teflon lined autoclave and age for 12-14 hours at 120 °C			13.06 19:20	14.06 8:33	120 °C	
crystallize at 170 °C for 24 hours			14.06 9:21	15.06 9:23	170 °C	
centrifuge and wash with distilled water until pH about 7			15.06			
dry at 60 °C for 12 hours			15.06	16.06	60 °C	
Prepare mixture of Perovskite and		1.539				
Zeolite		1.539				
calcine at 550 °C for 6 hours			16.06	17.06	550 °C 6h	

Figure 99: digitalized notes from the lab journal of batch 220609A ZSM-5+NCF-Co part 2

Recipe Zeolite ZSM-5 SiO_2/Al_2O_3 = 70 V1

Start Date:	23.06.2022
Batch:	ZSM-5 220623B
Prepared by:	Richard Buchinger

Working Step	mass needed (g)	actual mass (g)	Start Time	End Time	Temperature (°C)	pH (-)
Seed suspension S-1:						
Fill distilled water into beaker	4.9664	5.022	13:50			-
add EtOH	3.2149	3.215				-
add TPAOH solution	3.4335	3.516				-
add TEOS dropwise while stirring	3.6354	3.642		14:10		-
homogenize at roomtemperature for 2 hours	-	-	14:10	16:10		-
transfer into teflon lined autoclave	-					-
treat hydrothermally at 100 °C for 96 hours	-	-	16:13	16:15	100 °C	-
cool down to room temperature	-	-				-
nano-sized ZSM-5 aggregates:						
Fill distilled water into beaker	23.9200	23.978	16:00			-
Dissolve NaOH in water	0.5408	0.539				-
dissolve NaAlO2 in water	0.1524	0.163				
dissolve CTAB in water	0.5294	0.534				-
stir for 0,5 hours	-	-	16:10	16:40		-
add S-1 gel dropwise	5.0834	5.08				-

Figure 100: digitalized notes from the lab journal of batch 220623B ZSM-5+NCF-Co part 1

Working Step	mass needed (g)	actual mass (g)	Start Time	End Time	Temperature (°C)	pH (-)
prepare silica sol: silica	3.9096	4.195				-
water and add silica sol dropwise	5.8644	12.3		16:55		
stir for 2 hours			16:55	18:55		
transfer into teflon lined autoclave and age for 12-14 hours at 120 °C		15.54	19:01	08:00	120 °C	
crystallize at 170 °C for 24 hours			08:00	10:00	170 °C	
add Perovskite		1.449				
centrifuge and wash with distilled water until pH about 7						7
dry at 60 °C for 12 hours					60 °C	
calcine at 550 °C for 6 hours					550 °C 6h	

Figure 101: digitalized notes from the lab journal of batch 220623B ZSM-5+NCF-Co part 2

Recipe Zeolite ZSM-5 SiO_2/Al_2O_3 = 70 V1

Start Date:	23.06.2022
Batch:	ZSM-5 220623C
Prepared by:	Richard Buchinger

Working Step	mass needed (g)	actual mass (g)	Start Time	End Time	Temperature (°C)	pH (-)
Seed suspension S-1:						
Fill distilled water into beaker	4.9664	5.022	13:50			-
add EtOH	3.2149	3.215				-
add TPAOH solution	3.4335	3.516				-
add TEOS dropwise while stirring	3.6354	3.642		14:10		-
homogenize at roomtemperature for 2 hours	-	-	14:10	16:10		-
transfer into teflon lined autoclave	-					-
treat hydrothermally at 100 °C for 96 hours	-	-	16:13	16:15	100 °C	-
cool down to room temperature	-	-				-
nano-sized ZSM-5 aggregates:						
Fill distilled water into beaker	23.9200	23.978	16:00			-
Dissolve NaOH in water	0.5408	0.539				-
dissolve NaAlO2 in water	0.1524	0.163				
dissolve CTAB in water	0.5294	0.534				-
stir for 0,5 hours	-	-	16:10	16:40		-
add S-1 gel dropwise	5.0834	5.08				-

Figure 102: digitalized notes from the lab journal of batch 220623C ZSM-5+NCF-Co part 1

Working Step	mass needed (g)	actual mass (g)	Start Time	End Time	Temperature (°C)	pH (-)
prepare silica sol: silica	3.9096	4.195				-
water and add silica sol dropwise	5.8644	12.3		16:55		
stir for 2 hours			16:55	18:55		
transfer into teflon lined autoclave and age for 12-14 hours at 120 °C		15.37	27.06 19:00	28.06 8:00	120 °C	
add Perovskite		1.435				
crystallize at 170 °C for 24 hours			28.06 9:00	29.06 10:30	170 °C	
centrifuge and wash with distilled water until pH about 7			29.06			7
dry at 60 °C for 12 hours			29.06	30.06	60 °C	
calcine at 550 °C for 6 hours			30.06		550 °C 6h	

Figure 103: digitalized notes from the lab journal of batch 220623C ZSM-5+NCF-Co part 2

Recipe Zeolite ZSM-5 SiO_2/Al_2O_3 = 70 V1

Start Date:	21.07.2022
Batch:	ZSM-5 220721D
Prepared by:	Richard Buchinger

Working Step	mass needed (g)	actual mass (g)	Start Time	End Time	Temperature (°C)	pH (-)
Seed suspension S-1:						
Fill distilled water into beaker	2.4832	2.506	13:10			-
add EtOH	1.6075	1.61				-
add TPAOH solution	1.7167	1.713				-
add TEOS dropwise while stirring	1.8177	1.821		13:20		-
homogenize at roomtemperature for 2 hours	-	-	13:20	16:00		-
transfer into teflon lined autoclave	-					-
treat hydrothermally at 100 °C for 96 hours	-	-	16:30	16:30	100 °C	-
cool down to room temperature	-	-				-
nano-sized ZSM-5 aggregates:						
Fill distilled water into beaker	23.9200	24.02	14:50			-
Dissolve NaOH in water	0.5408	0.54				-
dissolve NaAlO2 in water	0.1524	0.158				
dissolve CTAB in water	0.5294	0.53				-
stir for 0,5 hours	-	-	15:00	15:40		-
add S-1 gel dropwise	5.0834	5.16				-

Figure 104: digitalized notes from the lab journal of batch 220721D ZSM-5+NCF-Co part 1

Working Step	mass needed (g)	actual mass (g)	Start Time	End Time	Temperature (°C)	pH (-)
prepare silica sol: silica	3.9096	3.98				-
water and add silica sol dropwise	5.8644	12.3		15:45		
stir for 2 hours			15:45	17:30		
Gel and		16.2				
Perovskite		1.44				
stir for 20 min			17:30	17:50		
transfer into teflon lined autoclave and age for 12-14 hours at 120 °C			18:10	07:35	120 °C	
crystallize at 170 °C for 24 hours			26.07 8:35	27.07 8:35	170 °C	
centrifuge and wash with distilled water until pH about 7			27.05			7
dry at 60 °C for 12 hours			27.05	28.05		
calcine at 550 °C for 6 hours			28.05	29.05	550 °C 6h	

Figure 105: digitalized notes from the lab journal of batch 220721D ZSM-5+NCF-Co part 2

Recipe Zeolite ZSM-5 SiO_2/Al_2O_3 = 70 V1

Start Date:	21.07.2022
Batch:	ZSM-5 220721E
Prepared by:	Richard Buchinger

Working Step	mass needed (g)	actual mass (g)	Start Time	End Time	Temperature (°C)	pH (-)
Seed suspension S-1:						
Fill distilled water into beaker	2.4832	2.506	13:10			-
add EtOH	1.6075	1.61				-
add TPAOH solution	1.7167	1.713				-
add TEOS dropwise while stirring	1.8177	1.821		13:20		-
homogenize at roomtemperature for 2 hours	-	-	13:20	16:00		-
transfer into teflon lined autoclave	-					-
treat hydrothermally at 100 °C for 96 hours	-	-	16:30	16:30	100 °C	-
cool down to room temperature	-	-				-
nano-sized ZSM-5 aggregates:						
Fill distilled water into beaker	23.9200	24.02	14:50			-
Dissolve NaOH in water	0.5408	0.54				-
dissolve NaAlO2 in water	0.1524	0.158				
dissolve CTAB in water	0.5294	0.53				-
stir for 0,5 hours	-	-	15:00	15:40		-
add S-1 gel dropwise	5.0834	5.16				-

Figure 106: digitalized notes from the lab journal of batch 220721E ZSM-5+NCF-Co part 1

Working Step	mass needed (g)	actual mass (g)	Start Time	End Time	Temperature (°C)	pH (-)
prepare silica sol: silica	3.9096	3.98				-
water and add silica sol dropwise	5.8644	12.3		15:45		
stir for 2 hours			15:45	17:45		
transfer into teflon lined autoclave and age for 12-14 hours at 120 °C		18.3	18:10	07:35	120 °C	
crystallize at 170 °C for 24 hours			26.07 8:35	27.07 8:35	170 °C	
add Perovskite		1.63				
centrifuge and wash with distilled water until pH about 7			27.05			7
dry at 60 °C for 12 hours			27.05	28.05	60 °C	
calcine at 550 °C for 6 hours			28.05	29.05	550 °C 6h	

Figure 107: digitalized notes from the lab journal of batch 220721E ZSM-5+NCF-Co part 2

Recipe Zeolite ZSM-5 SiO_2/Al_2O_3 = 70 V1

Start Date:	22.09.2022
Batch:	ZSM-5 220922A
Prepared by:	Richard Buchinger

Working Step	mass needed (g)	actual mass (g)	Start Time	End Time	Temperature (°C)	pH (-)
Seed suspension S-1:					RT	
Fill distilled water into beaker	2.4832	2.483	14:10		RT	-
add EtOH	1.6075	1.6231			RT	-
add TPAOH solution	1.7167	1.7212		14:15	RT	-
add TEOS dropwise while stirring	1.8177	1.8231	14:17	14:20	RT	-
homogenize at roomtemperature for 2 hours	-	-	14:20	16:20	RT	-
transfer into teflon lined autoclave	-				RT	-
treat hydrothermally at 100 °C for 96 hours	-	-	22.09 16.30	26.09 16.30	100 °C	-
cool down to room temperature	-	-			RT	-
nano-sized ZSM-5 aggregates:						
Fill distilled water into beaker	23.9200	23.922	16:00			-
Dissolve NaOH in water	0.5408	0.5405				-
dissolve NaAlO2 in water	0.1524	0.1521				
dissolve CTAB in water	0.5294	0.5291		16:10		-
stir for 0,5 hours	-	-	16:10	16:40		-
add S-1 gel dropwise	5.0834	5.037	17:00	17:05		-

Figure 108: digitalized notes from the lab journal of batch 220922A ZSM-5+NCF-Co part 1

Working Step	mass needed (g)	actual mass (g)	Start Time	End Time	Temperature (°C)	pH (-)
prepare silica sol: silica	3.9096	3.93				-
water and add silica sol dropwise	5.8644	12.3		17:15		
stir for 2 hours			17:15	19:15		
transfer into teflon lined autoclave and age for 12-14 hours at 120 °C	15	15.023	26.09 19:20	27.09 7:30	120 °C	
crystallize for 24 hours at 170 °C			27.09 8:30	28.09 8:30	170 °C	
centrifuge and wash until pH 7			28.09			7
dry in oven overnight 60-120 °C			28.09	29.09	100 °C	
Weigh in Zeolite		0.673				
NCF-Co	0.5774	0.578				
calcine at 550 °C 6 hours			29.09	30.09	550 °C 6h	

Figure 109: digitalized notes from the lab journal of batch 220922A ZSM-5+NCF-Co part 2

Recipe Zeolite ZSM-5 SiO_2/Al_2O_3 = 70 V1

Start Date:	22.09.2022
Batch:	ZSM-5 220922D
Prepared by:	Richard Buchinger

Working Step	mass needed (g)	actual mass (g)	Start Time	End Time	Temperature (°C)	pH (-)
Seed suspension S-1:					RT	
Fill distilled water into beaker	2.4832	2.483	14:10		RT	-
add EtOH	1.6075	1.6231			RT	-
add TPAOH solution	1.7167	1.7212		14:15	RT	-
add TEOS dropwise while stirring	1.8177	1.8231	14:17	14:20	RT	-
homogenize at roomtemperature for 2 hours	-	-	14:20	16:20	RT	-
transfer into teflon lined autoclave	-				RT	-
treat hydrothermally at 100 °C for 96 hours	-	-	22.09 16.30	26.09 16.30	100 °C	-
cool down to room temperature	-	-			RT	-
nano-sized ZSM-5 aggregates:						
Fill distilled water into beaker	23.9200	23.922	16:00			-
Dissolve NaOH in water	0.5408	0.5405				-
dissolve NaAlO2 in water	0.1524	0.1521				
dissolve CTAB in water	0.5294	0.5291		16:10		-
stir for 0,5 hours	-	-	16:10	16:40		-
add S-1 gel dropwise	5.0834	5.037	17:00	17:05		-

Figure 110: digitalized notes from the lab journal of batch 220922D ZSM-5+NCF-Co part 1

Working Step	mass needed (g)	actual mass (g)	Start Time	End Time	Temperature (°C)	pH (-)
prepare silica sol: silica	3.9096	3.93				-
water and add silica sol dropwise	5.8644	12.3		17:15		
stir for 1.5 hours			17:15	18:45		
prepare Zeolite		19.99	10:48			
Perovskite (05-15.07.22) mixture		2.08		18:50		
stir for 0.5 hours			18:50	19:20		
transfer into teflon lined autoclave and age for 12-14 hours at 120 °C	16.556	16.612	26.09 19:20	27.09 7:30	120 °C	
crystallize for 24 hours at 170 °C			27.09 8:30	28.09 8:30	170 °C	
centrifuge and wash until pH 7			28.09			7
dry in oven overnight 60-120 °C			28.09	29.09		
calcine at 550 °C 6 hours			29.09	30.09		

Figure 111: digitalized notes from the lab journal of batch 220922D ZSM-5+NCF-Co part 2

The raw data from the XRF measurements can be seen in Table 23.

Table 23: Raw Data from XRF analysis, n.n. means below detection limit

wt%	220922A	220721E	220721D	220623C	220922D	220623B	220609A
MoO_3	n.n.	n.n.	n.n.	n.n.	n.n.	n.n.	n.n.
Nb_2O_5	n.n.	n.n.	n.n.	n.n.	n.n.	n.n.	n.n.
ZrO_2	n.n.	n.n.	n.n.	n.n.	n.n.	n.n.	n.n.
SrO	n.n.	n.n.	n.n.	n.n.	n.n.	n.n.	n.n.
As_2O_3	n.n.	n.n.	n.n.	n.n.	n.n.	n.n.	n.n.
PbO	n.n.	0.02%	n.n.	0.01%	0.01%	n.n.	n.n.
ZnO	n.n.	0.02%	n.n.	n.n.	n.n.	n.n.	n.n.
CuO	0.05%	0.05%	0.05%	0.01%	0.04%	0.02%	0.03%
NiO	0.03%	0.03%	0.04%	0.02%	0.04%	0.02%	0.02%
Co_3O_4	2.87%	3.16%	2.86%	2.44%	3.05%	2.71%	2.83%
Fe_2O_3	20.02%	23.01%	20.53%	19.11%	22.45%	20.99%	22.52%
MnO	0.11%	0.13%	0.10%	0.08%	0.13%	0.08%	0.08%
Cr_2O_3	0.03%	0.06%	0.04%	0.04%	0.03%	0.03%	0.03%
V_2O_5	n.n.	0.02%	n.n.	n.n.	0.02%	n.n.	n.n.
TiO_2	0.03%	0.09%	0.05%	0.03%	0.02%	0.05%	0.05%
CaO	7.43%	8.84%	5.85%	6.91%	6.14%	7.29%	8.33%
K_2O	0.07%	0.08%	0.02%	0.08%	0.17%	0.10%	0.03%
Cl	0.26%	0.07%	0.10%	0.59%	1.02%	0.45%	0.07%
SO_3	0.13%	0.42%	0.14%	0.13%	0.23%	0.15%	0.06%
P_2O_5	0.02%	1.25%	0.23%	0.03%	0.04%	0.03%	n.n.
SiO_2	64.03%	58.86%	66.39%	64.46%	58.10%	63.07%	62.37%
Al_2O_3	2.08%	2.46%	1.87%	1.77%	2.03%	1.63%	1.99%
MgO	0.19%	0.31%	0.17%	0.17%	0.29%	0.12%	0.16%
Na_2O	2.65%	1.10%	1.58%	4.11%	6.21%	3.26%	1.44%

10 List of Figures

11 List of Tables

12 References

[1] L. Lindenthal *et al.*, "Novel perovskite catalysts for CO2 utilization - Exsolution enhanced reverse water-gas shift activity," *Applied Catalysis B: Environmental,* vol. 292, p. 120183, 2021/09/05/ 2021, doi: https://doi.org/10.1016/j.apcatb.2021.120183.

[2] H. Göthel, "Fischer-Tropsch-Synthese," in *Mineralöle und verwandte Produkte: Ein Handbuch für das Laboratorium*, C. Żerbe Ed. Berlin, Heidelberg: Springer Berlin Heidelberg, 1952, pp. 1190-1225.
[3] C. J. R. Frazão and T. Walther, "Syngas and Methanol-Based Biorefinery Concepts," *Chemie Ingenieur Technik,* https://doi.org/10.1002/cite.202000108 vol. 92, no. 11, pp. 1680-1699, 2020/11/01 2020, doi: https://doi.org/10.1002/cite.202000108.
[4] L. Lindenthal *et al.*, "Novel Perovskite Catalysts for CO2 Utilization - Exsolution Enhanced Reverse Water-Gas Shift Activity," *Applied Catalysis B-environmental,* p. 120183, 2021.
[5] M. W. Chase, Jr. "*NIST-JANAF Themochemical Tables*." (accessed 20.05, 2022).
[6] "Chapter 5.3.3 - Application of Hydrogen by Use of Chemical Reactions of Hydrogen and Carbon Dioxide," in *Science and Engineering of Hydrogen-Based Energy Technologies*, P. E. V. de Miranda Ed.: Academic Press, 2019, pp. 279-289.
[7] J. Popovic *et al.*, "High Temperature Water Gas Shift Reactivity of Novel Perovskite Catalysts," *Catalysts,* vol. 10, p. 582, 05/22 2020, doi: 10.3390/catal10050582.
[8] S. Mitchell, N.-L. Michels, and J. Pérez-Ramírez, "From powder to technical body: the undervalued science of catalyst scale up," *Chemical Society Reviews,* 10.1039/C3CS60076A vol. 42, no. 14, pp. 6094-6112, 2013, doi: 10.1039/C3CS60076A.
[9] T. Maesen and B. Marcus, "Chapter 1 The zeolite scene—An overview," in *Studies in Surface Science and Catalysis*, vol. 137, H. van Bekkum, E. M. Flanigen, P. A. Jacobs, and J. C. Jansen Eds.: Elsevier, 2001, pp. 1-9.
[10] J. Zhang *et al.*, "Synthesis, characterization and application of Fe-zeolite: A review," *Applied Catalysis A: General,* vol. 630, p. 118467, 2022/01/25/ 2022, doi: https://doi.org/10.1016/j.apcata.2021.118467.
[11] J. Xu, Y. Qin, H. Wang, F. Guo, and J. Xie, "Recent advances in copper-based zeolite catalysts with low-temperature activity for the selective catalytic reduction of NOx with hydrocarbons," *New Journal of Chemistry,* 10.1039/C9NJ04735B vol. 44, no. 3, pp. 817-831, 2020, doi: 10.1039/C9NJ04735B.
[12] C. Heard *et al.*, "Zeolite (In)Stability under Aqueous or Steaming Conditions," *Advanced Materials,* vol. 32, p. 2003264, 11/05 2020, doi: 10.1002/adma.202003264.
[13] "High Purity Aluminas." https://products.sasol.com/pic/products/home/grades/ZA/5pural-and-catapal/index.html (accessed 14.11, 2022).
[14] J. Popovic, "Institutsseminar_09.01.2019_Janko."
[15] Brunauer, S. Macko, P. Emmett, Teller, and Edward, "Brunauer, S., Emmett, P. H. & Teller, E. Adsorption of gases in multimolecular layers. J. Am. Chem. Soc. 60, 309-319," *Journal of the American Chemical Society,* vol. 60, pp. 309-319, 01/01 1938, doi: 10.1021/ja01269a023.
[16] U. König, R. Angélica, N. Norberg, and L. Gobbo, *Rapid X-ray diffraction (XRD) for grade control of bauxites*. 2012.
[17] "TDP 0 Desktop Tabletten Presse." https://www.lfatabletpresses.com/de/tdp-0-desktop-tabletten-presse (accessed 18.11, 2022).
[18] A. Corma, C. Corell, and J. Pérez-Pariente, "Synthesis and characterization of the MCM-22 zeolite," *Zeolites,* vol. 15, no. 1, pp. 2-8, 1995/01/01/ 1995, doi: https://doi.org/10.1016/0144-2449(94)00013-I.
[19] P. H. L. Quintela, W. S. Lima, B. J. B. d. Silva, A. O. S. d. Silva, and M. G. F. Rodrigues, "Effect of the simultaneous presence of sodium and potassium cations on the hydrothermal synthesis of MCM-22 zeolite," *Research, Society and Development,* vol. 10, no. 14, p. e192101421744, 10/30 2021, doi: 10.33448/rsd-v10i14.21744.
[20] H. Chen *et al.*, "Conversion of methanol to propylene over nano-sized ZSM-5 zeolite aggregates synthesized by a modified seed-induced method with CTAB," *RSC Advances,* 10.1039/C6RA14753D vol. 6, no. 80, pp. 76642-76651, 2016, doi: 10.1039/C6RA14753D.